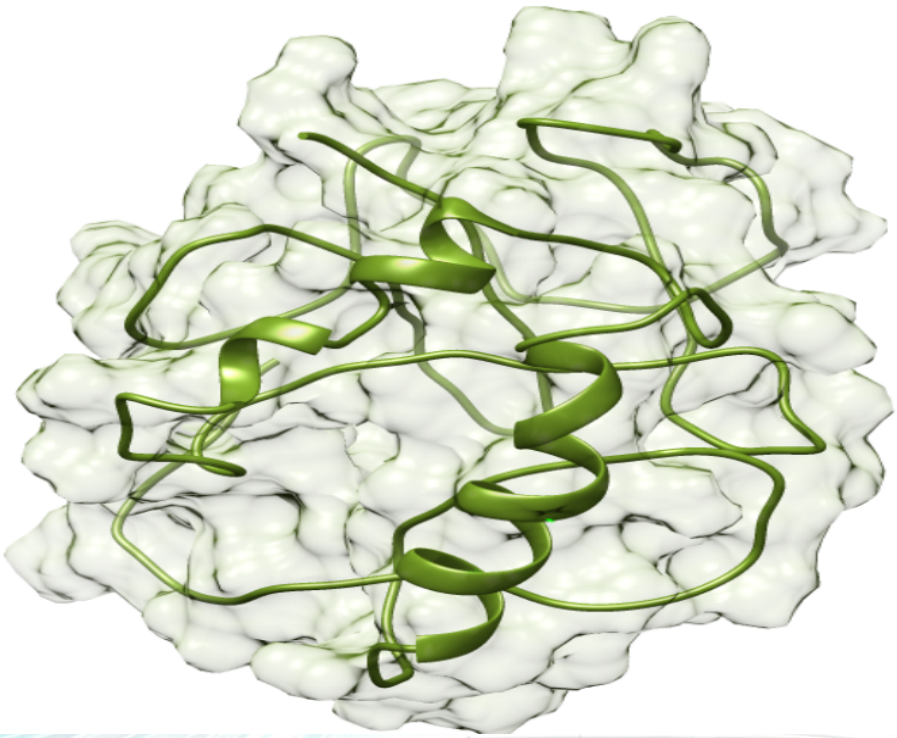
Volume 2, Issue 3, 2026

Online ISSN: 3068-1812
Print ISSN: 3071-3048

Advances in World Medical Research

In silico Identification of Potential Hepatitis B Virus HBx Inhibitors Through Molecular Docking Analysis

Maryam Aliza, Bibi Haleema



CSCHOLAR
Publishing INC
https://awmr.cscholar.com/

Article metadata are indexed and discoverable through the following services:

CNKI 中国知网 www.cnki.net · 万方数据 WANFANG DATA · Clarivate Research Commons · Google Scholar · Crossref · Scilit

Advances in World Medical Research

Volume 2, Issue 3, 2026

Quarterly

Editor-in-Chief:

Wei Zhang China Academy of Chinese Medical Science zhangw@blcu.edu.cn

Deputy Editor-in-Chief:

Han Chen Beijing Jizhi Yuewei Technology Co., Ltd. chenhan@ic-creation.cn

Standing Editorial Board Members：

For more details, please visit: https://awmr.cscholar.com/about/editorialTeam

Editorial Board Member:

For more details, please visit: https://awmr.cscholar.com/about/editorialTeam

Cover Design: ConnectSix Scholar Publishing INC

Publishing Unit: ConnectSix Scholar Publishing INC

Publisher's website: http://www.cscholar.com/

Publisher's address:

6547 N Academy Blvd #2265

Colorado Springs CO 80918

US

Website of the journal *Advances in World Medical Research*:

https://awmr.cscholar.com/

Table of contents

Research Progress on Neural Mechanisms and Intervention Strategies of Cognitive Impairment Associated with Obstructive Sleep Apnea	Yejun Du Weikai Zhang Zhanfeng Yan	1-19
In silico Identification of Potential Hepatitis B Virus HBx Inhibitors Through Molecular Docking Analysis	Maryam Aliza Bibi Haleema	20-31
In Silico Prediction of Distinct HMW PAH-Associated Pathways in Allergic Rhinitis: Chemokine-Related Targets of BaP and Metabolic Enzyme Targets of BaA/DBA	Yue He Yibo He Junfeng Xi An Chang Zeyu Guo Xianzhi Liu Jiayu Li Jiaxuan Li Zhao Wang Dong Chen	32-48
Qiliqiangxin Capsule in Patients with Chronic Heart Failure Complicated by Coronary Artery Disease: A Systematic Review and Meta-Analysis of Randomized Trials	Kaijuan Wang Jinhao Xu Xiangying Zheng Fengshuo Chang Jingen Li	49-77
CD8+ T Cell Exhaustion and Tumor Immune Checkpoint Blockade: Mechanisms, Heterogeneity, and Combination Intervention Strategies	Gang Liu	78-86
Call for Papers: Advances in World Medical Research	Editorial Materials	87-88

Advances in World Medical Research, 2026, 2(3), 1-19
https://doi.org/10.71204/zkb2g519

Research Progress on Neural Mechanisms and Intervention Strategies of Cognitive Impairment Associated with Obstructive Sleep Apnea

Yejun Du [1], Weikai Zhang [1], Zhanfeng Yan [1, *]

[1] Dongzhimen Hospital, Beijing University of Chinese Medicine, Beijing 100700, China

*** Correspondence**:

Zhanfeng Yan

15210682430@163.com

Received: 28 May 2026/ Accepted: 30 July 2026/ Published online: 19 September 2026

Abstract

Obstructive sleep apnea (OSA) is a prevalent sleep-related breathing disorder that is closely associated with cognitive impairment. However, the efficacy of conventional interventions remains limited, and exploring its neural mechanisms and adjunctive therapeutic strategies has become a research hotspot. This paper provides a narrative review of the research progress in neuroimaging mechanisms and intervention strategies for OSA-related cognitive impairment. Regarding neural mechanisms, this article focuses on two core mechanisms: dysfunction of the glymphatic system and unstable alterations in dynamic brain functional networks. Multimodal neuroimaging evidence demonstrates that patients with OSA exhibit distinct glymphatic system impairment and compromised dynamic reorganization ability of brain functional networks, characterized by "excessive persistence" and "abnormal transitions" of functional connectivity states. Pivotal mediation analyses have revealed for the first time the causal pathway of "glymphatic dysfunction → decreased brain network efficiency → cognitive impairment." In terms of intervention strategies, this article points out that continuous positive airway pressure (CPAP) has limited efficacy in improving cognitive function, accompanied by poor patient adherence. Non-invasive neuromodulation techniques represented by repetitive transcranial magnetic stimulation (rTMS) and transcranial direct current stimulation (tDCS) show potential as adjunctive interventions due to their direct regulation of cortical excitability and neuroplasticity. Current research is limited by predominant cross-sectional designs, lack of standardized imaging biomarkers, and small sample sizes in intervention studies. Future research should focus on developing predictive models based on multimodal radiomics and artificial intelligence, exploring physical interventions targeting the glymphatic system, and conducting long-term randomized controlled trials enriched with biomarkers. This review aims to provide theoretical evidence and novel insights for the early identification and precise intervention of OSA-related cognitive impairment.

Keywords: Obstructive Sleep Apnea; Cognitive Impairment; Glymphatic System; Dynamic Brain Functional Networks; Non-invasive Neuromodulation; Continuous Positive Airway Pressure

1. Introduction

1.1. Clinical Association Between Obstructive Sleep Apnea and Cognitive Impairment

Obstructive Sleep Apnea (OSA) is a prevalent sleep-disordered breathing disorder characterized by recurrent upper airway collapse during sleep. It is mainly manifested as pathophysiological alterations including intermittent hypoxemia, hypercapnia, sleep fragmentation and increased sympathetic nerve activity. Epidemiological data indicate that approximately 425 million adults aged 30 to 69 worldwide suffer from moderate to severe OSA (Greenstone & Hack, 2014). The prevalence in China has also been rising year by year ("Guidelines for the diagnosis and treatment", 2012), and the country currently bears the world's heaviest disease burden of OSA. A multi-level meta-analysis reported that the overall prevalence of OSA in China is 11.8%, with a marked upward temporal trend: the figure surged from 8.1% in 2000–2005 to 26.9% in 2021–2024 (Niu et al., 2025). In terms of absolute population size, the number of OSA patients in China has exceeded 170 million (Benjafield et al., 2019). Notably, around 80% of potential OSA patients have not received timely diagnosis, resulting in a substantial gap between disease prevalence and clinical diagnosis (Yi et al., 2023).

OSA substantially elevates the risks of cardiovascular diseases, metabolic disorders and cerebrovascular events (Bradley & Floras, 2009; Coughlin et al., 2004). In recent years, its link with cognitive impairment has become a research hotspot at the intersection of sleep medicine and neuroscience. Patients with OSA present with multidimensional cognitive deficits, among which impairments in attention, executive function, visual and verbal working memory are most prominent (Zhang et al., 2025). A systematic review and meta-analysis further quantified the strength of this association, reporting that the prevalence of mild cognitive impairment (MCI) reaches 39% among OSA patients, and the prevalence of OSA is also 39% in individuals with MCI. The overall odds ratio for their correlation was 1.65, indicating a bidirectional relationship between OSA and cognitive dysfunction (Ren et al., 2025).

The biological mechanisms underlying OSA-related cognitive impairment have been extensively investigated. Intermittent hypoxia and sleep fragmentation, the hallmark pathological features of OSA, can trigger neuroinflammation, oxidative stress, neuronal damage, altered synaptic plasticity and blood-brain barrier dysfunction. These pathological cascades ultimately impair learning and memory abilities (Zhang et al., 2025). Moreover, the interplay between sleep disturbances and neurodegenerative diseases has attracted growing attention. Disordered sleep architecture is not only a common comorbidity of Alzheimer's disease (AD) and Parkinson's disease (PD), but may also be involved in their early pathogenesis (Hassan Mohmmed Ahmed et al., 2025). According to an official workshop report from the American Thoracic Society (ATS), OSA acts as a risk factor for preclinical AD, and exerts adverse effects on the incidence, clinical manifestations and progression of AD and other types of dementia (Lal et al., 2022). Given the above evidence, exploring the mechanisms linking OSA to cognitive impairment is of great clinical value for the early identification and comprehensive intervention of these diseases. In this review, the terms "cognitive impairment", "cognitive dysfunction", "neurocognitive impairment", and "mild

cognitive impairment (MCI)" are used to describe different degrees of cognitive decline in OSA patients. Unless otherwise specified, "cognitive impairment" serves as the overarching term encompassing all objectively measured deficits in attention, executive function, memory, and processing speed. When referring to the specific clinical diagnosis of MCI (defined by Petersen criteria or equivalent), the term "mild cognitive impairment" is used. The occasional use of "neurocognitive damage" or "cognitive dysfunction" reflects the original authors' phrasing in cited studies, and does not imply a distinct pathophysiological entity. For clarity, all cognitive outcome measures in this review are interpreted within the framework of domain-specific performance rather than as categorical diagnoses.

1.2. Limitations of Current Mechanistic Understanding and Intervention Strategies

Although numerous studies have confirmed a significant association between OSA and cognitive impairment, the underlying neural mechanisms remain incompletely elucidated, and existing intervention strategies also have evident limitations.

In terms of mechanisms, most conventional studies have focused on how OSA-related pathophysiological changes, including intermittent hypoxia and sleep fragmentation, directly induce brain tissue damage and cognitive decline. However, less attention has been paid to the systemic characteristics of OSA-associated brain injury, particularly the impaired dynamic reorganization of whole-brain networks. In recent years, dysfunction of the glymphatic system and destabilized dynamic functional brain networks have been proposed as two core neuroimaging mechanisms of OSA-related cognitive impairment. Studies have demonstrated a consistent correlation between sleep disturbances and impaired glymphatic clearance, with OSA exerting the most pronounced effect (Ghaderi et al., 2025; Xiong et al., 2024). Nevertheless, how glymphatic dysfunction specifically affects the dynamic reorganization of brain networks, as well as the temporal sequence and causal pathways between the two, remain to be further clarified. Additionally, the vast majority of relevant studies adopt a cross-sectional design, which makes it difficult to distinguish causality from mere correlation. As stated in the ATS workshop report, despite solid biological plausibility, sufficient evidence is still lacking to verify the bidirectional causal relationship between OSA and pathological brain aging (Lal et al., 2022).

With regard to interventions, continuous positive airway pressure (CPAP) serves as the first-line therapy for OSA, which effectively alleviates nocturnal hypoxia and sleep fragmentation. However, available evidence reveals substantial heterogeneity in the cognitive benefits of CPAP, and its effects vary across different cognitive domains in existing studies (Lal et al., 2022). More importantly, long-term adherence to CPAP therapy is generally poor, with the non-adherence rate ranging from 30% to 60% among adult OSA patients. The adherence is even lower in children and adolescents (Rotenberg et al., 2016; Sawyer et al., 2011). This practical dilemma highlights an urgent need for alternative and adjunct therapeutic approaches. Furthermore, the ATS report indicated that current research on the cognitive effects of OSA treatments predominantly centers on CPAP, while high-quality evidence supporting other therapeutic modalities remains scarce (Lal et al., 2022).

1.3. Objectives and Structure of the Present Article

This article aims to review the research progress regarding neural mechanisms and intervention strategies for cognitive impairment associated with obstructive sleep apnea (OSA). The discussion is mainly organized into three parts. First, neuroimaging mechanisms: focusing on glymphatic system dysfunction and destabilized dynamic functional brain networks, this section summarizes how multimodal imaging evidence reveals the pathological basis of OSA-related brain damage, and explores the coupling pathways between the two mechanisms as well as their correlations with cognitive deficits. Second, innovative intervention strategies: on the basis of analyzing the limitations of conventional CPAP therapy, it reviews the application prospects and working mechanisms of non-invasive neuromodulation techniques represented by repetitive transcranial magnetic stimulation (rTMS) and transcranial direct current stimulation (tDCS) in the treatment of OSA-related cognitive impairment. Third, future research directions: in view of existing research gaps, this paper puts forward key research priorities including the development of multimodal radiomics models, exploration of glymphatic system-targeted interventions, and clinical trials enriched with biomarkers. It is expected to provide theoretical references for the early identification and precise intervention of OSA-related cognitive impairment.

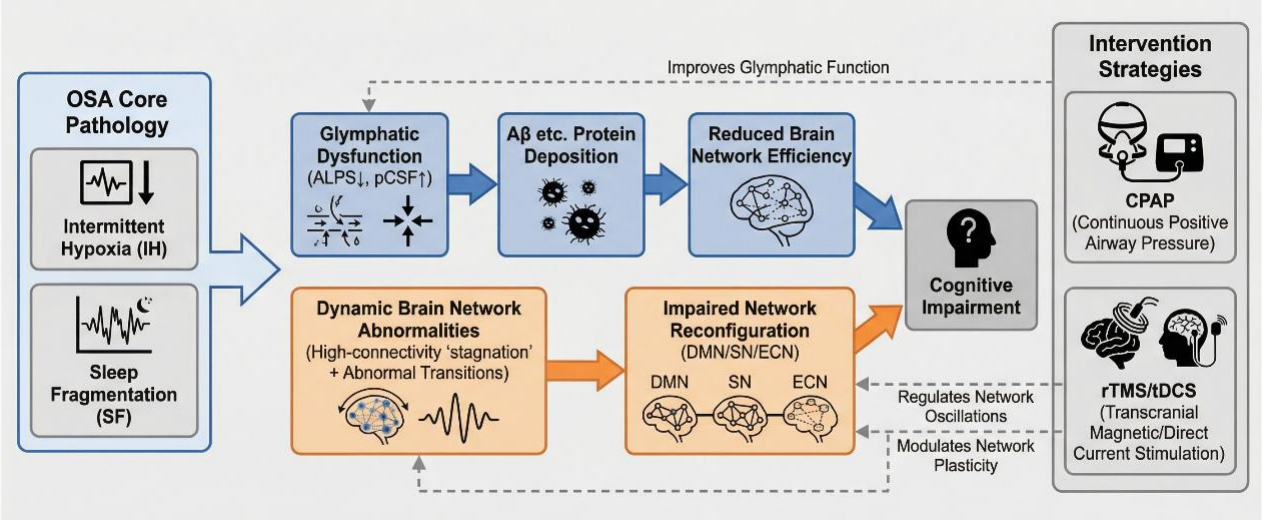


Figure 1. Pathways underlying OSA-related cognitive impairment

Figure 1 Schematic illustration of the two major pathways linking OSA to cognitive impairment and the potential intervention targets.

Abbreviations: pCSF, parenchymal cerebrospinal fluid; DTI- ALPS, diffusion tensor imaging- based analysis along the perivascular space; DMN, default mode network; SN, salience network; ECN, executive control network; CPAP, continuous positive airway pressure; rTMS, repetitive transcranial magnetic stimulation; tDCS, transcranial direct current stimulation.

Left panel: Core OSA pathologies (intermittent hypoxia and sleep fragmentation) drive cognitive dysfunction via two cascades. Pathway A (glymphatic dysfunction): OSA impairs glymphatic clearance, evidenced by reduced DTI- ALPS index (ALPS↓) and increased pCSF volume (pCSF↑), leading to accumulation of neurotoxic proteins (e.g., Aβ), which in turn decreases global brain network efficiency and ultimately causes cognitive decline. Pathway B (dynamic network instability): OSA disrupts the dynamic reorganization of large- scale brain networks (DMN, SN, ECN), manifesting as prolonged dwell time in high- connectivity states and aberrant state

transitions, which directly impair cognitive performance. Right panel: Potential interventions. CPAP alleviates nocturnal hypoxia and may partially restore glymphatic function. rTMS and tDCS modulate cortical excitability and network oscillations to correct aberrant dynamic connectivity. Solid arrows indicate pathological progression; dashed arrows indicate modulatory effects of interventions.

2. Neuroimaging Mechanisms of OSA-Related Cognitive Impairment

In recent years, advances in neuroimaging techniques have greatly deepened the understanding of the neural mechanisms underlying OSA-related cognitive impairment. Multimodal imaging evidence, ranging from macroscopic brain networks to the microscopic glymphatic system, has gradually delineated the complex pathological profiles of OSA-associated brain damage. This section mainly elaborates on two cutting-edge mechanisms: glymphatic system dysfunction and destabilization of dynamic brain networks.

2.1. Glymphatic System Dysfunction

The glymphatic system is a recently discovered pathway responsible for clearing metabolic waste in the brain, and its function largely relies on the convective exchange between cerebrospinal fluid and interstitial fluid during sleep (Yankova et al., 2021). Characterized by sleep fragmentation and intermittent hypoxia, OSA can severely impair this system and further facilitate the abnormal deposition of neurotoxic proteins (Keil et al., 2026).

2.1.1. Imaging Evidence of Impaired Glymphatic Function

The primary imaging biomarkers for evaluating glymphatic function include the diffusion tensor imaging-based analysis along the perivascular space (DTI-ALPS) index and parenchymal cerebrospinal fluid (pCSF) mapping derived from multi-echo T2 imaging. A systematic review and meta-analysis conducted by Ghaderi demonstrated that patients with severe OSA exhibited a markedly reduced DTI-ALPS index compared with healthy controls, with a pooled effect size of -0.95, confirming substantial glymphatic system impairment in this population. Meta-regression analysis further identified the apnea-hypopnea index (AHI) and Epworth Sleepiness Scale (ESS) score as major sources of heterogeneity, indicating that hypoxia burden and daytime sleepiness are closely linked to impaired glymphatic function (Ghaderi et al., 2025). Xiong et al. (2024) also reported a significantly lower ALPS index in OSA patients relative to controls, and this index was positively correlated with cognitive performance scores. Zhou et al. adopted multi-echo FAST-T2 MRI to compare untreated OSA patients, CPAP-treated OSA patients and healthy individuals. The results showed that untreated OSA patients had remarkably larger pCSF volume in the whole-brain gray matter, white matter and Alzheimer's disease (AD)-vulnerable brain regions. By contrast, pCSF levels in the CPAP group were comparable to those in healthy controls. Notably, pCSF burden was positively correlated with cortical amyloid-β (Aβ) deposition, suggesting that glymphatic dysfunction may mediate impaired Aβ clearance in OSA. This finding provides a mechanistic explanation for the epidemiological association between OSA and AD (Keil et al., 2026). In studies on Parkinson's disease (PD) complicated with OSA, Nepozitek et al. (2025) found that the ALPS index in newly diagnosed, treatment-naive PD patients was significantly negatively

correlated with AHI, oxygen desaturation index and the proportion of stage N1 sleep. Such correlations were not observed in PD patients without OSA. This evidence suggests that OSA may accelerate the pathological progression of neurodegenerative diseases by disrupting glymphatic function.

2.1.2. Correlation with Cognitive-Related Brain Regions

Glymphatic dysfunction is anatomically associated with structural and functional alterations in cognition-related brain regions. Xiong et al. (2024) found that the ALPS index was moderately positively correlated with the Montreal Cognitive Assessment (MoCA) scores in OSA patients. More importantly, mediation analysis conducted by Xiong et al. revealed that the global efficiency of brain networks exerted a partial mediating effect between glymphatic dysfunction and cognitive impairment, with an indirect effect value of 4.58 and a mediating effect proportion of 26.9%. This finding firstly established the causal chain of *glymphatic dysfunction → decreased brain network efficiency → cognitive impairment* in patients with OSA.

In terms of regional specificity, Keil et al. (2026) demonstrated that elevated pCSF was particularly prominent in AD-vulnerable brain regions of untreated OSA patients, including the posterior cingulate cortex, precuneus and medial temporal lobe. These areas are not only early-affected sites of AD pathology, but also core nodes of the default mode network (DMN), which play pivotal roles in episodic memory and self-referential processing. Impaired Aβ clearance resulting from glymphatic dysfunction may initially manifest in these regions, offering a mechanistic interpretation for the regional specificity of OSA-related cognitive impairment.

2.1.3. Technical Limitations and Confounding Factors of Glymphatic Imaging Biomarkers

It is important to recognize that both the DTI- ALPS index and parenchymal cerebrospinal fluid (pCSF) mapping are indirect surrogate markers of glymphatic function, rather than direct measures of CSF- interstitial fluid exchange. The DTI- ALPS index, derived from diffusion tensor imaging along the perivascular space, can be influenced by multiple confounders including cerebral small vessel disease, white matter hyperintensities, and age- related microstructural changes, all of which are common in OSA populations. Furthermore, the ALPS index assumes a specific orientation of perivascular diffusion, which may not hold true in regions with complex fiber crossings or in the presence of substantial motion artifacts. Similarly, pCSF elevation, as quantified by multi- echo T2 imaging, reflects the volumetric expansion of CSF spaces within the parenchyma; however, this increase is not specific to impaired clearance function. It can also result from brain atrophy, age- related sulcal widening, small vessel disease, or altered intracranial pressure dynamics. Thus, interpreting pCSF burden solely as a marker of metabolic waste clearance requires caution. The reproducibility of both biomarkers across different MRI scanners, field strengths, and post- processing pipelines remains to be systematically evaluated. Future studies should incorporate complementary techniques (e.g., contrast- enhanced MRI or PET tracers) to validate these imaging surrogates and should adjust for vascular and neurodegenerative confounders in statistical analyses.

2.2. Destabilization of Dynamic Functional Brain Networks

Traditional resting-state functional magnetic resonance imaging (rs-fMRI) studies generally assume that functional brain connectivity remains stable during scanning. However, recent research

has revealed the time-varying characteristics of functional brain networks. Due to intermittent hypoxia and disrupted sleep architecture, patients with OSA exhibit impaired capacity for dynamic network reorganization, presenting with unstable network states.

2.2.1. Application of Dynamic Functional Connectivity Analysis

Dynamic functional connectivity (dFC) analysis adopts the sliding-window approach to capture time-varying patterns of functional connections (Allen et al., 2014; Calhoun et al., 2014). Widely used analytical frameworks include independent component analysis (ICA)-based time-varying functional network connectivity (FNC), multiplier temporal derivative (MTD)-based state transition analysis, and graph theory-based dynamic network metrics (Preti et al., 2017; Shine et al., 2016; Zalesky et al., 2014). Yu et al. (2025) combined ICA with the sliding-window method and identified two reproducible functional connectivity states among 82 male OSA patients and 48 healthy controls. State I was characterized by strong functional connectivity with a low occurrence frequency, while State II showed weak functional connectivity and occurred more frequently. The results indicated that OSA patients with mild cognitive impairment (OSA-MCI) had longer dwell time and higher occupancy rate in the strong-connectivity state, alongside shorter dwell time and lower occupancy rate in the weak-connectivity state. The number of state transitions tended to rise in the patient group and was positively correlated with cognitive scores. These findings suggest that the prolonged retention of brain functional networks in the strong-connectivity state may reflect compensatory neural recruitment, yet persistent activation of this state could eventually deplete the reserve of network plasticity. Wang et al. (2025) applied the MTD method to analyze dFC features in 111 OSA patients and distinguished five connectivity states, consisting of four high-connectivity states and one low-connectivity state. Significant alterations in fractional time (FT) and mean dwell time (MDT) of State 1, State 3 and State 4 were observed in patients with moderate to severe OSA. Specifically, FT and MDT of State 1 were negatively correlated with hypoxia-related parameters, whereas those of State 3 were positively correlated with total sleep time. Notably, FT of State 3 was inversely associated with the visuospatial and executive function subscores of the Montreal Cognitive Assessment (MoCA), indicating that aberrations in specific dynamic connectivity states may be directly linked to executive dysfunction.

2.2.2. Dynamic Functional States and Cognitive Impairment

The aforementioned studies reveal two predominant patterns of aberrant dynamic functional states in OSA patients: excessive dwell time in high-connectivity states, indicating impaired network flexibility, and abnormal transitions between low- and high-connectivity states, which reflects disrupted network stability. Collectively, these two patterns hinder the brain from efficiently reorganizing network resources when confronted with cognitive demands.

Yu et al. (2025) further identified the core brain networks affected by dynamic functional abnormalities. Compared with healthy controls, OSA patients exhibited widespread aberrant functional connectivity within the high-connectivity state, mainly involving the salience network (SN), default mode network (DMN) and executive control network (ECN), along with reduced connectivity in the low-connectivity state. These networks undertake core roles in attentional orientation, introspective monitoring and cognitive control during cognitive processing.

Progressive deterioration of dFC was observed during the transition from OSA with normal cognition (OSA-NC) to OSA with mild cognitive impairment (OSA-MCI), suggesting that dynamic network metrics may serve as early imaging biomarkers for OSA-related cognitive impairment.

As summarized in the review by Rosenzweig et al. (2015), OSA patients present with abnormal or diminished blood oxygen level-dependent (BOLD) activation in specific brain regions including the hippocampus and prefrontal cortex during cognitive tasks. Such alterations in neurovascular coupling are likely associated with disturbed dynamic networks. Intermittent hypoxia impairs cerebrovascular reactivity, while sleep fragmentation disrupts synaptic homeostasis. The combined effects of these two factors ultimately undermine the dynamic reorganization capacity of functional brain networks.

The dynamic functional connectivity (dFC) metrics discussed above are derived from resting- state BOLD fMRI, which is inherently sensitive to physiological noise and motion artifacts. Patients with OSA often present with intermittent hypoxia, abnormal cerebrovascular reactivity, sleep deprivation, and relatively large head movements during scanning, all of which can confound BOLD signal fluctuations. In particular, changes in respiration and heart rate can induce low- frequency oscillations that mimic or contaminate neural connectivity patterns. Notably, none of the primary studies included in this review explicitly reported the use of physiological monitoring (e.g., simultaneous recording of cardiac and respiratory signals) or retrospective correction methods (e.g., RETROICOR, RVHRCOR) to remove such artifacts. Head motion parameters were generally matched between groups, but the potential residual effects of motion on dynamic state transitions were not systematically quantified. Furthermore, the risk of patients falling asleep during the scan is seldom addressed, which could dramatically alter connectivity states. Therefore, while the observed aberrant dFC patterns are consistent with the hypothesis of network instability, caution is warranted in attributing these findings solely to neuronal dysfunction; vascular and non- neuronal physiological contributions cannot be excluded. Future dFC studies in OSA should adopt rigorous artifact control strategies and report detailed procedures for handling physiological noise and motion.

2.3. Coupling Between Glymphatic Dysfunction and Brain Network Inefficiency

The two mechanisms described above are not independent but are linked in a sequential causal chain. Glymphatic dysfunction, by impairing the clearance of neurotoxic metabolites such as amyloid-β, creates a hostile microenvironment that undermines synaptic efficacy and the stability of large-scale functional connections (Benveniste et al., 2019; He & Sun, 2025; Yankova et al., 2021). The spatial overlap between regions of elevated pCSF (e.g., posterior cingulate cortex, precuneus, medial temporal lobe) and the core nodes of the default mode network provides anatomical support for this coupling. Mediation analyses (as detailed in Section 2.1.2) have quantitatively established that reduced global network efficiency partially mediates the relationship between glymphatic impairment and cognitive deficits. Thus, the pathway of glymphatic dysfunction → decreased brain network efficiency → cognitive impairment represents a unifying framework that integrates micro- and macro- level imaging findings.

3. Limitations of Conventional Interventions and Innovations in Non-Invasive Neuromodulation Techniques

Continuous positive airway pressure (CPAP) serves as the mainstay of conventional treatment for OSA. Although it effectively relieves nocturnal hypoxia and sleep fragmentation, it suffers from poor long-term patient adherence and shows limited efficacy in reversing established damage to brain functional networks (Gurbani et al., 2025). In recent years, non-invasive brain stimulation (NIBS) techniques, represented by repetitive transcranial magnetic stimulation (rTMS) and transcranial direct current stimulation (tDCS), have emerged as a cutting-edge research direction for intervening in OSA-related cognitive impairment. These techniques enable targeted regulation of activities in specific brain regions and facilitate neural plasticity.

3.1. Efficacy and Limitations of Continuous Positive Airway Pressure

A meta-analysis revealed that CPAP treatment yielded significant improvements only in the Trail Making Test Part B, which reflects cognitive flexibility, whereas no robust overall effects were observed on other cognitive domains including information processing speed, executive function and working memory (Durtette et al., 2024). Another study similarly indicated that CPAP mainly alleviated daytime sleepiness and improved processing speed and visual search ability, with insufficient evidence supporting its benefits for higher-order cognitive functions such as executive function and memory (Durtette et al., 2024). Therefore, merely relieving upper airway obstruction is inadequate to reverse established brain network damage, highlighting the necessity to develop adjunctive therapeutic strategies.

3.2. Application Prospects of Non-Invasive Neuromodulation Techniques

Non-invasive brain stimulation (NIBS) modulates the excitability of cortical neurons via externally applied electric or magnetic fields, thereby altering the functional states of distant brain networks. Unlike CPAP, which improves brain function indirectly by relieving upper airway obstruction, NIBS enables direct targeting of cognition-related neural circuits. It offers an alternative therapeutic option for OSA patients who cannot tolerate CPAP or continue to suffer from persistent cognitive impairment after CPAP treatment (Yao et al., 2023; Yu et al., 2024; Zhao et al., 2024).

3.2.1. Clinical Evidence of rTMS and tDCS

Direct evidence of TMS in patients with OSA: Han et al. (2023) conducted a randomized controlled trial (RCT) to explore the effects of transcranial magnetic stimulation (TMS) on cognitive function in OSA patients. A total of 42 patients diagnosed with OSA via polysomnography were enrolled. Intermittent theta burst stimulation (iTBS) was delivered over the left dorsolateral prefrontal cortex (DLPFC), with parameters set as 2-second stimulation followed by an 8-second interval. Each session consisted of three trains of 600 pulses, with a 15-minute break between trains. The results demonstrated significant improvements in visual memory, sustained attention and working memory in the active stimulation group. Quantitative electroencephalography (EEG) recordings acquired before and after intervention revealed that TMS markedly increased the relative power spectral density of theta and beta bands in the parietal,

temporal and anterior brain regions, indicating that TMS ameliorates cognitive function by regulating cortical neural oscillations.

Indirect evidence from cross-diagnostic meta-analyses: Although studies focusing specifically on NIBS for OSA remain limited, high-quality meta-analyses on other neurological disorders provide valuable references. A meta-analysis by Begemann et al. (2020) including 82 RCTs found that both TMS and tDCS yielded small yet statistically significant improvements in working memory, and tDCS also exerted notable benefits on attention and alertness. A key finding was that the pro-cognitive effects of NIBS were consistent across diagnoses. Similar effect sizes were observed in various brain disorders such as dementia, Parkinson's disease and schizophrenia, suggesting that NIBS acts by modulating general brain network states rather than targeting disease-specific pathways. This conclusion is highly generalizable to patients with OSA.

Exploration of tDCS application: To date, no RCTs have reported the direct use of tDCS in OSA patients. Nevertheless, studies on Alzheimer's disease (AD) and mild cognitive impairment (MCI) have shown that anodal tDCS applied to the left DLPFC or parietal cortex can enhance episodic memory and executive function (Rektorová et al., 2025). Given the overlapping neuropathological mechanisms between OSA and AD, including impaired amyloid-β clearance and glymphatic dysfunction, tDCS possesses considerable translational potential for clinical use in OSA populations.

3.2.2. Potential Neural Mechanisms: From Neural Oscillations to Brain Network Remodeling and Glymphatic Modulation

The mechanisms by which non-invasive brain stimulation (NIBS) alleviates OSA-related cognitive impairment can be elaborated from three aspects: neural oscillations, brain network remodeling and glymphatic system regulation.

Modulation of cortical neural oscillations: Han et al. (2023) firstly verified in OSA patients that TMS significantly elevated the power spectral density of theta and beta bands after intervention. Theta oscillations are closely implicated in the encoding and retrieval of working memory, while beta oscillations participate in sustained attention and cognitive control. TMS-induced alterations in oscillatory rhythms serve as electrophysiological markers of neural plasticity, reflecting persistent enhancement of cortical excitability following stimulation.

Remodeling of unstable functional brain networks: Neuroimaging-based mechanistic studies indicate that NIBS may exert therapeutic effects by regulating dynamic connectivity patterns of large-scale brain networks. A recent review in *Nature Reviews Neurology* noted that advances in NIBS, including state-dependent protocols, network-based strategies, multifocal and subcortical paradigms, personalized electric field modeling and accelerated stimulation regimens, offer great promise for the diagnosis and management of neurological disorders (Rektorová et al., 2025).

Indirect regulation of glymphatic function: Impaired amyloid-β (Aβ) clearance resulting from glymphatic dysfunction is one of the core mechanisms underlying OSA-related cognitive impairment (Liu et al., 2023). Whether NIBS can indirectly improve glymphatic function by adjusting sleep architecture or cerebral hemodynamics has become a major research focus. Latest evidence suggests that accelerated iTBS is well tolerated and yields clinically meaningful cognitive

benefits in patients with Alzheimer's disease, which may be linked to the modulation of Aβ deposition (Rektorová et al., 2025). For OSA populations, exploring the synergistic effects of TMS and CPAP — whereby TMS restores cortical excitability and CPAP relieves nocturnal hypoxia — represents a key direction for future investigations.

4. Limitations of Current Studies and Key Directions for Future Research

4.1. Limitations of Existing Studies

Despite remarkable progress in the research on OSA-related cognitive impairment in recent years, several critical limitations remain, hindering the translation of basic research findings into clinical practice.

First, most studies adopt a cross-sectional design, resulting in a lack of longitudinal evidence to confirm causality. The vast majority of current investigations into the association between OSA and cognitive impairment are cross-sectional, which cannot distinguish causal relationships from mere correlations. A bidirectional interaction may exist between the two conditions: OSA impairs cognitive function via intermittent hypoxia and sleep fragmentation, while cognitive decline may in turn disrupt sleep architecture, thus forming a vicious cycle. Large-sample and long-term longitudinal cohort studies are urgently required to clarify this complex interplay.

Second, imaging biomarkers lack standardization and external validation. Although emerging imaging biomarkers have shown promising application prospects, substantial variations in imaging parameters, analytical pipelines and threshold settings across studies reduce the comparability of results. To date, there are no unified operational specifications for these biomarkers, nor replications in independent external cohorts, which limits their clinical application.

Third, intervention studies are plagued by small sample sizes and inconsistent treatment adherence. Conventional therapies represented by CPAP can effectively alleviate nocturnal hypoxia and sleep fragmentation, yet the long-term adherence rate among patients is generally below 50%. A multicenter randomized controlled trial demonstrated that 12-month CPAP treatment significantly improved functional connectivity of the default mode network and cortical thickness, but failed to produce notable changes in Montreal Cognitive Assessment scores. This indicates that relieving upper airway obstruction alone may be insufficient to reverse established brain network damage, and a longer intervention period may be necessary. For non-invasive neuromodulation techniques, high-quality randomized controlled trials specifically targeting OSA patients are still scarce. Major shortcomings include small sample sizes, inconsistent stimulation parameters and a lack of long-term follow-up data.

Fourth, the causal relationship between the glymphatic system and brain networks remains unclear. Multiple studies have confirmed glymphatic dysfunction and aberrant brain networks in OSA patients, both of which are correlated with cognitive performance. However, how glymphatic dysfunction specifically affects the dynamic reorganization of brain networks, as well as the temporal sequence and causal pathways linking the two, needs to be further elucidated through longitudinal imaging studies and animal experiments.

4.2. Key Priorities for Future Research

This section proposes major research directions from three perspectives: the development of multimodal radiomics models, exploration of glymphatic system-targeted interventions, and implementation of relevant clinical trials.

4.2.1. Multimodal Radiomics Models and AI-Based Prediction

Transition from unimodal to multimodal integration: Most current studies evaluate OSA-related brain damage using a single imaging modality. Nevertheless, glymphatic dysfunction, abnormal dynamic brain networks and cerebral structural changes interact intricately, so a single modality cannot fully characterize the overall pathological features. Future research should integrate multimodal data including structural MRI, functional MRI and angiography to establish combined radiomics models. As commented by Jackson and Rosenzweig in *AJRCCM*, integrating high-density polysomnography with perivascular imaging enables direct verification of the arousal-vascular uncoupling hypothesis. Repeated respiratory event-related microarousals in OSA patients may impair norepinephrine-mediated slow vascular pulsation, thereby disrupting glymphatic function (Jackson & Rosenzweig, 2025).

Artificial intelligence-driven predictive models: The Sleep-Brain-Aging Vulnerability (SBAV) framework proposed by Sheikh Ibrahim further demonstrates the potential of multi-omics integration. This hierarchical model incorporates genomics, proteomics, endocrine biomarkers, EEG sleep microarchitecture and neuroimaging features. It improves the accuracy of identifying cognitive risks associated with OSA in female patients by 35%–42% compared with traditional AHI stratification. This paradigm indicates that future model development should fully account for heterogeneity in gender, age and genetic background (Sheikh Ibrahim, 2025).

4.2.2. Exploration of Glymphatic System-Targeted Interventions

Protective effects of CPAP on glymphatic function: Recent longitudinal studies have yielded compelling evidence that CPAP can ameliorate glymphatic function. A 4-year follow-up study by Jackson and Rosenzweig (2025) involving over 1,000 community participants demonstrated a dose-response relationship between OSA severity and reduced DTI-ALPS index. Patients with alleviated OSA presented a relative increase in ALPS index, and changes in this index mediated the association between AHI variations and alterations in visual memory. Additionally, Keil et al. (2026) reported that pCSF levels in CPAP-treated patients were comparable to those in healthy controls, while untreated patients had markedly elevated pCSF, which was positively correlated with Aβ deposition. Another study found that the volume of perivascular spaces in the basal ganglia remained stable among OSA patients with persistent CPAP adherence, whereas a significant progression was observed in the non-adherent group (Sommer et al., 2025). Collectively, these findings suggest that CPAP may slow the progression of cerebral small vessel disease by restoring glymphatic function.

Direct modulation techniques for glymphatic function: Conventional interventions act on the glymphatic system indirectly by relieving nocturnal hypoxia, while physical therapies targeting this system are emerging. An ongoing open-label study conducted at the Mayo Clinic (Mayo Clinic, n.d.) is the first to evaluate the efficacy of the Automated Manual Lymph Drainage Device

(AMLDT, Neuroglide) on glymphatic function in OSA patients. Primary outcome measures include changes in plasma Aβ42, Aβ40, Aβ42/Aβ40 ratio, phosphorylated tau 217 (p-tau-217), neurofilament light chain and glial fibrillary acidic protein. Eligible participants are required to have received stable CPAP treatment for no less than six months. This study aims to assess the incremental benefits of combining lymph drainage therapy with CPAP, and provide evidence for the "CPAP-plus" combined intervention strategy.

4.2.3. Biomarker Enrichment and Long-Term Follow-Up Clinical Trials

Biomarker enrichment strategies: A 12-month follow-up study by Frias et al. on patients with Alzheimer's disease comorbid with OSA found that cognitive decline progressed more slowly in individuals with good CPAP adherence compared with those with poor adherence. Baseline sleep architecture, sleep efficiency and sleeping posture were predictive of cognitive outcomes, indicating these parameters can serve as enrichment biomarkers to identify patients most likely to benefit from treatment (Frias et al., 2025). Ma et al. further demonstrated that plasma neurofilament light chain (NfL) outperformed Aβ-related biomarkers in distinguishing OSA patients with concomitant mild cognitive impairment (MCI). When combined with conventional indicators, its area under the curve (AUC) reached 0.907 (Ma et al., 2026). In future clinical trials, plasma NfL, glial fibrillary acidic protein (GFAP) and p-tau-217 can be incorporated into enrollment criteria or stratified randomization design to enhance statistical power.

Long-term follow-up and real-world evidence: Most existing intervention studies adopt a follow-up period of 3 to 12 months. However, the development and progression of OSA-related cognitive impairment is a chronic process. Randomized controlled trials with a follow-up duration of at least 2 to 3 years are warranted to clarify whether interventions can prevent progression to dementia. Meanwhile, pragmatic clinical trials based on real-world data should be conducted to evaluate long-term adherence and therapeutic effects of interventions under routine clinical settings.

5. Discussion and Conclusions

Research on the mechanisms and innovative interventions for cognitive impairment associated with obstructive sleep apnea has become a cutting-edge hotspot at the intersection of sleep medicine and neuroscience. This article reviews recent advances in this field, and the main conclusions are summarized as follows. First, glymphatic dysfunction and destabilization of dynamic functional brain networks are two core neuroimaging mechanisms underlying OSA-related cognitive impairment, with a well-established mediating coupling pathway between them. At the micro level, multimodal imaging evidence based on the DTI-ALPS index and pCSF mapping consistently confirms evident glymphatic impairment in OSA patients. A systematic review and meta-analysis by Ghaderi et al. reported a significant reduction in the DTI-ALPS index among patients with severe OSA relative to healthy controls, verifying substantial glymphatic dysfunction in this population (Ghaderi et al., 2025). Li et al. further found that patients with severe OSA exhibited markedly attenuated global and anterior BOLD-CSF coupling, which was closely correlated with cognitive decline. Notably, both cognitive function and cortical glymphatic function were significantly improved after effective treatment (Li et al., 2025). At the macro level, dynamic functional network

analyses have identified two unstable patterns in OSA patients: excessive dwell time in specific connectivity states and abnormal state transitions, accompanied by impaired dynamic reorganization of the default mode network, salience network and executive control network (Huang et al., 2023; Li et al., 2022; Wang et al., 2025). Mediation analyses have established a causal chain from glymphatic dysfunction to reduced network efficiency and subsequently to cognitive impairment (Xiong et al., 2024).

It is worth emphasizing that the association between glymphatic dysfunction and cognitive impairment is not unique to OSA. Recent systematic reviews and meta-analyses have demonstrated a consistent link between sleep disorders and impaired glymphatic clearance, with OSA exerting the strongest effect, which supports the dose-response relationship and relevant cognitive analyses (De la Herrán-Arita, 2026; Ghaderi et al., 2025; Wostyn & Nedergaard, 2026). A review by De la Herrán-Arita further regarded the glymphatic system as a key physiological bridge connecting sleep disturbances and the molecular pathogenesis of neurodegenerative diseases. Common clinical conditions including OSA, chronic insomnia and circadian rhythm disorders can fundamentally disrupt glymphatic clearance (De la Herrán-Arita, 2026). Collectively, the above evidence indicates that OSA-related glymphatic dysfunction ultimately leads to multidimensional cognitive deficits by compromising global brain network efficiency.

Second, continuous positive airway pressure (CPAP) yields limited and highly heterogeneous effects on cognitive function in OSA patients, while non-invasive neuromodulation techniques show promising potential as adjunct interventions. Although CPAP effectively corrects nocturnal hypoxia and sleep fragmentation, meta-analyses have revealed inconsistent cognitive improvements across studies (Lal et al., 2022). Simply alleviating upper airway obstruction is insufficient to reverse established brain network damage, creating an urgent need for complementary therapeutic approaches.

Represented by repetitive transcranial magnetic stimulation (rTMS) and transcranial direct current stimulation (tDCS), non-invasive brain stimulation (NIBS) can directly modulate neuronal excitability in targeted brain regions, enhance neural plasticity and regulate dynamic connectivity of large-scale brain networks. It provides a novel treatment option for OSA patients who are intolerant to CPAP or suffer from persistent cognitive impairment after CPAP therapy. A high-quality umbrella review by Wu et al. confirmed that NIBS, particularly rTMS and tDCS, significantly improves overall cognition, language ability, executive function and memory in patients with Alzheimer's disease and mild cognitive impairment (Wu et al., 2025).

In direct evidence from OSA populations, a randomized controlled trial by Han et al. demonstrated that iTBS applied over the left dorsolateral prefrontal cortex remarkably improved visual memory, sustained attention and working memory in OSA patients. The intervention also increased the relative power spectral density of theta and beta bands in the parietal, temporal and anterior brain regions, indicating that TMS ameliorates cognition by regulating cortical neural oscillations (Han et al., 2023). Future research should further explore the synergistic effects of NIBS combined with CPAP, as well as the potential mechanisms whereby NIBS restores glymphatic function indirectly via modulating sleep architecture.

Third, research on OSA-related cognitive impairment is evolving from the traditional hypoxia-brain injury paradigm toward an integrated diagnosis and treatment model featuring multimodal mechanism interpretation, targeted intervention and precise patient stratification. This paradigm shift is mainly driven by three factors. First, the rapid advancement of multimodal neuroimaging techniques enables systematic exploration of mechanisms ranging from glymphatic function to dynamic brain networks, and provides objective biomarkers for accurate identification of individuals at high risk of cognitive decline. Second, interventions targeting the glymphatic system and dynamic brain networks are progressing from theoretical research to clinical validation. Third, biomarker enrichment strategies are expected to enhance the statistical power and clinical translation efficiency of clinical trials. Future studies should prioritize large-sample, multicenter randomized controlled trials with a follow-up period of no less than 2 to 3 years, to clarify the efficacy of different interventions in preventing progression to dementia. Additionally, it is essential to develop multimodal radiomics prediction models integrating structural MRI, functional MRI and angiography, so as to facilitate precise stratified management of OSA-related cognitive impairment. The establishment of this new paradigm will lay a more solid theoretical foundation and offer practical approaches for the early identification and effective intervention of OSA-associated cognitive deficits.

Author Contributions:

Conceptualization, Z.F.Y.; methodology, Y.J.D.; resources, Z.F.Y.; data curation, Y.J.D. and W.K.Z.; writing ─ original draft preparation, Y.J.D. and W.K.Z.; writing ─ review and editing, Z.F.Y.; visualization, Y.J.D.; supervision, Z.F.Y.; project administration, Z.F.Y.; funding acquisition, Z.F.Y. All authors have read and agreed to the published version of the manuscript.

Funding:

The project is supported by the following grants:National Population Health Science Data Center, Chinese Academy of Medical Sciences (Grant No. NCMI202409A08).

Institutional Review Board Statement:

Not applicable.

Informed Consent Statement:

Not applicable.

Data Availability Statement:

No new data were created or analyzed in this study. Data sharing is not applicable to this article.

Acknowledgments:

The authors would like to thank all participants and staff who contributed to this study.

Conflict of Interest:

The authors declare no conflict of interest.

References

Allen, E. A., Damaraju, E., Plis, S. M., et al. (2014). Tracking whole-brain connectivity dynamics in the resting state. Cerebral Cortex, 24(3), 663–676.

Begemann, M. J., Brand, B. A., Ćurčić-Blake, B., et al. (2020). Efficacy of non-invasive brain stimulation on cognitive functioning in brain disorders: A meta-analysis. Psychological Medicine, 50(15), 2465–2486.

Benjafield, A. V., Ayas, N. T., Eastwood, P. R., et al. (2019). Estimation of the global prevalence and burden of obstructive sleep apnoea: A literature-based analysis. The Lancet Respiratory Medicine, 7(8), 687–698.

Benveniste, H., Liu, X., Koundal, S., et al. (2019). The glymphatic system and waste clearance with brain aging: A review. Gerontology, 65(2), 106–119.

Bradley, T. D., & Floras, J. S. (2009). Obstructive sleep apnoea and its cardiovascular consequences. The Lancet, 373(9657), 82–93.

Calhoun, V. D., Miller, R., Pearlson, G., et al. (2014). The chronnectome: Time-varying connectivity networks as the next frontier in fMRI data discovery. Neuron, 84(2), 262–274.

Coughlin, S. R., Mawdsley, L., Mugarza, J. A., et al. (2004). Obstructive sleep apnoea is independently associated with an increased prevalence of metabolic syndrome. European Heart Journal, 25(9), 735–741.

De la Herrán-Arita, A. K. (2026). When sleep fails, brain clearance suffers: The role of glymphatic impairment in clinical neurology. Acta Neurologica Belgica, 126(3), 783–792.
https://doi.org/10.1007/s13760-025-02959-w

Durtette, A., Dargent, B., Gierski, F., et al. (2024). Impact of continuous positive airway pressure on cognitive functions in adult patients with obstructive sleep apnea: A systematic review and meta-analysis. Sleep Medicine, 123, 7–21.

Frias, C. L., Almeria, M., Castejon, J., Artero, C., Caruana, G., Elias-Mas, A., Uscamaita, K., Hawkins, V., Ray, N. J., Buongiorno, M., Cullell, N., & Krupinski, J. (2025). A pilot study: The effect of CPAP intervention on sleep architecture and cognition in Alzheimer's disease patients with obstructive sleep apnea. Neurology International, 17(9), Article 147. https://doi.org/10.3390/neurolint17090147

Ghaderi, S., Mohammadi, S., & Fatehi, F. (2025). Glymphatic pathway dysfunction in severe obstructive sleep apnea: A meta-analysis. Sleep Medicine, 131, 106528.

Greenstone, M., & Hack, M. (2014). Obstructive sleep apnoea. BMJ, 348, g3745.

Guidelines for the diagnosis and treatment of obstructive sleep apnea hypopnea syndrome (revised 2011). (2012). In Proceedings of the 4th Northeast China Academic Conference on Respiratory Diseases & the 11th Annual Conference of Jilin Society of Respiratory Diseases (pp. 67–70).

Gurbani, N., Naismith, S., Rosenzweig, I., et al. (2025). Should we treat sleep apnoea to prevent dementia? Current Treatment Options in Neurology, 27(1), 26.

Han, X., Cai, S., Gui, H., et al. (2023). Transcranial magnetic stimulation cortical oscillations and improve cognition in obstructive sleep apnea patients. Brain and Behavior, 13(4), e2958.

Hassan Mohmmed Ahmed, A. F., Emam Mohamed Ahmed, N. M. A., Abdulwahid Elsamany, A. A., et al. (2025). The role of sleep disturbances in Alzheimer's disease progression: A systematic review. Cureus, 17(6), e86450.

He, Z., & Sun, J. (2025). Clearance mechanisms of the glymphatic/lymphatic system in the brain: New therapeutic perspectives for cognitive impairment. Cognitive Neurodynamics, 19(1), 111.

Huang, Y., Shen, C., Zhao, W., et al. (2023). Multilayer network analysis of dynamic network reconfiguration in patients with moderate-to-severe obstructive sleep apnea and its association with neurocognitive function. Sleep Medicine, 112, 333–341.

Jackson, M. L., & Rosenzweig, I. (2025). Perivascular dynamics, sleep apnea, and memory: Interpreting a moving target. American Journal of Respiratory and Critical Care Medicine, 211(12), 2244–2246.

Keil, S. A., Li, Y., Krieger, A. C., et al. (2026). Increased MRI-derived parenchymal cerebral spinal fluid mapping in untreated obstructive sleep apnea patients. Neurobiology of Disease, 221, 107325.

Lal, C., Ayappa, I., Ayas, N., et al. (2022). The link between obstructive sleep apnea and neurocognitive impairment: An official American thoracic society workshop report. Annals of the American Thoracic Society, 19(8), 1245–1256.

Li, H., Li, L., Li, K., et al. (2022). Abnormal dynamic functional network connectivity in male obstructive sleep apnea with mild cognitive impairment: A data-driven functional magnetic resonance imaging study. Frontiers in Aging Neuroscience, 14, 977917.

Li, Y., Lin, S., Guo, Z., et al. (2025). Decoupling of global signal and cerebrospinal fluid inflow is associated with cognitive decline in patients with obstructive sleep apnoea. Sleep Medicine, 129, 330–338.

Liu, G., Yang, C., Wang, X., et al. (2023). Oxygen metabolism abnormality and Alzheimer's disease: An update. Redox Biology, 68, 102955.

Ma, L., Liu, N., Feng, Y., et al. (2026). Exploration of plasma biomarkers of neurodegeneration in obstructive sleep apnea-related mild cognitive impairment. Clinical Otolaryngology, 51(1), 92–100.

Mayo Clinic. (n.d.). A study of automated manual lymphatic drainage therapy for obstructive sleep apnea. https://www.mayo.edu/research/clinical-trials/cls-20597241

Nepozitek, J., Marecek, S., Rottova, V., et al. (2025). Glymphatic dysfunction evidenced by DTI-ALPS is related to obstructive sleep apnea intensity in newly diagnosed Parkinson's disease. npj Parkinson's Disease, 11(1), 160.

Niu, Y., Sun, S., Wang, Y., et al. (2025). Spatiotemporal trends in the prevalence of obstructive sleep apnoea across China: A multilevel meta-analysis incorporating geographic and demographic stratification (2000-2024). Nature and Science of Sleep, 17, 879–903.

Preti, M. G., Bolton, T. A., & Van De Ville, D. (2017). The dynamic functional connectome: State-of-the-art and perspectives. NeuroImage, 160, 41–54.

Rektorová, I., Pupíková, M., Fleury, L., et al. (2025). Non-invasive brain stimulation: Current and future applications in neurology. Nature Reviews Neurology, 21(12), 669–686.

Ren, Y., Chen, S., Wang, H., et al. (2025). Unraveling the bidirectional links between obstructive sleep apnea and mild cognitive impairment: A systematic review and meta-analysis. Sleep Medicine, 132, 106562.

Rosenzweig, I., Glasser, M., Polsek, D., et al. (2015). Sleep apnoea and the brain: A complex relationship. The Lancet Respiratory Medicine, 3(5), 404–414.

Rotenberg, B. W., Murariu, D., & Pang, K. P. (2016). Trends in CPAP adherence over twenty years of data collection: A flattened curve. Journal of Otolaryngology - Head & Neck Surgery, 45(1), 43.

Sawyer, A. M., Gooneratne, N. S., Marcus, C. L., et al. (2011). A systematic review of CPAP adherence across age groups: Clinical and empiric insights for developing CPAP adherence interventions. Sleep Medicine Reviews, 15(6), 343–356.

Sheikh Ibrahim, H. (2025). SBAV: A sex-stratified precision framework for predicting sleep apnea–driven neurodegeneration in aging women [Conference abstract]. Innovation in Aging, 9(Suppl. 2), igaf122.4257. https://doi.org/10.1093/geroni/igaf122.4257

Shine, J. M., Bissett, P. G., Bell, P. T., et al. (2016). The dynamics of functional brain networks: Integrated network states during cognitive task performance. Neuron, 92(2), 544–554.

Sommer, R., Hill, E. A., Ramirez, J., et al. (2025). Continuous positive airway pressure and progression of enlarged perivascular spaces in adults with obstructive sleep apnea. Neurology, 105(8), e213955.

Wang, J., Wang, Z., Wang, X., et al. (2025). Altered brain dynamic functional connectivity in patients with obstructive sleep apnea and its association with cognitive performance. Sleep Medicine, 128, 174–182.

Wostyn, P., & Nedergaard, M. (2026). Ocular glymphatic dysfunction as a potential link between obstructive sleep apnea and retinal structural changes. Comment on Pusic Sesar et al. Multimodal assessment of ocular parameters in patients with severe obstructive sleep apnea with emphasis on retinal structural changes. Life 2025, 15, 1307. Life, 16(2), Article 214. https://doi.org/10.3390/life16020214

Wu, M., Song, W., Wang, X., et al. (2025). Efficacy of non-invasive brain stimulation interventions on cognitive impairment: An umbrella review of meta-analyses of randomized controlled trials. Journal of NeuroEngineering and Rehabilitation, 22(1), 22.

Xiong, Z., Bai, M., Wang, Z., et al. (2024). Resting-state fMRI network efficiency as a mediator in the relationship between the glymphatic system and cognitive function in obstructive sleep apnea hypopnea syndrome: Insights from a DTI-ALPS investigation. Sleep Medicine, 119, 250–257.

Yankova, G., Bogomyakova, O., & Tulupov, A. (2021). The glymphatic system and meningeal lymphatics of the brain: New understanding of brain clearance. Reviews in the Neurosciences, 32(7), 693–705.

Yao, L., Wang, Y., Gao, Y., Gao, H., & Guo, X. (2023). The role of the fronto-parietal network in modulating sustained attention under sleep deprivation: An functional magnetic resonance imaging study. Frontiers in Psychiatry, 14, Article 1289300. https://doi.org/10.3389/fpsyt.2023.1289300

Yi, H. J., Liao, X. Y., Pi, M. Y., et al. (2023). Establishment of a new telemedicine-based model for the diagnosis and treatment of obstructive sleep apnea: Study protocol for a non-inferiority randomized controlled trial. Chinese General Practice, 26(3), 380–385.

Yu, R., Li, Y., Zhao, K., et al. (2025). The contributions of resting-state functional-MRI studies to our understanding of male patients with obstructive sleep apnea: A systematic review. Frontiers in Neurology, 16, 1532037.

Yu, S., Wang, S., & Sun, H. (2024). Effects of repetitive transcranial magnetic stimulation on inhibitory control in first-episode schizophrenia: Behavioral and neural mechanisms. Frontiers in Psychiatry, 15, Article 1496562. https://doi.org/10.3389/fpsyt.2024.1496562

Zalesky, A., Fornito, A., Cocchi, L., et al. (2014). Time-resolved resting-state brain networks. Proceedings of the National Academy of Sciences of the United States of America, 111(28), 10341–10346.

Zhang, X., Xu, H., Yin, S., et al. (2025). Obstructive sleep apnea and memory impairments: Clinical characterization, treatment strategies, and mechanisms. Sleep Medicine Reviews, 81, 102092.

Zhao, X., Liu, J., Shao, Z., Liu, X., Wang, Z., Yuan, K., Zhang, B., Li, Y., Sheng, X., Zhu, Y., & Guo, Y. (2024). Restoration of abnormal sleep EEG power in patients with insomnia disorder after 1Hz rTMS over left DLPFC. Frontiers in Psychiatry, 15, Article 1431837. https://doi.org/10.3389/fpsyt.2024.1431837

License: Copyright (c) 2026 Author.
All articles published in this journal are licensed under the Creative Commons Attribution 4.0 International License (CC BY 4.0). This license permits unrestricted use, distribution, and reproduction in any medium, provided the original author(s) and source are properly credited. Authors retain copyright of their work, and readers are free to copy, share, adapt, and build upon the material for any purpose, including commercial use, as long as appropriate attribution is given.

Advances in World Medical Research, 2026, 2(3), 20-31
https://doi.org/10.71204/qbf0ba53

In silico Identification of Potential Hepatitis B Virus HBx Inhibitors Through Molecular Docking Analysis

Maryam Aliza [1, *], Bibi Haleema [2]

[1] Department of Bioinformatics, The Islamia University of Bahawalpur, Bahawalpur 63100, Pakistan

[2] Department of Genomics and Bioinformatics, Cholistan University of Veterinary and Animal Sciences, Bahawalpur 63100, Pakistan

*** Correspondence**:

Maryam Aliza

alizamaryam4678@gmail.com

Received: 16 August 2026/ Accepted: 25 September 2026/ Published online: 30 September 2026

Abstract

Hepatitis B virus (HBV) remains a major contributor to chronic liver disease worldwide and represents a significant global health challenge. The HBx protein plays an important role in HBV replication and viral pathogenesis and is therefore considered a promising therapeutic target. In the present study, an in silico molecular docking approach was employed to identify potential HBx inhibitors from a selected group of fourteen compounds. The three-dimensional structure of the HBx protein was predicted using the I-TASSER server, and the selected compounds were subjected to molecular docking using PyRx and AutoDock Vina. The docking results revealed that several compounds exhibited favorable predicted binding affinities toward HBx, with SC75741 showing the most favorable docking score (−9.8 kcal/mol), followed by Rutin (−9.1 kcal/mol), Cynarin (−8.6 kcal/mol), and Ledipasvir (−8.4 kcal/mol). Notably, Cynarin, which is not currently an approved anti-HBV drug, demonstrated a favorable docking score and interactions with several important HBx residues, highlighting its potential as a candidate lead compound for further investigation. Overall, the findings suggest that the identified compounds, particularly SC75741, Rutin, Cynarin, and Ledipasvir, may serve as potential candidates for HBx-targeted anti-HBV drug discovery.

Keywords: Hepatitis; Bioinformatics; HBV; HBx; Computational Drug Design

1. Introduction

Hepatitis B virus (HBV) is a member of the *Hepadnaviridae* family of enveloped DNA viruses (Hamadalnil & Altayb, 2024). Acute hepatitis caused by HBV infection can develop into chronic hepatitis B, liver fibrosis, cirrhosis, and hepatocellular carcinoma (Saeed et al., 2023). Chronic HBV infections increase the risk of liver cancer and cirrhosis and are therefore considered a silent

killer disease (Ahmadi et al., 2024). HBV is a partially double-stranded DNA virus. Nine genotypes, A to I, and a potential tenth genotype, J, have been identified; full-genome analysis indicates that these genotypes differ by more than 8% (Velkov et al., 2018). According to a worldwide genotypic study, genotypes C (26%), D (22%), E (18%), A (14%), and B (11%) are responsible for 96% of chronic HBV infections (Velkov et al., 2018).

Four copies of the viral mRNA are translated into seven proteins: three surface proteins (S, M, and L), polymerase (P), core protein or capsid (C), additional protein (e), and transactivator X protein (Mohebbi et al., 2023). Of the four HBV open reading frames that partially overlap, the HBx gene is the smallest. It encodes a regulatory protein of 154 amino acids and a molecular mass of 17 kDa and is composed of 452 nucleotides (Pathak et al., 2014). HBV can remain undetectable for long periods, resulting in progressive immune-mediated liver damage (Baei et al., 2025). Since HBV can progress slowly over decades, not everyone infected with the virus develops symptoms. Some individuals may experience nausea, vomiting, fever, dark urine, tremors, low appetite, jaundice, blood in the stool, and diarrhea (Gholizadeh et al., 2023).

Hepatitis B spreads when the blood or seminal fluid of an infected person enters another person’s body (Rizzo et al., 2022). HBV is mostly transmitted through contact with contaminated blood or body fluids, breastfeeding by an infected person, travel to regions with high HBV infection rates, sharing personal items, sharing needles, and exposure among drug users and medical staff (Tufon et al., 2019). During delivery, HBV can also be transferred from an infected mother to a newborn (Naderi et al., 2023). According to the World Health Organization's (WHO) 2024 Global Hepatitis Report, there are 254 million people living with HBV worldwide, with an estimated 1.2 million new HBV infections occurring annually (Ugbaja et al., 2025). Iran is one of the countries where HBV prevalence is low to medium (2.2%). Currently, Pakistan and Egypt account for almost 80% of the worldwide hepatitis burden.

The entire HBV virion consists of a nucleocapsid containing relaxed circular DNA (rcDNA) and an outer membrane layer. Heparan sulfate proteoglycans and sodium taurocholate co-transporting polypeptide (NTCP) interact sequentially with HBV to facilitate infection of hepatocytes (Ko et al., 2018). Following fusion of the viral and cellular membranes, the viral particle is internalized through endocytosis. The viral capsid is released into the cytoplasm and transported through endosomal regions and cytosol by the nuclear pore (Hu et al., 2019) . The HBV X protein (HBx) is necessary for HBV replication (Tsukuda & Watashi, 2020). Cell invasion and proliferation are influenced by several signaling pathways that are affected by HBx. HBx contributes to oncogenesis in addition to chromosomal instability and viral replication. It regulates oxidative stress, migration, angiogenesis, oncogenesis, and DNA methylation (Shaikh et al., 2022).

Unfortunately, most approved anti-HBV medications have certain therapeutic limitations despite their efficacy (Martyn et al., 2023). Long-term use of HBV polymerase inhibitors and nucleotide analogs (lamivudine, adefovir, entecavir) can lead to drug resistance with mutations in the Pol "Tyr-Met-Asp-Asp (YMDD)" motif; some patients experience adverse effects from interferon (pegIFN-α) treatment (Parvez et al., 2019).

2. Materials and Methods

2.1. Sequence Retrieval

The FASTA sequence of the target protein was retrieved from UniProtKB using the accession number Q69027, corresponding to the HBV protein X of genotype C subtype ayr (UniProt Consortium, 2021). The protein consists of 154 amino acids. After downloading the sequence in FASTA format, it was submitted to the I-TASSER server for structure prediction.

2.2. Structure Prediction

The three-dimensional (3D) structure of the HBx protein was predicted using I-TASSER, which predicts stable and accurate protein structure (Yang et al., 2015). The FASTA sequence was provided as the input. Among the five candidate models generated by the server, the model with the highest C-score was selected as the best-predicted structure. The protein was subsequently processed using SWISS-PDB Viewer to clean the structure, and the cleaned protein structure was saved for molecular docking analysis.

2.3. Ligand Preparation

The selected natural compounds were retrieved from the PubChem database (Kim et al., 2023), an open repository maintained by the National Center for Biotechnology Information (NCBI) that provides comprehensive information on chemical structures and their biological activities (Schoch et al., 2020).

To generate 3D structures, the canonical SMILES (Simplified Molecular Input Line Entry System) notation of each compound was obtained from PubChem and entered into ChemDraw software. ChemDraw was used to generate the corresponding 2D structure and 3D conformations for further analysis. The energy of each ligand was minimized using the Molecular Mechanics 2 (MM2) force field to optimize bond angles, torsional angles, and bond lengths, thereby obtaining a low-energy and more stable molecular conformation. The energy-minimized structures were then saved in PDB format. Subsequently, the energy-minimized 3D structures were imported into PyRx, where the Open Babel module was used to further prepare the ligands and convert them into PDBQT format for molecular docking (Dallakyan & Olson, 2015).

2.4. Molecular Docking

Molecular docking was performed after preparing of the protein and ligand structures to identify compounds with the strongest binding affinity towards the target protein. PyRx, an open-source virtual screening platform that utilizes AutoDock Vina, was used for the docking analysis (Che et al., 2023; Kanwal et al., 2017). The prepared HBx structure was used as the receptor, while the selected compounds were used as ligands. Blind docking was subsequently performed by setting a grid box that surrounded the entire HBx protein structure. This approach ensured that all potential binding pockets were explored during docking, allowing potential active sites to be identified. The best docking pose for each ligand was selected based on the lowest binding energy (kcal/mol) score. Lowest binding energy values indicate stronger predicted interactions between the ligand and target protein.

The docking results were further analyzed and visualized using Discovery Studio Visualizer to characterize the interactions between the ligand and the protein binding site (Baroroh et al., 2023). Molecular interactions, including hydrogen bonds, hydrophobic interactions, and van der Waals forces, were determined to analyze the binding pose and predicted stability of the ligand-protein complexes.

3. Results

3D structure of HBx was predicted using the I-TASSER server. The final protein structure obtained after cleaning was used for evaluating the binding affinities of the selected antiviral compounds against the HBx protein (Figure 1).

The predicted structure of the protein was validated by using multiple structural assessment tools, like ERRAT, Verify3D, and PROCHECK, to evaluate the overall quality and consistency (Figure 2 (a,b) (Patil et al., 2025). These methods of assessment assess the non-bonded atomic interactions, sequence-structure compatibility, and chiral fidelity of the model, confirming its relevance for ensuing computational analysis (Table 1) (Rasool et al., 2018). The Ramachandran plot analysis showed that 98% of residues were located in favored regions and only 30 residues were in disallowed regions.

A total of fourteen ligands were selected for molecular docking analysis against the HBx protein (Figure 3). The optimized ligand structures were later used for molecular docking to evaluate their binding affinity. The selected fourteen compounds were subjected to molecular docking against the HBx protein using PyRx. The binding affinities of the docked complexes were analyzed, and the compounds were ranked according to their docking scores from strongest to weakest binding. Among the screened compounds, SC75741 showed the strongest binding affinity towards the HBx protein. The binding energies of docked compounds are displayed in Table 2.

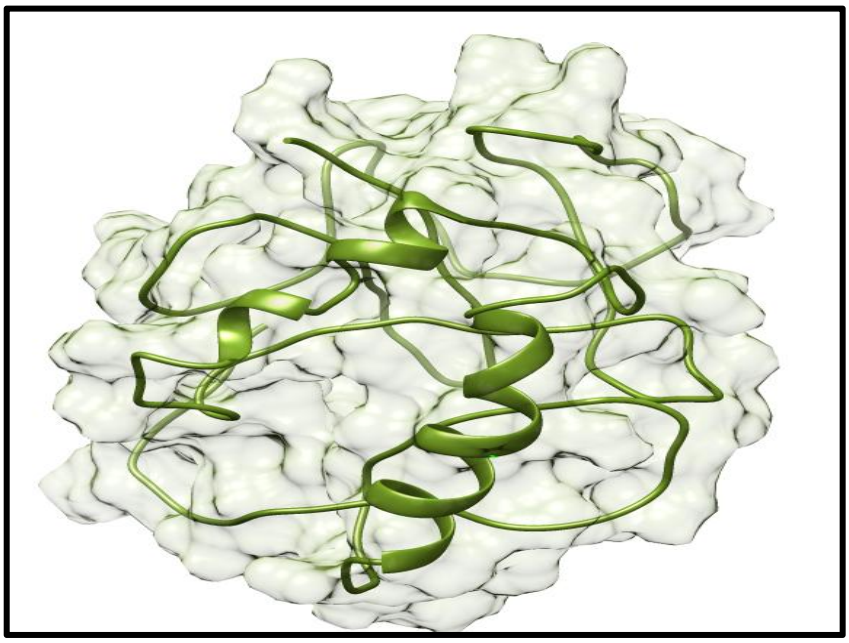


Figure 1. 3D predicted structure of HBx protein

Table 1. Results of structure validation

Analyses	Values
Overall quality factor	60.6897%
Compatibility	89.61%
Allowed region	89.7%

Table 2. Binding energies of docked compounds against HBx

Rank	Compounds	Binding energy (Kcal/mol)	classification
1	Sc75741	-9.8	Strong binder
2	Bilobetin	-9.6	Strong binder
3	Rutin	-9.1	Strong binder
4	Cynarin	-8.6	Strong binder
5	Ledipasvir	-8.4	Strong binder
6	Oleanolic acid	-8.2	Strong binder
7	Luteoline	-8.2	Strong binder
8	Betulinic acid	-7.6	Moderate binder
9	Ellagic acid	-7.3	Moderate binder
10	Resveratrol	-7.1	Moderate binder
11	Curcumin	-6.8	Moderate binder
12	Turmerone	-6.4	Moderate binder
13	Lamivudine	-5.4	Weak binder
14	1,8-cineole (Eucalyptol)	-5.2	Weak binder

The docking analysis demonstrated differences in the predicted binding affinities among the fourteen compounds, indicating variation in their interactions with the HBx binding region. Compounds exhibiting more favorable docking scores were considered to have stronger predicted binding interactions with the target protein and were therefore prioritized for further interaction analysis. The docked complexes of all fourteen compounds were imported into BIOVIA Discovery Studio Visualizer for detailed interaction profiling. Visualization of each complex in both three-dimensional (3D) and two-dimensional (2D) interaction modes revealed the specific amino acid residues of HBx involved in hydrogen bonding, hydrophobic contacts, π–π stacking, and van der Waals interactions with each ligand (Table 3; Figure 4).

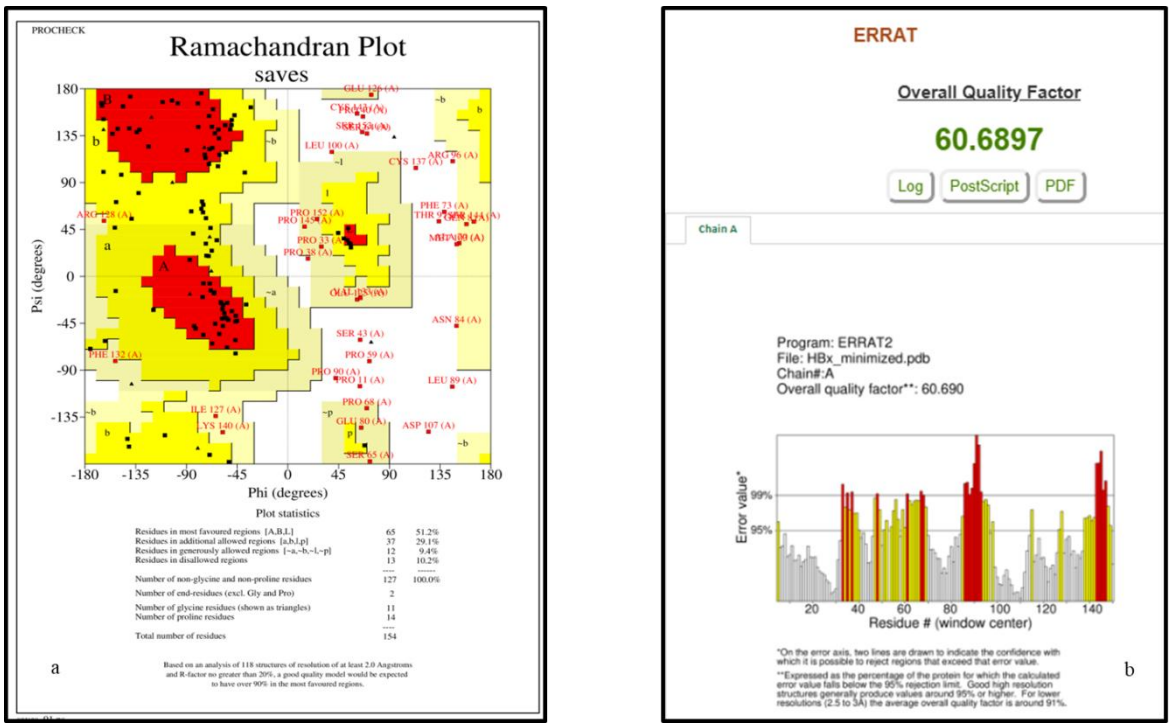


Figure 2. a) Ramachandran plot and b) ERRAT graph of predicted structure

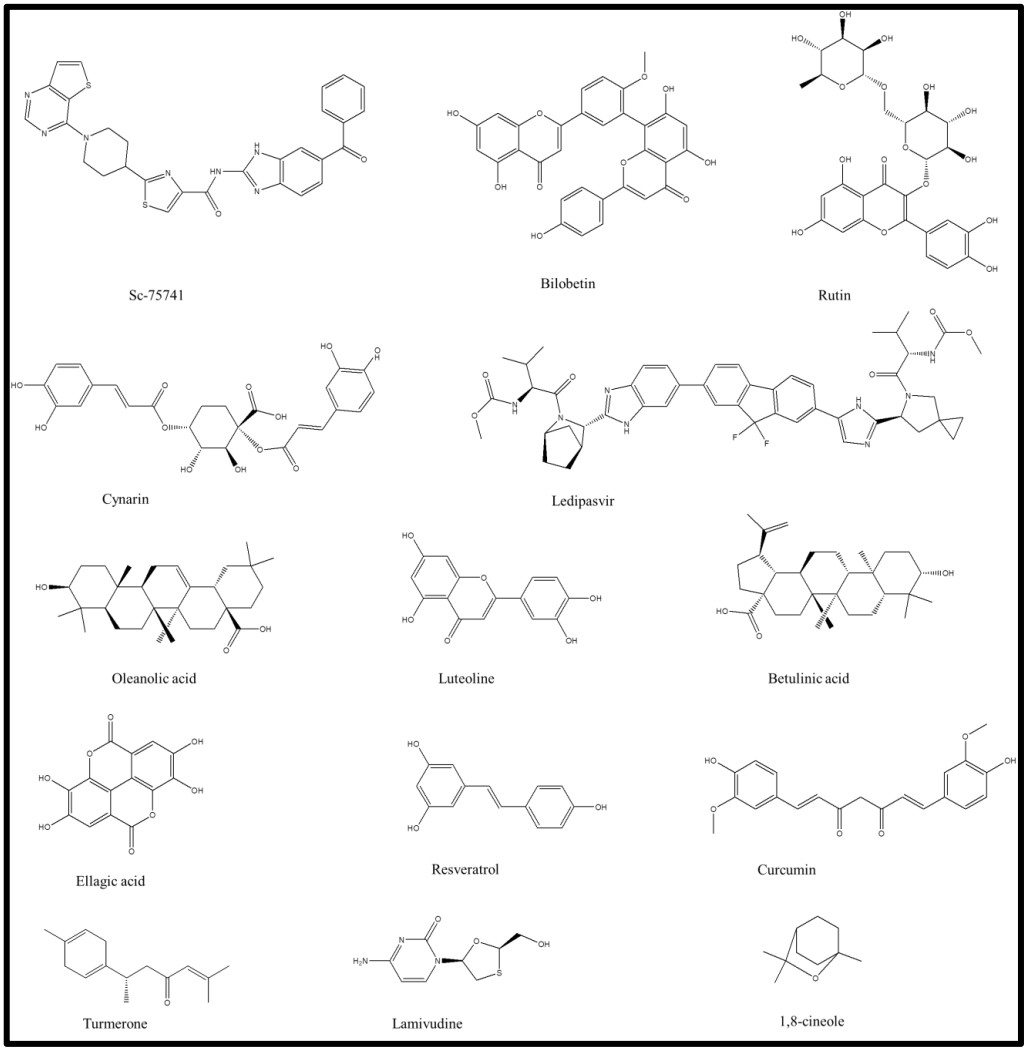


Figure 3. Two-dimensional chemical structures of the fourteen ligands

The interaction analysis provided additional structural insights into the predicted binding modes of the selected compounds. The identification of multiple types of non-covalent interactions helped characterize the ligand-binding patterns and provided a basis for comparing the binding modes of the fourteen compounds. In particular, the interaction profile of SC75741 was further examined to identify the residues and intermolecular interactions potentially contributing to its favorable docking score. Interestingly, it was observed that all the screened compounds bound at a similar binding site (Table 3).

Table 3. Interacting residues of HBx for all complexes

Rank	Compounds	Residues
1	Sc 75741	Leu-9, Asp-10, Arg-13, Val-15, Thr-74, Ala-767, Ser-78, Ile-127, Arg-128, Leu-129, Pro-147, Cys-148, Pro-152, Ser-153
2	Bilobetin	Cys-7, Gln-8, Leu-9, Arg-13, Val-15, Cys-17, Thr-74, Ser-75, Ala-76, Ser-78, Ile-127, Arg-128, Leu-129, Cys-143, Ser-144, Pro-145, Phe-150, Phe-151, Pro-152,
3	Rutin	Leu-9, Asp-10, Arg-13, Arg-72, Thr-74, Ala-76, Arg-77, Ser-78, Ile-127, Arg-128, Leu-129, Lys-130, Ser-144, Pro-145, Pro-152
4	Cynarin	Leu-9, Asp-10, Arg-13, Val-15, Ala-62, Phe-63, Ser-64, Arg-72, Thr-74, Ala-76, Ser-78, Ile-127, Arg-128, Leu-129, Lys-130, Phe-132, Arg-138, His-139, Ser-144,
5	Ledipasvir	Leu-9, Asp-10, Pro-11, Ala-12, Arg-13, Val-15, Pro-36, Pro-38, Thr-74, Ser-75, Ala-76, Ile-127, Arg-128, Leu-129, Lys-130, Ser-144, Pro-145, Pro-152, Ser-153
6	Oleanolic acid	Leu-9, Arg-13 Val-15, Thr-74, Ala-76, Ile-127, Arg-128, Leu-129, Pro-152, Ser-153
7	Luteoline	Leu-9, Arg-13 Val-15, Arg-72, Thr-74, Ala-76, Ser-78, Ile-127, Arg-128, Leu-129, Lys-130, Ser-144, Pro-145, Pro-152
8	Buetulinic acid	Leu-9, Asp-10, Arg-13 Val-15, Thr-74, Ser-75, Ala-76, Ile-127, Arg-128, Leu-129, Pro-147, Cys-148, Pro-152, Ser-153
9	Ellagic acid	Cys-7, Leu-9, Asp-10, Arg-13, Val-15, Cys-17, Thr-74, Ser-75, Ala-76, Arg-128, Pro-152, Ser-153
10	Resveratrol	Leu-9, Arg-13, Val-15, Arg-72, Thr-74, Ala-76, Ser-78, Ile-127, Arg-128, Leu-129, Lys-130, Ser-144, Pro-145, Cys-148, Pro-152
11	Curcumin	Leu-9, Arg-13, Val-15, Ala-76, Ser-78, Ile-127, Arg-128, Leu-129, Cys-143, Ser-144, Pro-145, Cys-148, Pro-152
12	Turmerone	Leu-9, Thr-74, Ala-76, Ser-78, Ile-127, Arg-128, Leu-129, Lys-130, Ser-144, Pro-145, Pro-152
13	Lamivudine	Arg-13, Val-15, Ala-76, Ser-78, Ile-127, Arg-128, Leu-129, Ser-144, Pro-145, Ala-146, Pro-147, Cys-148, Pro-152
14	1,8-cineole (Eucalyptol)	Cys-7, Leu-9, Arg-13, Val-15, Thr-74, Ser-75, Ala-76, Leu-129, Ser-153

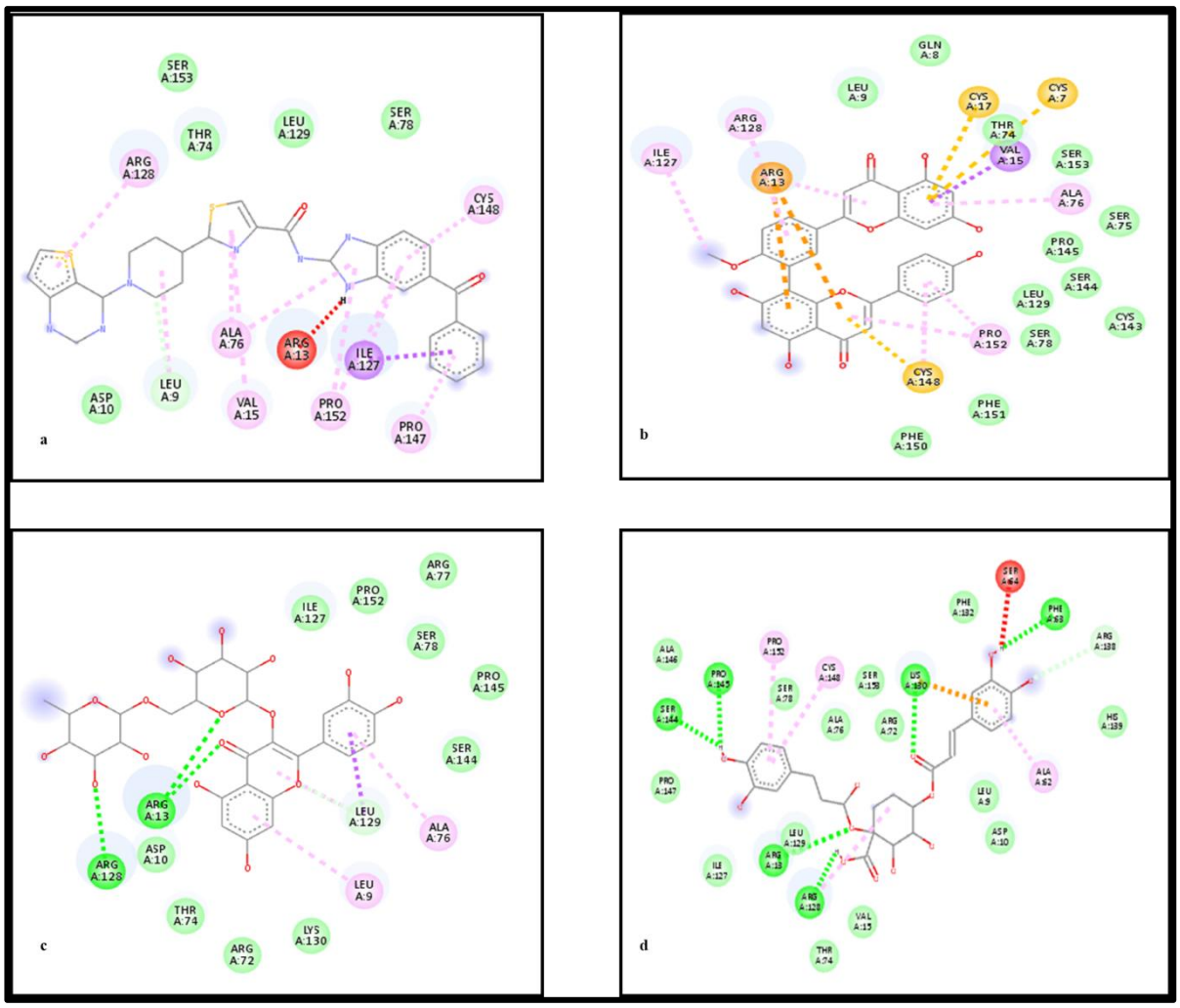


Figure 4. Two-dimensional interactions of a) Sc757241 – HBx complex, b) Bilobetin – HBx complex, c) Rutin – HBx complex and d) Cynarin – HBx complex.

4. Discussion

The present study investigates the inhibitory potential of selected natural compounds against the HBx protein using molecular docking. HBx plays a key role in HBV replication and is a multifunctional regulatory protein involved in the progression of hepatocellular carcinoma and viral chronicity, making it a high-valuecandidate for therapeutic targeting. Molecular docking showed that SC75741 (-9.8 Kcal/mol), Bilobetin (-9.6 Kcal/mol), Rutin (-9.1 Kcal/mol), Cynarin (-8.6 Kcal/mol), and Ledipasvir (-8.4 Kcal/mol) exhibited the strongest binding affinities towards the HBx protein. These compounds were therefore classified as strong binders to HBX. Lamivudine (-5.4 Kcal/mol), 1,8-cineole (-5.2 Kcal/mol) showed the weakest binding affinities. Lower binding energy values indicated more favorable predicted protein-ligand interactions.

The protein-ligand interaction analysis further supported the docking results. Several common amino acid residues were identified among the top-ranked compounds, including Leu-9, Arg-13, Val-15, Thr-74, Ala-76, Ile-127, Arg-128, Leu-129, Pro-152, and Ser-153. These residues may play key roles in ligand binding within the binding pockets of HBx. The repeated occurrence of these residues in the binding profiles of the top-ranked ligands suggests that they may represent an important binding region within the HBx protein. The existence of hydrophobic interactions

and hydrogen bonds may contribute to the stability of the ligand-protein complexes and potentially explain the favorable binding energies noted for the leading compounds.

Among the selected compounds, Cynarin displayed distinct binding capability, with a favorable binding energy of -8.6 Kcal/mol. It interacted with many key residues participating in binding interactions, including Leu-9, Arg-13, Thr-74, Arg-128, Leu-129, Pro-152, and Ser-153. Cynarin is not currently an approved drug for the treatment of HBV infection; its binding energy and interaction profile suggest that it could serve as a promising lead compound for the development of novel HBx inhibitors.

The findings of the present study are consistent with previous computational studies that have identified HBx as an attractive molecular target for anti-HBV drug discovery. The identification of favorable binding interactions between the selected compounds and HBx provides a basis for further computational and experimental investigations aimed at developing effective HBx-targeted therapies for HBV infection.

5. Conclusion

This study identified potential inhibitors of the HBx protein through molecular docking analysis. Among the fourteen compounds evaluated, SC75741, Bilobetin, Rutin, Cynarin, and Ledipasvir exhibited the strongest binding affinities and favorable interactions with key HBx residues. Cynarin showed promising binding characteristics despite not being an approved anti-HBV drug, highlighting its potential as a novel lead compound. These findings provide a basis for further computational and experimental studies to validate the inhibitory activity and therapeutic potential of these compounds against the HBx protein.

Author Contributions:

Conceptualization, M.A.; methodology, B. H.; resources, M.A.; data curation, B. H.; writing—original draft preparation, M.A. and B. H.; writing—review and editing, M.A.; visualization, B. H.; supervision, M.A.; project administration, M.A.; funding acquisition, M.A. All authors have read and agreed to the published version of the manuscript.

Funding:

This research received no external funding.

Institutional Review Board Statement:

Not applicable.

Informed Consent Statement:

Not applicable.

Data Availability Statement:

Not applicable.

Acknowledgments:

The authors gratefully acknowledge the support of the Department of Genomics and Bioinformatics, CUVAS, throughout the study.

Conflict of Interest:

The authors declare no conflict of interest.

References

Ahmadi, N., Aghasadeghi, M., Hamidi-Fard, M., Motevalli, F., & Bahramali, G. (2024). Reverse vaccinology and immunoinformatic approach for designing a bivalent vaccine candidate against hepatitis A and hepatitis B viruses. Molecular Biotechnology, 66(9), 2362–2380. https://doi.org/10.1007/s12033-023-00867-z

Baei, B., Askari, P., Askari, F. S., Kiani, S. J., & Mohebbi, A. (2025). Pharmacophore modeling and QSAR analysis of anti-HBV flavonols. PLOS ONE, 20(1), Article e0316765. https://doi.org/10.1371/journal.pone.0316765

Baroroh, U., Muscifa, Z. S., Destiarani, W., Rohmatullah, F. G., & Yusuf, M. (2023). Molecular interaction analysis and visualization of protein-ligand docking using Biovia Discovery Studio Visualizer. Indonesian Journal of Computational Biology, 2(1), 22 – 30. https://doi.org/10.24198/ijcb.v2i1.46322

Che, X., Liu, Q., & Zhang, L. (2023). An accurate and universal protein-small molecule batch docking solution using AutoDock Vina. Results in Engineering, 19, Article 101335. https://doi.org/10.1016/j.rineng.2023.101335

Dallakyan, S., & Olson, A. J. (2015). Small-molecule library screening by docking with PyRx. In J. E. Hempel, C. H. Williams, & C. C. Hong (Eds.), Chemical biology: Methods and protocols (Methods in Molecular Biology, Vol. 1263, pp. 243 – 250). Springer. https://doi.org/10.1007/978-1-4939-2269-7_19

Gholizadeh, O., Akbarzadeh, S., Ghazanfari Hashemi, M., Gholami, M., Amini, P., Yekanipour, Z., Tabatabaie, R., Yasamineh, S., Hosseini, P., & Poortahmasebi, V. (2023). Hepatitis A: Viral structure, classification, life cycle, clinical symptoms, diagnosis error, and vaccination. Canadian Journal of Infectious Diseases and Medical Microbiology, 2023, Article 4263309. https://doi.org/10.1155/2023/4263309

Hamadalnil, Y., & Altayb, H. N. (2024). In silico molecular study of hepatitis B virus X protein as a therapeutic target. Journal of Biomolecular Structure and Dynamics, 42(8), 4002–4015. https://doi.org/10.1080/07391102.2023.2217920

Hu, J., Protzer, U., & Siddiqui, A. (2019). Revisiting hepatitis B virus: Challenges of curative therapies. Journal of Virology, 93(20), Article e01032-19. https://doi.org/10.1128/JVI.01032-19

Kanwal, S., Jamil, F., Ali, A., & Sehgal, S. A. (2017). Comparative modeling, molecular docking, and revealing of potential binding pockets of RASSF2; a candidate cancer gene. Interdisciplinary Sciences: Computational Life Sciences, 9(2), 214 – 223. https://doi.org/10.1007/s12539-016-0145-z

Kim, S., Chen, J., Cheng, T., Gindulyte, A., He, J., He, S., Li, Q., Shoemaker, B. A., Thiessen, P. A., Yu, B., Zaslavsky, L., Zhang, J., & Bolton, E. E. (2023). PubChem 2023 update. Nucleic Acids Research, 51(D1), D1373–D1380. https://doi.org/10.1093/nar/gkac956

Ko, C., Chakraborty, A., Chou, W.-M., Hasreiter, J., Wettengel, J. M., Stadler, D., Bester, R., Asen, T., Zhang, K., Wisskirchen, K., McKeating, J. A., Ryu, W.-S., & Protzer, U. (2018). Hepatitis B virus genome recycling and de novo secondary infection events maintain stable cccDNA levels. Journal of Hepatology, 69(6), 1231 – 1241. https://doi.org/10.1016/j.jhep.2018.08.012

Martyn, E., Eisen, S., Longley, N., Harris, P., Surey, J., Norman, J., Brown, M., Sultan, B., Maponga, T. G., Iwuji, C., Flanagan, S., Ghosh, I., Story, A., & Matthews, P. C. (2023). The forgotten people: Hepatitis B virus (HBV) infection as a priority for the inclusion health agenda. eLife, 12, Article e81070. https://doi.org/10.7554/eLife.81070

Mohebbi, A., Ghorbanzadeh, T., Naderifar, S., Khalaj, F., Askari, F. S., & Sammak, A. S. (2023). A fragment-based drug discovery developed on ciclopirox for inhibition of hepatitis B virus core protein: An in silico study. PLOS ONE, 18(5), Article e0285941. https://doi.org/10.1371/journal.pone.0285941

Naderi, M., Hosseini, S. M., Besharat, S., Behnampour, N., Shahramian, I., & Moradi, A. (2023). Clinical and virological aspects of core and pre-core mutations in three generations of chronic hepatitis B virus patients. Future Virology, 18(6), 349 – 358. https://doi.org/10.2217/fvl-2022-0216

Parvez, M. K., Rehman, M. T., Alam, P., Al-Dosari, M. S., Alqasoumi, S. I., & Alajmi, M. F. (2019). Plant-derived antiviral drugs as novel hepatitis B virus inhibitors: Cell culture and molecular docking study. Saudi Pharmaceutical Journal, 27(3), 389 – 400. https://doi.org/10.1016/j.jsps.2018.12.008

Pathak, R. K., Baunthiyal, M., Taj, G., & Kumar, A. (2014). Virtual screening of natural inhibitors to the predicted HBx protein structure of hepatitis B virus using molecular docking for identification of potential lead molecules for liver cancer. Bioinformation, 10(7), 428–435. https://doi.org/10.6026/97320630010428

Patil, V. S., Harish, D. R., Charla, R., Bhandare, V. V., Gujarathi, S. S., Beerwala, F. A., Patil, P. P., Jalalpure, S. S., Hegde, H. V., & Roy, S. (2025). Flavonoids of Andrographis paniculata regulate hepatitis B virus replication and hepatocellular carcinoma progression: Evidence from computational and experimental studies. BMC Complementary Medicine and Therapies, 25(1), Article 95. https://doi.org/10.1186/s12906-025-04807-z

Rasool, M., Malik, A., Waquar, S., Tul-Ain, Q., Jafar, T. H., Rasool, R., Kalsoom, A., Ghafoor, M. A., Sehgal, S. A., Gauthaman, K., Naseer, M. I., Al-Qahtani, M. H., & Pushparaj, P. N. (2018). In-silico characterization and in-vivo validation of albiziasaponin-A, iso-orientin, and salvadorin using a rat model of Alzheimer's disease. Frontiers in Pharmacology, 9, Article 730. https://doi.org/10.3389/fphar.2018.00730

Rizzo, G. E. M., Cabibbo, G., & Craxì, A. (2022). Hepatitis B virus-associated hepatocellular carcinoma. Viruses, 14(5), Article 986. https://doi.org/10.3390/v14050986

Saeed, U., Piracha, Z. Z., Alrokayan, S., Hussain, T., Almajhdi, F. N., & Waheed, Y. (2023). Immunoinformatics and evaluation of peptide vaccines derived from global hepatitis B viral

HBx and HBc proteins critical for covalently closed circular DNA integrity. Microorganisms, 11(12), Article 2826. https://doi.org/10.3390/microorganisms11122826

Schoch, C. L., Ciufo, S., Domrachev, M., Hotton, C. L., Kannan, S., Khovanskaya, R., Leipe, D., McVeigh, R., O'Neill, K., Robbertse, B., Sharma, S., Soussov, V., Sullivan, J. P., Sun, L., Turner, S., & Karsch-Mizrachi, I. (2020). NCBI Taxonomy: A comprehensive update on curation, resources and tools. Database, 2020, Article baaa062. https://doi.org/10.1093/database/baaa062

Shaikh, I. A., Muddapur, U. M., C, K., Badiger, S., Kulkarni, M., Mahnashi, M. H., Alshamrani, S. A., Huneif, M. A., More, S. S., Khan, A. A., & Iqubal, S. M. S. (2022). In silico molecular docking and simulation studies of protein HBx involved in the pathogenesis of hepatitis B virus-HBV. Molecules, 27(5), Article 1513. https://doi.org/10.3390/molecules27051513

Tsukuda, S., & Watashi, K. (2020). Hepatitis B virus biology and life cycle. Antiviral Research, 182, Article 104925. https://doi.org/10.1016/j.antiviral.2020.104925

Tufon, K. A., Meriki, H. D., Kwenti, T. E., Tony, N. J., Malika, E., Bolimo, A. F., Kouanou, Y. S., Nkuo-Akenji, T., & Anong, D. N. (2019). HBV transmission risk assessment in healthcare workers, household and sexual contacts of HBV infected patients in the Southwest Region of Cameroon. Oman Medical Journal, 34(4), 313–321. https://doi.org/10.5001/omj.2019.62

Ugbaja, S. C., Mushebenge, A. G.-A., Kumalo, H., Ngcobo, M., & Gqaleni, N. (2025). Potential benefits of in silico methods: A promising alternative in natural compound's drug discovery and repurposing for HBV therapy. Pharmaceuticals, 18(3), Article 419. https://doi.org/10.3390/ph18030419

UniProt Consortium (2021). UniProt: The universal protein knowledgebase in 2021. Nucleic Acids Research, 49(D1), D480–D489. https://doi.org/10.1093/nar/gkaa1100

Velkov, S., Ott, J. J., Protzer, U., & Michler, T. (2018). The global hepatitis B virus genotype distribution approximated from available genotyping data. Genes, 9(10), Article 495. https://doi.org/10.3390/genes9100495

Yang, J., Yan, R., Roy, A., Xu, D., Poisson, J., & Zhang, Y. (2015). The I-TASSER Suite: Protein structure and function prediction. Nature Methods, 12(1), 7 – 8. https://doi.org/10.1038/nmeth.3213

License: Copyright (c) 2026 Author.
All articles published in this journal are licensed under the Creative Commons Attribution 4.0 International License (CC BY 4.0). This license permits unrestricted use, distribution, and reproduction in any medium, provided the original author(s) and source are properly credited. Authors retain copyright of their work, and readers are free to copy, share, adapt, and build upon the material for any purpose, including commercial use, as long as appropriate attribution is given.

Advances in World Medical Research, 2026, 2(3), 32-48
https://doi.org/10.71204/13dkj505

In Silico Prediction of Distinct HMW PAH-Associated Pathways in Allergic Rhinitis: Chemokine-Related Targets of BaP and Metabolic Enzyme Targets of BaA/DBA

Yue He [1, #], Yibo He [1, #], Junfeng Xi [1], An Chang [2], Zeyu Guo [1], Xianzhi Liu [1], Jiayu Li [1], Jiaxuan Li [1], Zhao Wang [3, 4, *], Dong Chen [1, 5, *]

[1] Department of ORL-HN, The First Affiliated Hospital of Jinzhou Medical University, Jinzhou 121001, China

[2] Department of Drug Administration, The First Affiliated Hospital of Jinzhou Medical University, Jinzhou 121001, China

[3] Department of Otorhinolaryngology, Dongzhimen Hospital, The First Affiliated Hospital of Beijing University of Chinese Medicine, Beijing 100029, China

[4] Institute of Traditional Chinese Medicine Otorhinolaryngology Head and Neck Surgery, Dongzhimen Hospital, Beijing University of Chinese Medicine, Beijing 100700, China

[5] Liaoning Province Clinical Medical Research Center for Allergic Diseases, Jinzhou 121001, China

[#] Yue He and Yibo He contributed equally to this work.

*** Correspondence**:

Zhao Wang

entdoctorwang@126.com

Dong Chen

drchendong@jzmu.edu.cn

Received: 8 June 2026/ Accepted: 20 August 2026/ Published online: 30 September 2026

Abstract

Polycyclic aromatic hydrocarbons (PAHs), major atmospheric pollutants, have been associated with allergic respiratory disease, but the molecular links between individual PAHs and allergic rhinitis (AR) remain incompletely characterized. This in silico study explored predicted associations of three high-molecular-weight PAHs—benzo[a]pyrene (BaP), benzo[a]anthracene (BaA), and dibenz[a,h]anthracene (DBA)—with AR-related molecular networks. We integrated ADMET prediction (ADMETlab 2.0), multi-source target identification, network topology analysis (STRING and Cytoscape), functional enrichment (DAVID), and molecular docking (AutoDock Vina). ADMET analysis generated multiple toxicological alerts for all three compounds. Network analysis identified 191, 138, and 159 overlapping targets for the BaP–AR, BaA–AR, and DBA–

AR datasets, respectively. BaP-associated targets were preferentially enriched in chemotaxis and chemokine signaling, whereas BaA- and DBA-associated targets were more strongly enriched in xenobiotic and cytochrome P450-related metabolic pathways. Molecular docking yielded energetically favorable predicted poses between BaP and chemokine-related hub proteins (CCL2, CCL5, CXCL8, CXCL12, and CXCR4) and between BaA/DBA and metabolic hub proteins, including ABCB1, CYP1A2, and CYP3A4. Taken together, these analyses generate a hypothesis that BaP may be preferentially associated with chemokine-related inflammatory networks, whereas BaA and DBA may be associated with metabolic-enzyme networks that could influence endogenous inflammatory mediator metabolism or drug disposition. Given its computational scope, this study yields in silico-generated hypotheses and candidate targets warranting experimental validation.

Keywords: Polycyclic Aromatic Hydrocarbons; Allergic Rhinitis; Network Toxicology; Molecular Docking; In Silico Analysis

1. Introduction

Allergic rhinitis (AR) is an immunoglobulin E-mediated type I hypersensitivity reaction triggered by inhaled allergens. Pathologically, it is characterized by a Th2-biased immune response in the nasal mucosa. This response activates B lymphocytes to generate allergen-specific IgE, facilitates inflammatory-cell recruitment, and is associated with epithelial injury, glandular hyperplasia, and mucosal-barrier dysfunction (Zhang et al., 2021). The hallmark symptoms include paroxysmal sneezing, rhinorrhea, nasal pruritus, and congestion (Bousquet et al., 2020). AR affects hundreds of millions of people worldwide, impairs quality of life, and represents a substantial public-health burden (Colás et al., 2017; Cox, 2016). Although genetic predisposition and common environmental allergens, such as pollen and dust mites, are established contributors (Bernstein et al., 2024), epidemiological evidence also associates air-pollutant exposure with AR susceptibility and symptom severity (Li et al., 2022; Lu et al., 2022). Long-term exposure to specific PM2.5 constituents has likewise been associated with allergic diseases (Feng et al., 2023).

Polycyclic aromatic hydrocarbons (PAHs) are atmospheric contaminants generated mainly by incomplete combustion of organic materials (Srogi, 2007). Their lipophilicity and environmental persistence facilitate widespread distribution, bioaccumulation, and biological uptake (Abdel-Shafy & Mansour, 2016; Barbosa et al., 2023). Their carcinogenic and mutagenic effects are well documented (Holme et al., 2023; Liu et al., 2008), and epidemiological and experimental evidence has linked PAH exposure to immune dysregulation and allergic respiratory disease (Karimi et al., 2015; Yu et al., 2022). The selected high-molecular-weight PAHs differ structurally: BaA contains four fused aromatic rings, whereas BaP and DBA each contain five, and the three compounds have distinct ring-fusion geometries. These structural differences may alter molecular shape and target complementarity, providing a chemical rationale for comparing their predicted target profiles (Barbosa et al., 2023; Bukowska et al., 2022). Research has focused primarily on BaP, which has been associated with eosinophilic airway inflammation and aggravated nasal obstruction in experimental allergic models (Mizutani et al., 2007; Tajima et al., 2020). By contrast, the potential

molecular associations of BaA and DBA with AR remain poorly integrated and underexplored (Malik et al., 2013).

In this in silico study, we aimed to explore potential molecular associations of benzo[a]pyrene (BaP), benzo[a]anthracene (BaA), and dibenz[a,h]anthracene (DBA) with allergic rhinitis (AR). Our goal was to characterize the differential target profiles of these high-molecular-weight PAHs by integrating toxicity prediction, network toxicology, functional enrichment, and molecular docking. Specifically, we employed these computational approaches to map the predicted relationships between the PAHs and their potential targets. Through this comprehensive analysis, we sought to generate testable hypotheses and identify candidate targets associated with PAH-linked AR, thereby providing a computational framework for understanding environmental pollutant-immune interactions.

2. Methods

2.1. Integrated Network Toxicology-Based Analysis of PAHs

This study used an integrated computational approach to investigate three prototypical high-molecular-weight polycyclic aromatic hydrocarbons (HMW PAHs): benzo[a]pyrene (BaP), benzo[a]anthracene (BaA), and dibenz[a,h]anthracene (DBA). Their canonical SMILES strings were retrieved from the PubChem database (https://pubchem.ncbi.nlm.nih.gov/). The ADMET properties were then predicted using the ADMETlab 2.0 platform (https://admetmesh.scbdd.com/service/evaluation/cal), providing exploratory pharmacokinetic and toxicological descriptors for subsequent target-prioritization analyses (Xiong et al., 2021).

2.2. Screening and Identification of Potential PAHs Molecular Targets

Potential molecular targets of the PAHs were screened using a triple-database cross-validation strategy. First, compound names were standardized and SMILES strings were obtained from PubChem. Parallel queries were then performed across three databases: 1) ChEMBL (https://www.ebi.ac.uk/ChEMBL/), using standardized compound names (e.g., "Benzo[a]pyrene") and a species filter for "Homo sapiens"; 2) SEA database (https://sea.bkslab.org/), by submitting the SMILES strings for screening against "HUMAN" targets; and 3) TargetNet database (http://targetnet.scbdd.com/calcnet/index/), where SMILES strings were submitted to retain targets with a probability score greater than 0 (Prob > 0). The resulting target lists from all sources were integrated, and duplicates were removed. The combined list was then filtered through the UniProt database, restricting entries to 'Reviewed' proteins from 'Human' species, to obtain a non-redundant library of standardized target gene names (Coudert et al., 2023).

2.3. Compilation of AR-Associated Targets

Targets associated with allergic rhinitis (AR) were systematically retrieved from four databases: DrugBank (https://go.drugbank.com/), GeneCards (https://www.genecards.org/), OMIM (https://www.omim.org/), and TTD (https://db.idrblab.net/ttd/), using "allergic rhinitis" as a standardized search query. To maximize relevance, GeneCards entries were screened to retain only those with a relevance score exceeding the median. Following data integration and removal of

redundant entries, a standardized AR target library was constructed, encompassing 1363 unique targets.

2.4. Intersection Analysis of PAHs and Allergic Rhinitis Targets

The overlap between predicted PAH targets and AR-associated targets was identified and visualized using the jvenn tool on the Weishengxin online platform (Bardou et al., 2014). Specifically, the PAH target library and the AR target library were uploaded separately. The platform's standard intersection analysis was then performed, generating an interactive Venn diagram. This diagram provided key statistical metrics and directly listed the common targets shared between the two sets. These shared targets were carried forward for exploratory network and enrichment analyses.

2.5. Establishment of the Protein-Protein Interaction (PPI) Network and Determination of Hub Targets

Based on the common targets identified in the Venn analysis, a human PPI network was constructed in the STRING database (confidence threshold > 0.4, https://cn.string-db.org/). The PPI network was imported into Cytoscape (Shannon et al., 2003) for multiparametric topological analysis. Significant targets were screened using the CytoNCA plugin based on degree centrality, closeness centrality, betweenness centrality, and local average connectivity (LAC). High-density functional modules were identified using the MCODE plugin (parameters: degree cutoff=2, k-core=2). The top 10 hub candidate genes were predicted by the MCC algorithm of the CytoHubba plugin. Ultimately, core hub genes were defined as the triple intersection of: 1) CytoNCA-significant targets, 2) MCODE core module genes, and 3) CytoHubba top 10 genes.

2.6. GO and KEGG Pathway Enrichment Analysis

Potential intersecting target genes between PAHs and AR were analyzed using the DAVID database (Huang da et al., 2009), with species restricted to Homo sapiens. Comprehensive functional annotation was conducted through Gene Ontology (GO) analysis encompassing biological processes, molecular functions, and cellular components, alongside pathway enrichment analysis via the Kyoto Encyclopedia of Genes and Genomes (KEGG) resource. Results were visualized using the integrated Weishengxin modules as bar charts and pathway-oriented bubble maps to summarize predicted functional associations and pathway patterns.

2.7. Molecular Docking Analysis of PAHs against Hub Targets

The crystal structures of the selected hub target protein were retrieved from the RCSB Protein Data Bank (https://www.rcsb.org/). Ligand structures of PAHs were standardized using PubChem. Prior to molecular docking, the target protein structure was preprocessed to remove all water molecules and co-crystallized ligands using PyMOL. Subsequently, hydrogen atoms and Gasteiger partial charges were applied to both the receptor protein and the ligand molecules using AutoDockTools. A grid box covering the entire putative binding pocket of the receptor was defined for docking simulations. Molecular docking simulations were conducted under rigid conditions using AutoDock Vina (Trott & Olson, 2010). Predicted ligand poses were examined with the PLIP online tool (http://plip-tool.biotec.tu-dresden.de/), and visualized in PyMOL.

3. Results

3.1. Predicted Toxicological Profiles of the Selected PAHs

ADMETlab 2.0 predicted high plasma protein binding for BaP, BaA, and DBA (PPB > 97%). The predicted volume of distribution (1.057 - 1.281 L/kg) and clearance (5.990 - 8.051 mL/min/kg) were compatible with broad tissue distribution and relatively slow elimination. The platform also generated alerts related to carcinogenicity, genotoxicity, drug-induced liver injury, skin sensitization, and eye irritation, with predicted activity involving the aryl hydrocarbon receptor and antioxidant response element pathways. Respiratory toxicity alerts were additionally predicted for BaP and DBA. These computational outputs were used as exploratory context for target prioritization.

3.2. Predicted BaP-Associated Targets and Pathways in AR

To characterize the predicted molecular overlap between BaP and AR, BaP-associated targets obtained from ChEMBL, SEA, and TargetNet (n = 798) were integrated with AR-related targets from DrugBank, GeneCards, OMIM, and TTD (n = 1363). Intersection analysis identified 191 shared candidate targets (Figure 1A). A PPI network of these targets was constructed using STRING (Figure 1B) and analyzed in Cytoscape (Figure 1C). Three complementary algorithms were applied: CytoNCA for centrality-based screening (Figure 1D), CytoHubba for ranking the top 10 genes (Figure 1E), and MCODE for module detection (Figure 1F). The consensus intersection of these outputs (Figure 1G) prioritized five hub targets: CCL2, CCL5, CXCL8, CXCL12, and CXCR4. Their predicted interaction subnetwork is shown in Figure 1H.

Functional enrichment analysis of the 191 shared candidate targets identified 154 enriched KEGG pathways and 856 GO terms, including 593 biological-process, 74 cellular-component, and 189 molecular-function terms. The leading biological-process terms included chemotaxis, inflammatory response, chemokine-mediated signaling, xenobiotic metabolism, and cellular chemotaxis; leading cellular-component terms included the cell surface, plasma membrane, endoplasmic reticulum membrane, and extracellular space; and leading molecular-function terms included heme binding, oxidoreductase activity, monooxygenase activity, C-C chemokine-receptor activity, and iron-ion binding (Figure 2A). The top KEGG pathways included chemokine signaling, viral protein interaction with cytokines and cytokine receptors, lipid and atherosclerosis, chemical carcinogenesis, and drug metabolism-cytochrome P450 (Figure 2B). These enrichment results nominate chemokine-related processes as candidate associations.

Within the selected docking protocol, BaP yielded favorable predicted binding scores with CCL2, CCL5, CXCL8, CXCL12, and CXCR4 (Figure 3). The predicted poses included hydrophobic, π-stacking, and π-cation interactions, and the most negative docking score was observed for CXCR4 (−11.5 kcal/mol). These scores support prioritization of the five proteins for further study, but they do not confirm direct binding, functional modulation, or chemokine dysregulation in nasal tissue.

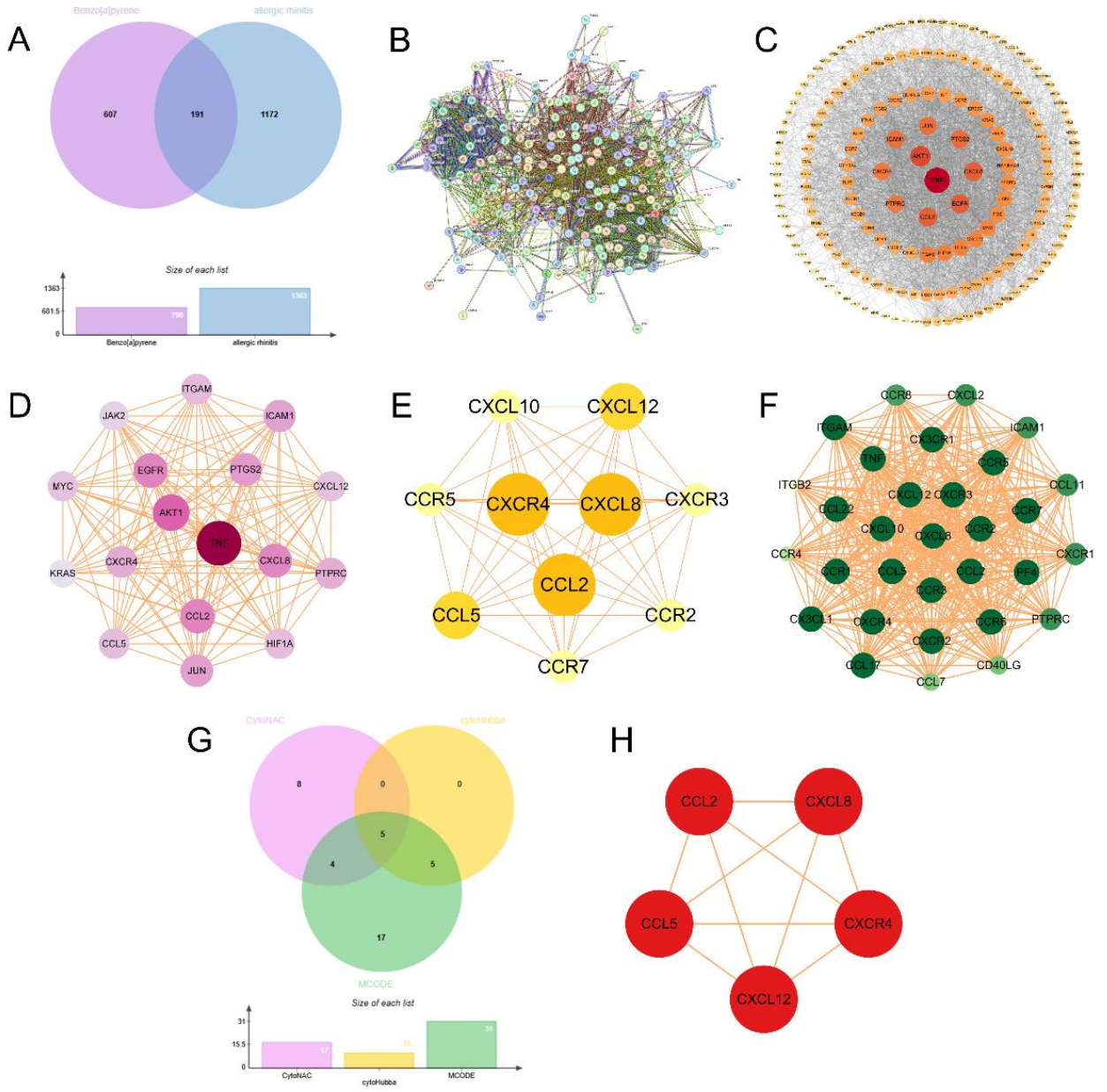


Figure 1. Computational Prioritization of BaP-Associated Targets in AR

Note: (A) Intersection analysis of BaP-associated targets (n = 798) and AR-related targets (n = 1363), yielding 191 shared candidate targets. (B-C) STRING PPI network and Cytoscape visualization. (D-F) CytoNCA centrality screening, CytoHubba ranking, and MCODE module analysis. (G-H) Consensus analysis prioritized CCL2, CCL5, CXCL8, CXCL12, and CXCR4 as chemokine-related hub targets.

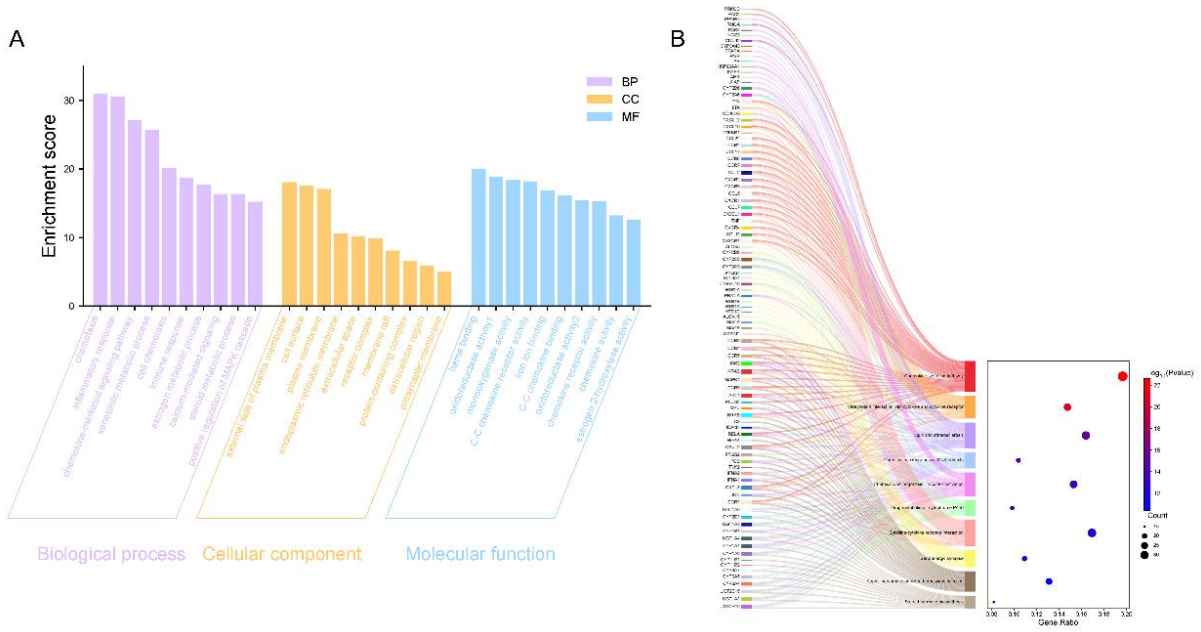


Figure 2. Functional Enrichment of Predicted BaP-AR Shared Targets

Note: (A) Top enriched GO terms for the 191 shared BaP-AR candidate targets across biological process, cellular component, and molecular function. (B) Top enriched KEGG pathways. The principal biological message is the computational enrichment of chemotaxis, inflammatory-response, and chemokine-signaling terms.

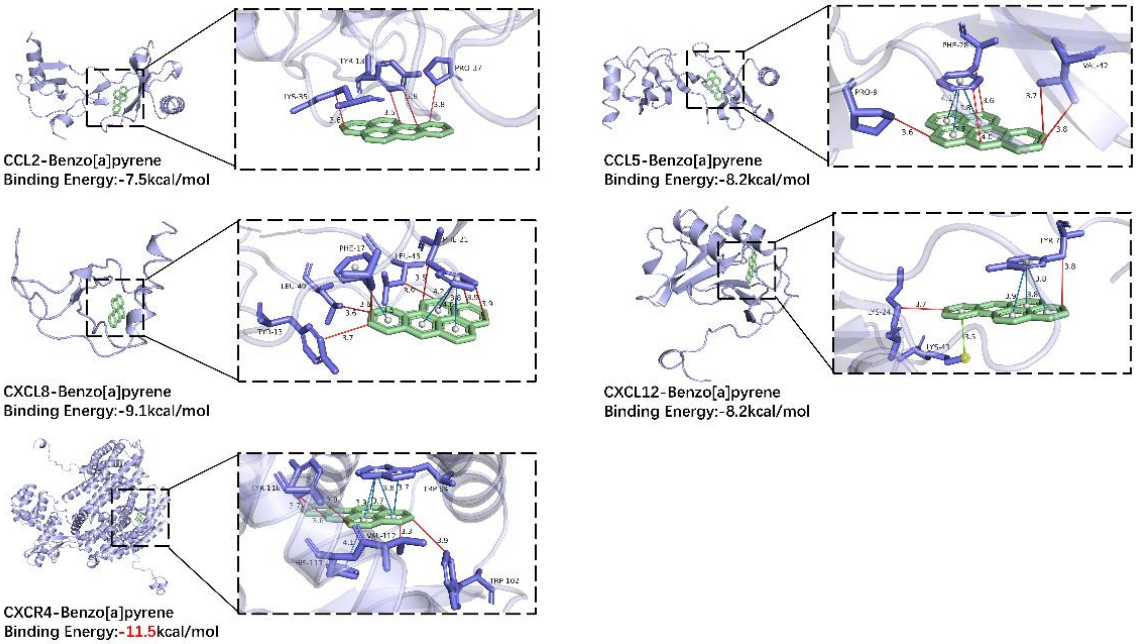


Figure 3. Predicted Docking Poses of BaP with Chemokine-Related Hub Proteins

Note: Representative computational docking poses of BaP with CCL2, CCL5, CXCL8, CXCL12, and CXCR4. Interaction annotations: hydrophobic (red), π-stacking (sky blue), π-cation (chartreuse).

3.3. Predicted BaA-Associated Targets and Pathways in AR

Using the same analytical approach, BaA-related targets (obtained from ChEMBL, SEA, and TargetNet; n = 788) were integrated with the previously described AR-related targets (n = 1363). A total of 138 potential BaA–AR association targets were identified through intersection analysis (Figure 4A). A protein-protein interaction (PPI) network was established based on these 138 targets

using the STRING database (Figure 4B), with subsequent visualization performed in Cytoscape (Figure 4C). The CytoNCA plugin was employed to filter nodes with betweenness centrality, closeness centrality, degree, and LAC values above the median (Figure 4D). We identified the top ten hub genes using the CytoHubba plugin (Figure 4E), and performed module clustering with MCODE (Figure 4F). The intersection of results derived from the three algorithms was illustrated using a Venn diagram (Figure 4G), yielding three core hub genes: ABCB1, CYP1A2, and CYP3A4. Their interaction network was subsequently visualized (Figure 4H).

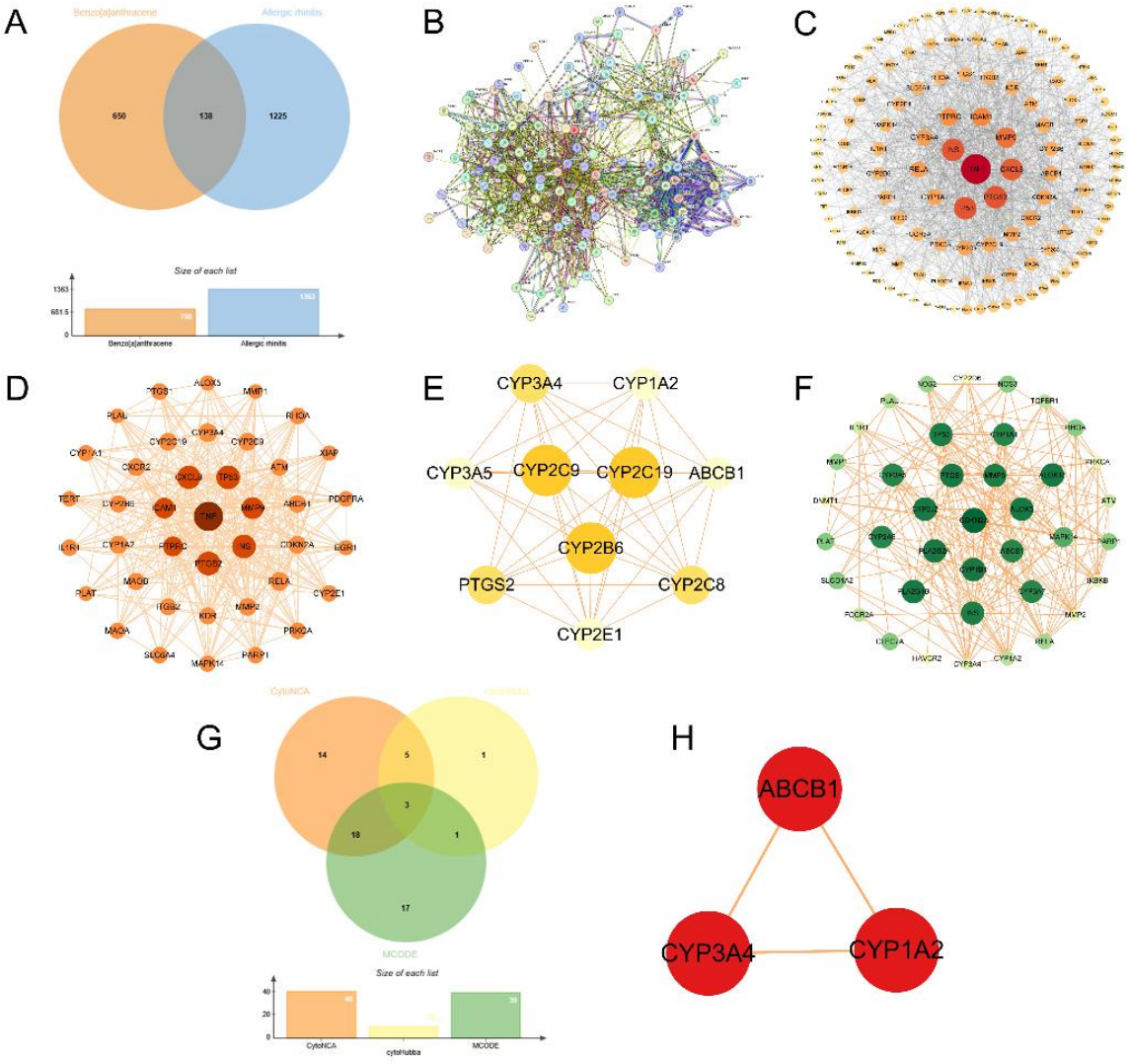


Figure 4. Computational Prioritization of BaA-Associated Targets in AR

Note: (A) Intersection of BaA-associated targets (n = 788) and AR-related targets (n = 1363), yielding 138 shared candidate targets. (B-F) PPI construction, network visualization, centrality screening, hub ranking, and module analysis. (G-H) Consensus analysis prioritized ABCB1, CYP1A2, and CYP3A4 as metabolic hub targets.

Enrichment analysis of the 138 shared candidate targets identified 124 enriched KEGG pathways and 649 GO terms, comprising 450 biological-process, 56 cellular-component, and 143 molecular-function terms. Leading biological-process terms included xenobiotic metabolism, inflammatory response, steroid metabolism, the cytochrome P450 epoxygenase pathway, and long-chain fatty acid biosynthesis; leading cellular-component terms included the cell surface, plasma membrane, endoplasmic reticulum membrane, and membrane raft; and leading molecular-function terms

included heme binding, iron-ion binding, oxidoreductase activity, monooxygenase activity, and estradiol 2-hydroxylase activity (Figure 5A). The top KEGG pathways included lipid and atherosclerosis, serotonergic synapse, arachidonic-acid metabolism, linoleic-acid metabolism, and chemical carcinogenesis (Figure 5B). These results prioritize metabolic and inflammatory pathways as computationally associated with the BaA–AR target overlap.

BaA yielded favorable predicted docking scores with ABCB1, CYP1A2, and CYP3A4, with values below −9 kcal/mol under the selected protocol (Figure 6). The predicted poses included hydrophobic, π-stacking, and π-cation contacts, and the most negative score was observed for CYP1A2 (−13.2 kcal/mol). These computational results identify candidate protein–ligand interactions for future testing.

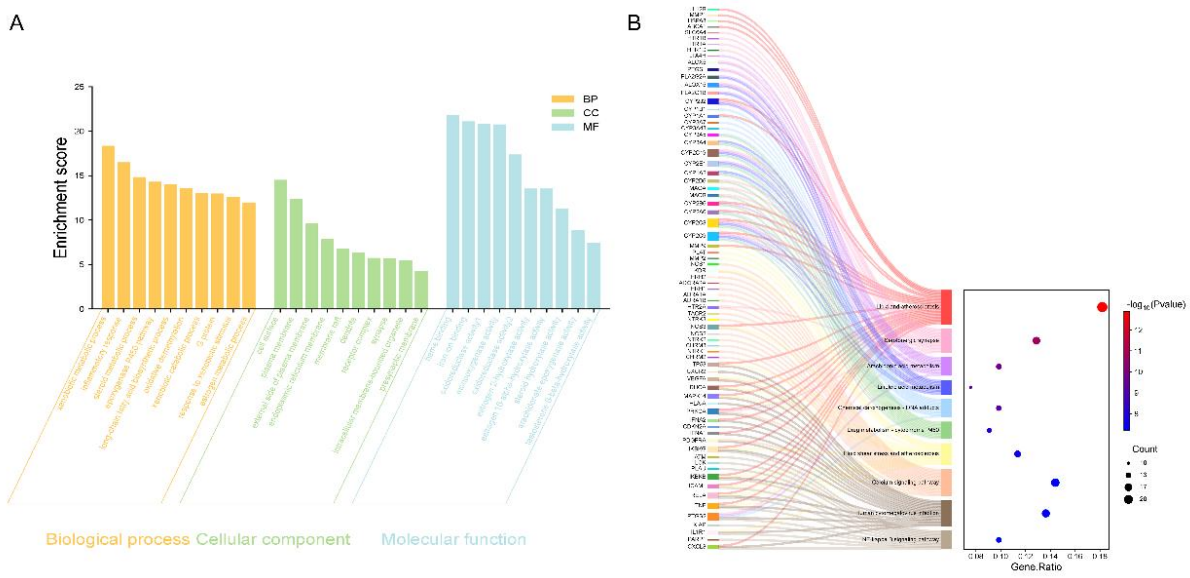


Figure 5. Functional Enrichment of Predicted BaA-AR Shared Targets

Note: (A) Top enriched GO terms for the 138 shared BaA-AR candidate targets. (B) Top enriched KEGG pathways. The principal biological message is enrichment of xenobiotic, lipid, arachidonic-acid, steroid, and cytochrome P450-related metabolic processes.

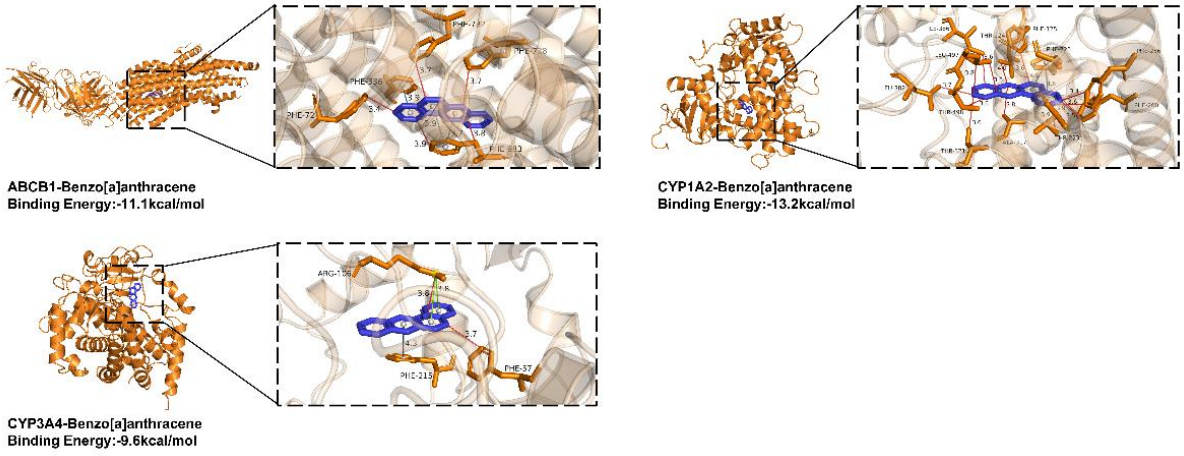


Figure 6. Predicted Docking Poses of BaA with Metabolic Hub Proteins

Note: Representative computational docking poses of BaA with ABCB1, CYP1A2, and CYP3A4. Interaction annotations: red for hydrophobic interactions; sky blue for π-stacking; chartreuse for π-cation interactions.

3.4. Predicted DBA-Associated Targets and Pathways in AR

DBA-associated targets (obtained from ChEMBL, SEA, and TargetNet; n = 891) were combined with AR-related targets (n = 1363). A total of 159 potential DBA–AR interaction targets were identified through intersection analysis (Figure 7A). We constructed a protein-protein interaction (PPI) network from the 159 candidate proteins with the STRING database (Figure 7B) and visualized it using Cytoscape (Figure 7C). Consistent with the methodology used in the benzo[a]anthracene investigation, a combination of topological and functional module analyses was performed, including node centrality screening via CytoNCA (Figure 7D), hub gene identification using CytoHubba (top 10 genes, Figure 7E), and module detection with MCODE (Figure 7F). The consensus core targets derived from the three algorithms were identified using a Venn diagram (Figure 7G), yielding six key hub genes: ABCB1, CYP1A2, CYP3A4, CYP2C9, CYP2C19, and UGT1A1. The interaction subnetwork among these genes was explicitly depicted (Figure 7H).

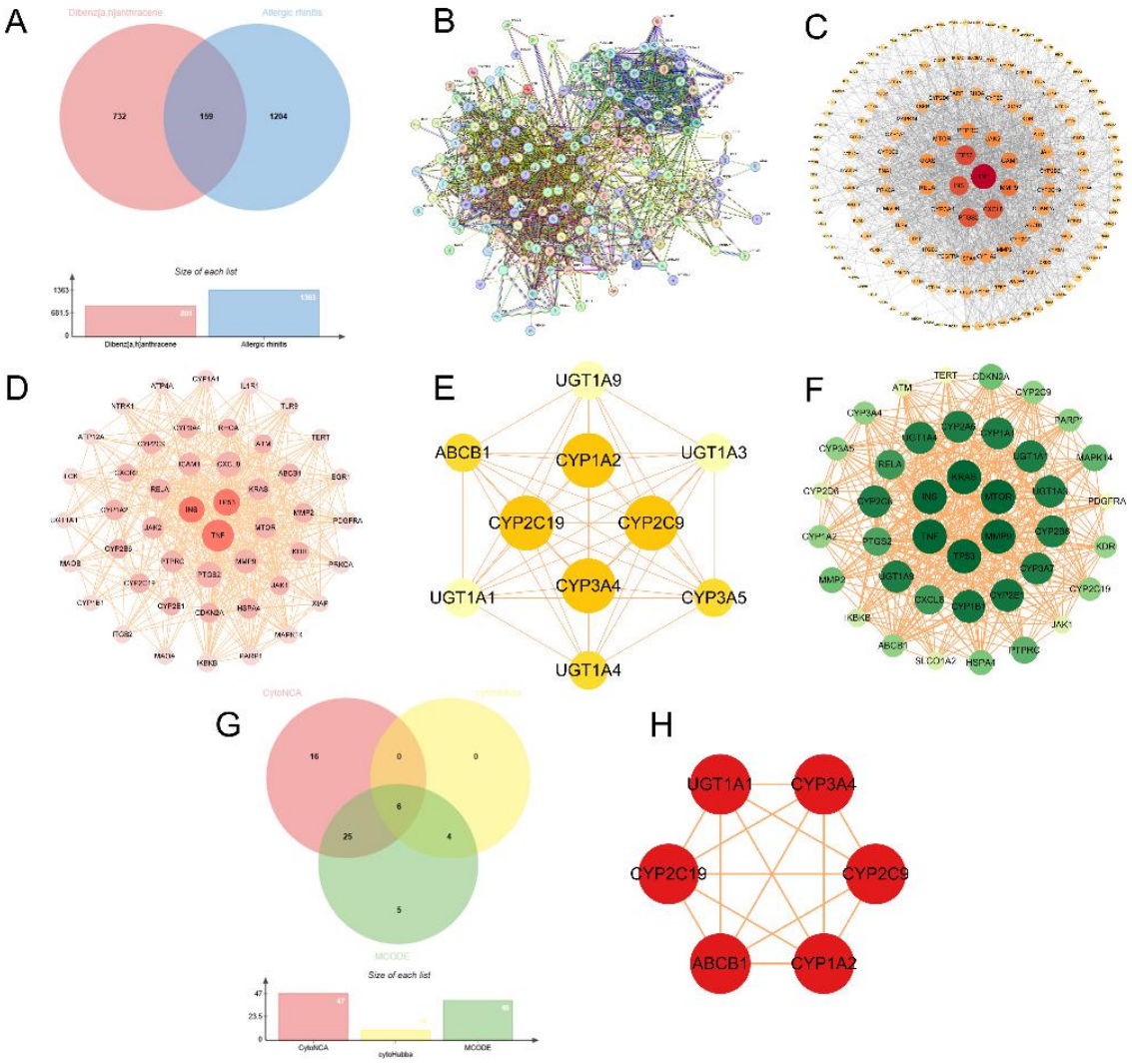


Figure 7. Computational Prioritization of DBA-Associated Targets in AR

Note: (A) Intersection of DBA-associated targets (n = 891) and AR-related targets (n = 1363), yielding 159 shared candidate targets. (B-F) PPI construction, network visualization, centrality screening, hub ranking, and module analysis. (G-H) Consensus analysis prioritized ABCB1, CYP1A2, CYP3A4, CYP2C9, CYP2C19, and UGT1A1 as metabolic hub targets.

Enrichment analysis of the 159 shared candidate targets identified 147 enriched KEGG pathways and 726 GO terms, comprising 482 biological-process, 70 cellular-component, and 174 molecular-function terms. Leading biological-process terms included xenobiotic metabolism, estrogen metabolism, steroid metabolism, inflammatory response, and the cytochrome P450 epoxygenase pathway; leading cellular-component terms included the cell surface, plasma membrane, endoplasmic reticulum membrane, and membrane raft; and leading molecular-function terms included heme binding, oxidoreductase activity, iron-ion binding, and monooxygenase activity (Figure 8A). The leading KEGG pathways included lipid and atherosclerosis, chemical carcinogenesis, metabolism of xenobiotics by cytochrome P450, and serotonergic synapse (Figure 8B). These results prioritize metabolic-enzyme networks as computationally associated with the DBA-AR target overlap.

DBA yielded favorable predicted docking scores with ABCB1, CYP1A2, CYP3A4, CYP2C9, CYP2C19, and UGT1A1, with values below −9 kcal/mol under the selected protocol (Figure 9). The predicted poses included hydrophobic, π-stacking, and π-cation contacts, and the most negative score was observed for CYP1A2 (−14.2 kcal/mol). These computational scores support target prioritization but do not establish direct binding, altered catalytic activity, or a causal role in AR.

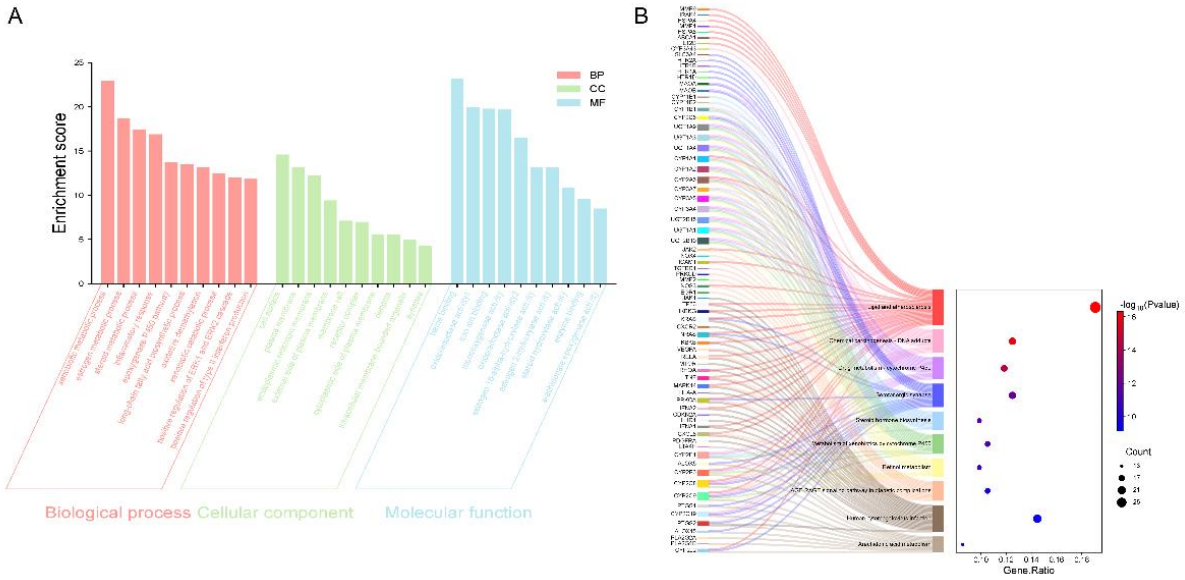


Figure 8. Functional Enrichment of Predicted DBA-AR Shared Targets

Note: (A) Top enriched GO terms for the 159 shared DBA-AR candidate targets. (B) Top enriched KEGG pathways. The principal biological message is enrichment of xenobiotic, steroid, estrogen, and cytochrome P450-related metabolic processes.

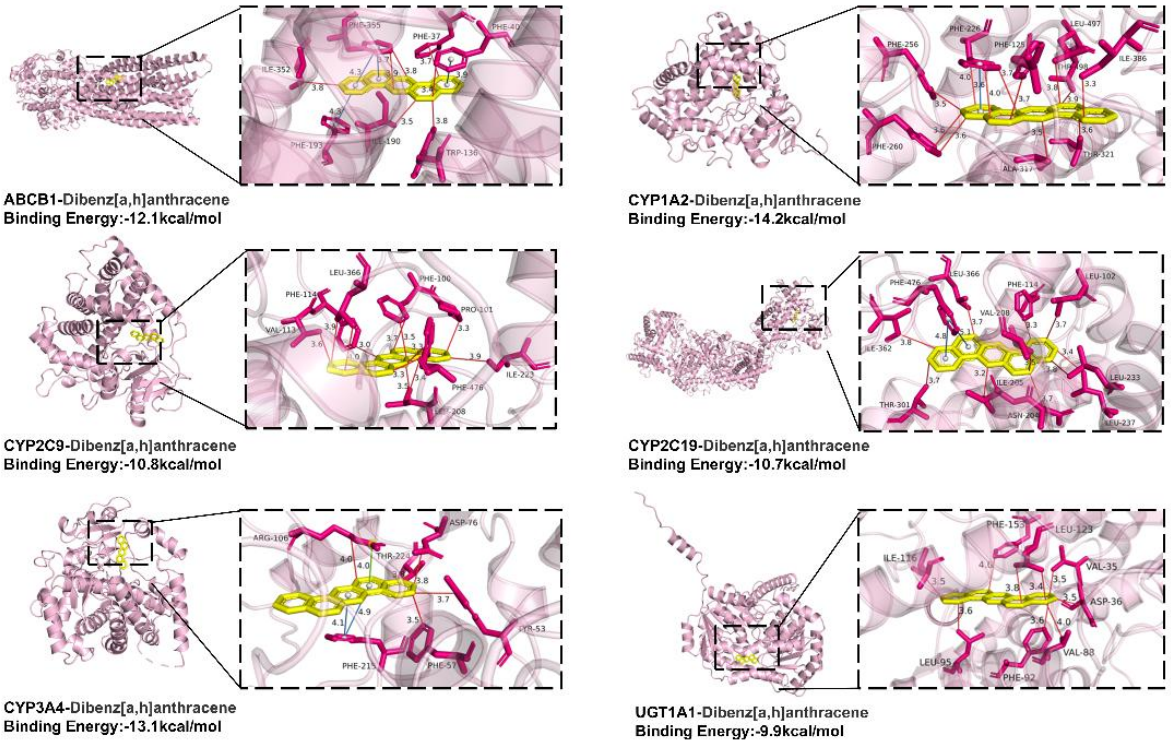


Figure 9. Predicted Docking Poses of DBA with Metabolic Hub Proteins

Note: Representative computational docking poses of DBA with ABCB1, CYP1A2, CYP3A4, CYP2C9, CYP2C19, and UGT1A1. Interaction annotations: hydrophobic (red), π-stacking (sky blue), π-cation (chartreuse).

4. Discussion

Allergic rhinitis (AR) is a prevalent inflammatory respiratory disease whose occurrence and severity have been associated with environmental pollution (Li et al., 2022). PAHs are persistent organic pollutants generated by incomplete combustion and are detected in particulate matter, vehicle exhaust, tobacco smoke, and other environmental media (Låg et al., 2020). PAH exposure has also been linked to altered regulatory T-cell function, providing biological plausibility for effects on allergic immune responses (Hew et al., 2015). Consistent with this, epidemiological evidence supports an association between PAH exposure and respiratory diseases in children, particularly asthma development and impaired respiratory function, with pediatric populations showing heightened susceptibility due to their smaller body size and immature immune systems (Wang et al., 2023). Nevertheless, epidemiological associations with mixed air pollution do not establish the contribution of an individual PAH to specific clinical AR phenotypes.

BaP, BaA, and DBA are environmentally relevant high-molecular-weight PAHs with distinct fused-ring structures. BaP, a classical PAH comprising five fused benzene rings, has been reported to possess carcinogenic and mutagenic properties. It was reported that BaP exposure was associated with nasal mucosal damage and respiratory irritation in an experimental model (Liu et al., 2024). Early investigations revealed that short-term intranasal BaP administration in guinea pig models of AR did not exacerbate rhinitis symptoms; however, prolonged treatment (22 weeks) was associated with aggravated nasal obstruction in an AR model (Mizutani et al., 2007). In vitro studies reported

that BaP enhanced basophil activation and stimulated IL-4 secretion in pollen-allergic subjects independently of allergen exposure (Lubitz et al., 2010). Additional in vivo studies have also associated BaP exposure with elevated mucus secretion and nasal tissue remodeling (Liu et al., 2024). These observations support investigating potential molecular links between BaP exposure and AR. However, they do not validate the specific target relationships predicted in the present analysis. The BaP-associated network prioritized CCL2, CCL5, CXCL8, CXCL12, and CXCR4. Chemokines and their receptors are relevant to clinically meaningful AR features because they coordinate inflammatory-cell trafficking, immune-cell recruitment, and epithelial-barrier responses (Li et al., 2022). In particular, CXCR4 has been implicated in mediating epithelial autophagy and compromising nasal epithelial barrier integrity via the CXCR4/miR-125b/FoxP3 pathway (Zheng et al., 2020). Thus, the predicted hub set offers a plausible molecular bridge to nasal inflammatory-cell infiltration and barrier dysfunction.

For BaA and DBA, existing case-control studies have reported an association between exposure to these compounds and the incidence of asthma (Al-Daghri et al., 2013; Jung et al., 2014); however, their potential association with AR remains unexplored. The analyses prioritized ABCB1 and several CYP enzymes and highlighted xenobiotic metabolism, arachidonic-acid metabolism, steroid metabolism, and cytochrome P450 epoxygenase pathways. In addition to xenobiotic and drug metabolism, CYP-associated networks participate in the processing of endogenous lipids and steroid hormones that can influence inflammatory signaling (Guengerich et al., 2016). The resulting hypothesis is therefore broader than drug disposition alone: BaA- or DBA-associated metabolic perturbation could theoretically alter endogenous inflammatory-mediator balance. Loratadine, for example, undergoes CYP3A4-mediated metabolism (Wang et al., 2025; Yumibe et al., 1996; Zhang et al., 2026), making altered drug handling a clinical possibility. Moreover, studies suggest that CYP1A2 may be involved in the metabolism of montelukast—a leukotriene receptor antagonist used in AR management—and that altered CYP1A2 activity could modulate its metabolic clearance (Filppula et al., 2011). CYP1A2 and CYP3A4, which were prioritized by the present analysis, have been reported to be involved in the metabolism of certain anti-allergy medications. Whether BaA or DBA binding could alter the catalytic activity of these enzymes and thereby affect drug disposition remains a testable hypothesis.

This study has several limitations. First, all findings are derived from computational predictions and depend on database completeness, target-prediction algorithms, enrichment backgrounds, network thresholds, available protein structures, and docking assumptions. Second, docking scores do not establish direct binding, target activation or inhibition, tissue exposure, or causal biological effects. Third, no clinical samples, nasal-mucosal measurements, exposure–response data, cell experiments, animal models, CYP activity assays, or pharmacokinetic analyses were included. Fourth, the analysis did not account for PAH mixtures, metabolites, exposure dose and route, temporal patterns, or interindividual variability. Accordingly, the proposed pathways should be viewed as hypothesis-generating and require independent experimental and clinical validation.

In summary, the integrated computational analysis generated a dual-pathway hypothesis: BaP-associated targets were preferentially linked to chemokine-related networks, whereas BaA- and DBA-associated targets were preferentially linked to metabolic-enzyme networks. This framework

may help prioritize biomarkers and experimental questions. Importantly, these findings represent computational hypotheses and candidate targets that warrant experimental validation.

5. Conclusion

Using computational toxicology, multi-algorithm network analysis, functional enrichment, and molecular docking, this study identified distinct predicted target patterns for three high-molecular-weight PAHs in relation to AR. BaP-associated targets were enriched in chemokine-related pathways and included CCL2, CCL5, CXCL8, CXCL12, and CXCR4, whereas targets associated with BaA and DBA were enriched in metabolic pathways and included CYP1A2, CYP3A4, and other metabolic proteins. These findings provide in silico hypotheses concerning inflammatory-cell recruitment, epithelial-barrier regulation, endogenous mediator metabolism, and possible drug-disposition effects.

Author Contributions:

Yue He: Writing-original draft, Formal analysis, Visualization. Yibo He: Writing-original draft, Formal analysis, Visualization. Junfeng Xi: Formal analysis, Data curation. An Chang: Writing-review & editing, Data curation. Zeyu Guo: Writing-review & editing, Formal analysis. Xianzhi Liu: Formal analysis, Data curation. Jiayu Li: Formal analysis, Data curation. Jiaxuan Li: Formal analysis, Data curation. Zhao Wang: Writing-original draft, Methodology, Supervision, Funding acquisition. Dong Chen: Writing-original draft, Methodology, Supervision, Funding acquisition. All authors have read and agreed to the published version of the manuscript.

Funding:

This work was supported by the Liaoning Provincial Science and Technology Program (Key Research and Development Program) [No. 2025JH2/101800361].

Institutional Review Board Statement:

Not applicable.

Informed Consent Statement:

Not applicable.

Data Availability Statement:

The datasets supporting the findings of this study are fully available within the paper and its supplementary information files. Requests for additional details can be directed to the corresponding author.

Conflict of Interest:

The authors declare no conflict of interest.

References

Abdel-Shafy, H. I., & Mansour, M. S. M. (2016). A review on polycyclic aromatic hydrocarbons: Source, environmental impact, effect on human health and remediation. Egyptian Journal of Petroleum, 25(1), 107-123.

Al-Daghri, N. M., Alokail, M. S., Abd-Alrahman, S. H., Draz, H. M., Yakout, S. M., & Clerici, M. (2013). Polycyclic aromatic hydrocarbon exposure and pediatric asthma in children: a case-control study. Environ Health, 12, 1.

Barbosa, F., Jr., Rocha, B. A., Souza, M. C. O., Bocato, M. Z., Azevedo, L. F., Adeyemi, J. A., Santana, A., & Campiglia, A. D. (2023). Polycyclic aromatic hydrocarbons (PAHs): Updated aspects of their determination, kinetics in the human body, and toxicity. J Toxicol Environ Health B Crit Rev, 26(1), 28-65.

Bardou, P., Mariette, J., Escudié, F., Djemiel, C., & Klopp, C. (2014). jvenn: an interactive Venn diagram viewer. Bmc Bioinformatics, 15(1), 293.

Bernstein, J. A., Bernstein, J. S., Makol, R., & Ward, S. (2024). Allergic Rhinitis: A Review. Jama, 331(10), 866-877.

Bousquet, J., Anto, J. M., Bachert, C., Baiardini, I., Bosnic-Anticevich, S., Walter Canonica, G., Melén, E., Palomares, O., Scadding, G. K., Togias, A., & Toppila-Salmi, S. (2020). Allergic rhinitis. Nat Rev Dis Primers, 6(1), 95.

Bukowska, B., Mokra, K., & Michałowicz, J. (2022). Benzo[a]pyrene-Environmental Occurrence, Human Exposure, and Mechanisms of Toxicity. Int J Mol Sci, 23(11).

Colás, C., Brosa, M., Antón, E., Montoro, J., Navarro, A., Dordal, M. T., Dávila, I., Fernández-Parra, B., Ibáñez, M. D. P., Lluch-Bernal, M., Matheu, V., Rondón, C., Sánchez, M. C., & Valero, A. (2017). Estimate of the total costs of allergic rhinitis in specialized care based on real-world data: the FERIN Study. Allergy, 72(6), 959-966.

Coudert, E., Gehant, S., de Castro, E., Pozzato, M., Baratin, D., Neto, T., Sigrist, C. J. A., Redaschi, N., & Bridge, A. (2023). Annotation of biologically relevant ligands in UniProtKB using ChEBI. Bioinformatics, 39(1).

Cox, L. (2016). The role of allergen immunotherapy in the management of allergic rhinitis. Am J Rhinol Allergy, 30(1), 48-53.

Feng, C., Shao, Y., Ye, T., Cai, C., Yin, C., Li, X., Liu, H., Ma, H., Yu, B., Qin, M., Chen, Y., Yang, Y., Xu, W., Zhu, Q., Jia, P., & Yang, S. (2023). Associations between long-term exposure to PM(2.5) chemical constituents and allergic diseases: evidence from a large cohort study in China. Sci Total Environ, 904, 166755.

Filppula, A. M., Laitila, J., Neuvonen, P. J., & Backman, J. T. (2011). Reevaluation of the microsomal metabolism of montelukast: major contribution by CYP2C8 at clinically relevant concentrations. Drug Metab Dispos, 39(5), 904-911.

Guengerich, F. P., Waterman, M. R., & Egli, M. (2016). Recent Structural Insights into Cytochrome P450 Function. Trends Pharmacol Sci, 37(8), 625-640.

Hew, K. M., Walker, A. I., Kohli, A., Garcia, M., Syed, A., McDonald-Hyman, C., Noth, E. M., Mann, J. K., Pratt, B., Balmes, J., Hammond, S. K., Eisen, E. A., & Nadeau, K. C. (2015). Childhood exposure to ambient polycyclic aromatic hydrocarbons is linked to epigenetic modifications and impaired systemic immunity in T cells. Clin Exp Allergy, 45(1), 238-248.

Holme, J. A., Vondráček, J., Machala, M., Lagadic-Gossmann, D., Vogel, C. F. A., Le Ferrec, E., Sparfel, L., & Øvrevik, J. (2023). Lung cancer associated with combustion particles and fine particulate matter (PM(2.5)) - The roles of polycyclic aromatic hydrocarbons (PAHs) and the aryl hydrocarbon receptor (AhR). Biochem Pharmacol, 216, 115801.

Huang da, W., Sherman, B. T., & Lempicki, R. A. (2009). Systematic and integrative analysis of large gene lists using DAVID bioinformatics resources. Nat Protoc, 4(1), 44-57.

Jung, K. H., Perzanowski, M., Rundle, A., Moors, K., Yan, B., Chillrud, S. N., Whyatt, R., Camann, D., Perera, F. P., & Miller, R. L. (2014). Polycyclic aromatic hydrocarbon exposure, obesity and childhood asthma in an urban cohort. Environ Res, 128, 35-41.

Karimi, P., Peters, K. O., Bidad, K., & Strickland, P. T. (2015). Polycyclic aromatic hydrocarbons and childhood asthma. Eur J Epidemiol, 30(2), 91-101.

Låg, M., Øvrevik, J., Refsnes, M., & Holme, J. A. (2020). Potential role of polycyclic aromatic hydrocarbons in air pollution-induced non-malignant respiratory diseases. Respir Res, 21(1), 299.

Li, S., Wu, W., Wang, G., Zhang, X., Guo, Q., Wang, B., Cao, S., Yan, M., Pan, X., Xue, T., Gong, J., & Duan, X. (2022). Association between exposure to air pollution and risk of allergic rhinitis: A systematic review and meta-analysis. Environ Res, 205, 112472.

Li, Z., Yu, S., Jiang, Y., & Fu, Y. (2022). Chemokines and chemokine receptors in allergic rhinitis: from mediators to potential therapeutic targets. Eur Arch Otorhinolaryngol, 279(11), 5089-5095.

Liu, G., Niu, Z., Van Niekerk, D., Xue, J., & Zheng, L. (2008). Polycyclic aromatic hydrocarbons (PAHs) from coal combustion: emissions, analysis, and toxicology. Rev Environ Contam Toxicol, 192, 1-28.

Liu, J., Chen, G., Qin, X., Sun, Q., & Guo, Z. (2024). Effects of Benzo[α]pyrene on Mucus Secretion and Tissue Remodeling in a Rat Model of Allergic Rhinitis. Ann Otol Rhinol Laryngol, 133(10), 886-892.

Lu, C., Liu, Z., Liao, H., Yang, W., Li, Q., & Liu, Q. (2022). Effects of early life exposure to home environmental factors on childhood allergic rhinitis: Modifications by outdoor air pollution and temperature. Ecotoxicol Environ Saf, 244, 114076.

Lubitz, S., Schober, W., Pusch, G., Effner, R., Klopp, N., Behrendt, H., & Buters, J. T. (2010). Polycyclic aromatic hydrocarbons from diesel emissions exert proallergic effects in birch pollen allergic individuals through enhanced mediator release from basophils. Environ Toxicol, 25(2), 188-197.

Malik, A. I., Rowan-Carroll, A., Williams, A., Lemieux, C. L., Long, A. S., Arlt, V. M., Phillips, D. H., White, P. A., & Yauk, C. L. (2013). Hepatic genotoxicity and toxicogenomic responses in Muta™Mouse males treated with dibenz[a,h]anthracene. Mutagenesis, 28(5), 543-554.

Mizutani, N., Nabe, T., Ohtani, Y., Han, H. Y., Fujii, M., Yoshino, S., Hirayama, T., & Kohno, S. (2007). Polycyclic aromatic hydrocarbons aggravate antigen-induced nasal blockage in experimental allergic rhinitis. J Pharmacol Sci, 105(3), 291-297.

Shannon, P., Markiel, A., Ozier, O., Baliga, N. S., Wang, J. T., Ramage, D., Amin, N., Schwikowski, B., & Ideker, T. (2003). Cytoscape: a software environment for integrated models of biomolecular interaction networks. Genome Res, 13(11), 2498-2504.

Srogi, K. (2007). Monitoring of environmental exposure to polycyclic aromatic hydrocarbons: a review. Environ Chem Lett, 5(4), 169-195.

Tajima, H., Tajiki-Nishino, R., Watanabe, Y., Kurata, K., & Fukuyama, T. (2020). Activation of aryl hydrocarbon receptor by benzo[a]pyrene increases interleukin 33 expression and eosinophil infiltration in a mouse model of allergic airway inflammation. J Appl Toxicol, 40(11), 1545-1553.

Trott, O., & Olson, A. J. (2010). AutoDock Vina: improving the speed and accuracy of docking with a new scoring function, efficient optimization, and multithreading. J Comput Chem, 31(2), 455-461.

Wang, S. Y., Chen, Q., Chen, Z. X., Chen, J., Yuan, J., Dai, L. S., Chen, L. G., & Zhang, X. D. (2025). Impact of metabolic enzyme activity variability on dabrafenib disposition. Front Pharmacol, 16, 1643618.

Wang, X., Wang, X., Qi, J., Gong, S., Wang, C., Li, L., Fan, L., Liu, H., Cao, Y., Liu, M., Han, X., Su, L., Yao, X., Tysklind, M., & Wang, X. (2023). Levels, distribution, sources and children health risk of PAHs in residential dust: A multi-city study in China. Sci Total Environ, 862, 160760.

Xiong, G., Wu, Z., Yi, J., Fu, L., Yang, Z., Hsieh, C., Yin, M., Zeng, X., Wu, C., Lu, A., Chen, X., Hou, T., & Cao, D. (2021). ADMETlab 2.0: an integrated online platform for accurate and comprehensive predictions of ADMET properties. Nucleic Acids Res, 49(W1), W5-w14.

Yu, Y. Y., Jin, H., & Lu, Q. (2022). Effect of polycyclic aromatic hydrocarbons on immunity. J Transl Autoimmun, 5, 100177.

Yumibe, N., Huie, K., Chen, K. J., Snow, M., Clement, R. P., & Cayen, M. N. (1996). Identification of human liver cytochrome P450 enzymes that metabolize the nonsedating antihistamine loratadine. Formation of descarboethoxyloratadine by CYP3A4 and CYP2D6. Biochem Pharmacol, 51(2), 165-172.

Zhang, Y., Lan, F., & Zhang, L. (2021). Advances and highlights in allergic rhinitis. Allergy, 76(11), 3383-3389.

Zhang, Z., Huang, X., Gan, C., Xue, S., He, Y., & Wen, C. (2026). In-vitro and in-vivo CYP3A4 Variants: Neratinib metabolism and drug interaction risk. Chem Biol Interact, 427, 111935.

Zheng, J., Zeng, M., Nian, J. B., Zeng, L. Y., Fu, Z., Huang, Q. J., & Wei, X. (2020). The CXCR4/miR-125b/FoxP3 axis regulates the function of the epithelial barrier via autophagy in allergic rhinitis. Am J Transl Res, 12(6), 2570-2584.

License: Copyright (c) 2026 Author.
All articles published in this journal are licensed under the Creative Commons Attribution 4.0 International License (CC BY 4.0). This license permits unrestricted use, distribution, and reproduction in any medium, provided the original author(s) and source are properly credited. Authors retain copyright of their work, and readers are free to copy, share, adapt, and build upon the material for any purpose, including commercial use, as long as appropriate attribution is given.

Advances in World Medical Research, 2026, 2(3), 49-77
https://doi.org/10.71204/y50qbv78

Qiliqiangxin Capsule in Patients with Chronic Heart Failure Complicated by Coronary Artery Disease: A Systematic Review and Meta-Analysis of Randomized Trials

Kaijuan Wang [1, #] , Jinhao Xu [1, #], Xiangying Zheng [1, #], Fengshuo Chang [2], Jingen Li [1, *]

[1] Department of Cardiovascular Medicine, Dongzhimen Hospital, Beijing University of Chinese Medicine, Beijing 100700, China

[2] Department of Geriatrics, Xiyuan Hospital, China Academy of Chinese Medical Science, Beijing 100091, China

[#] These authors are co-first authors of the article.

*** Correspondence**:

Jingen Li

lijingen198908@126.com

Received: 17 June 2026/ Accepted: 30 August 2026/ Published online: 30 September 2026

Abstract

To explore the clinical value and potential risk of Qiliqiangxin Capsule, we designed a systematic review and meta-analysis on randomized controlled trials (RCTs), targeting patients diagnosed with both chronic heart failure and coronary artery disease. Our search included eight commonly used databases, focusing on studies that assessed the effectiveness of Qiliqiangxin Capsule and guideline-directed medical therapy for patients whose condition was chronic heart failure complicated by coronary artery disease. We conducted the meta-analysis employing the meta and metafor packages running under R 4.5.3, whereas the risk of bias was assessed using the Cochrane Risk of Bias 2 (RoB 2) tool. After systematic screening procedure, we included 17 studies, involving 2000 eligible patients. The results showed that Qiliqiangxin Capsule combination treatment reduced the occurrences of the primary outcome [RR=0.38,95%CI (0.23,0.63)], left ventricular ejection fraction (LVEF) [MD=5.39,95%CI (4.62,6.16)], left ventricular end-diastolic diameter (LVEDD) [MD=-4.86,95% CI(-6.20,-3.51)], N-terminal B-type natriuretic peptide precursor (NT-proBNP) levels [SMD = -0.82, 95% CI (-0.97, -0.67)], the 6-minute walk test distance (6MWD) [MD=39.05,95%CI(19.90,58.20)], and the clinical efficacy [RR = 1.20, 95% CI (1.14, 1.25)] were also significantly improved. As for the safety evaluation, the incidence of adverse events was not found to differ meaningfully [RR = 0.95, 95% CI (0.60, 1.50)]. The combination of Qiliqiangxin Capsule and guideline-directed medical therapy can safely and effectively improve the heart failure rehospitalization and all-cause mortality in patients with chronic heart failure complicated by coronary artery disease, improve cardiac performance, increase physical capacity. However, further large sample trials are required to confirm the results.

Keywords: Qiliqiangxin Capsule; Chronic Heart Failure; Coronary Artery Disease; Meta-Analysis

1. Introduction

Heart failure (HF) (McDonagh et al., 2021) is widely recognized as a complex, end-stage cardiovascular syndrome. Recent epidemiological data indicates approximately 60 million people worldwide live with HF, with a rapidly increasing prevalence driven by population aging and improved survival following acute cardiovascular events (Bozkurt et al., 2025). Among the diverse etiologies of HF, coronary artery disease (CAD) ranks as the most frequent cause, being responsible for over half of all HF cases in many regions (Chinese Society of Cardiology et al., 2024). The coexistence of HF and CAD creates a synergistic pathophysiological burden, significantly exacerbating clinical symptoms and increasing a greater all-cause mortality risk than either condition alone (Yan et al., 2020).

In modern clinical management, the pharmacological approach to chronic heart failure (CHF) is anchored in guideline-directed medical therapy (GDMT), often referred to as the foundational quadruple therapy (McDonagh et al., 2023), while concomitant CAD is primarily managed with antiplatelet agents and lipid-lowering medications (McDonagh et al., 2021). Although these conventional therapies have demonstrated substantial efficacy in reducing mortality and improving cardiac function parameters, they exhibit notable limitations. Significant numbers of patients still have residual risks, recurrent hospitalizations, and inadequate improvements in long-term quality of life (Fiuzat et al., 2020).

Traditional Chinese Medicine (TCM) has garnered growing recognition for its unique, multi-target therapeutic profile in the management of cardiovascular diseases. Qiliqiangxin capsule, a well-established TCM formulation and formulated with 11 medicinal botanicals, has been included in national HF guidelines in China and has demonstrated promising cardioprotective effects, including reducing myocardial fibrosis and modulating neurohormonal activation (Cheang et al., 2024).

In the last decade, a large number of small-sample randomized controlled studies (RCTs) have been carried out, aimed to assessing the therapeutic benefits and safety of Qiliqiangxin capsule for CHF complicated by CAD. Preliminary evidence suggested that Qiliqiangxin Capsule, when added to conventional pharmacotherapy, may improve LVEF, reduced NT-proBNP levels, enhance physical capacity (e.g., 6-minute walk distance), and potentially lower rehospitalization rates. Notably, the recent landmark QUEST trial (Qiliqiangxin in Heart Failure: Assessment of Reduction in Mortality) provided robust evidence that Qiliqiangxin Capsule significantly reduced the composite risk of cardiovascular death and HF hospitalization in patients with reduced ejection fraction (Cheang et al., 2024). Despite these encouraging findings, comprehensive and rigorous systematic evaluations specifically targeting the subpopulation of CHF patients with concomitant CAD remain scarce. To address this critical lack of evidence, we performed a meta-analysis of trials examining Qiliqiangxin Capsule in patients with CHF complicated by CAD, comprehensively and systematically evaluating its efficacy and safety.

2. Materials and Methods

We designed and executed this systematic review under Preferred Reporting Items for Systematic Reviews and Meta-Analyses (PRISMA) 2020 statement (Page et al., 2021). Prospective registration in PROSPERO (ID number: 420251236471) and the completed PRISMA checklist is available in the Supplementary Materials (Table S1).

2.1. Eligibility Criteria

Studies were deemed eligible for inclusion if they satisfied all of the following conditions: (i) Adult patients with definite CHF and coexisting CAD, and whose HF symptom severity ranged from New York Heart Association (NYHA) class II to IV, irrespective of on age, sex, geographic region, or disease duration. (ii) Qiliqiangxin Capsule (4 capsules [1.2 g] per dose, three times daily) administered in combination with standard treatment for at least 12 weeks. (iii) Standard treatment alone or with placebo. Standard treatment included lipid-lowering therapy, vasodilators, antiplatelet agents, angiotensin-converting enzyme inhibitors (ACEI)/angiotensin receptor blockers (ARB)/angiotensin receptor-neprilysin inhibitors (ARNI), beta-blockers, mineralocorticoid receptor antagonists (MRA), and sodium-glucose cotransporter-2 inhibitors (SGLT2i). (iv) Reporting outcomes of interest.The primary outcome was the composite of HF rehospitalization or all-cause mortality. Secondary outcomes included left ventricular ejection fraction (LVEF), left ventricular end-diastolic dimension (LVEDD), N-terminal pro-B-type natriuretic peptide (NT-proBNP), 6-minute walk test distance (6MWD), clinical response rate (defined as improvement in NYHA functional class by ≥2 levels or achievement of class I as effective; no change or deterioration in NYHA functional class as ineffective), (Haijing and Zhigang, 2022) and the incidence of adverse events. (v) RCTs were eligible, irrespective of language (Chinese or English). Studies metting the following criteria have been excluded: (i) obviously erroneous information, duplicate publication; (ii) lack of recognized diagnostic criteria and established guidelines, rendering definitive diagnosis of CHF or CAD uncertain; (iii) concomitant use of other traditional Chinese medicine preparations in addition to the specified proprietary Chinese medicine during the treatment period; or (iv) .treatment duration <12 weeks.

2.2. Search Strategy

An extensive search was carried out in China (CNKI, VIP, Wanfang, and SinoMed) and English (PubMed, Web of Science, Embase, and Cochrane Library) databases, for all records published up to November 30, 2025. The search terms included heart failure, coronary disease, qiliqiangxin, and RCT. Table S2 contains a full account of the search strategies.

2.3. Literature Selection and Data Extraction

Reference management was facilitated by EndNote 21, and duplicate citations were excluded before screening. Two reviewers (W.K.J., X.J.H.) independently conducted a three-phase screening and data extraction process: (i) preliminary screening the title and abstract to eliminate duplicates and studies irrelevant to the research topic; (ii) full-text review of candidate studies using eligibility criteria; and (iii) standardized data extraction with independent cross-verification between reviewers. The extracted data elements included the first author's name, year, baseline patient characteristics

(sample size, sex distribution, mean age), intervention and comparison details, outcomes and randomization method. Disagreements were resolved by discussion or third-reviewer adjudication.

2.4. Risk of Bias Assessment

Methodological quality was evaluated in the Cochrane RoB 2 tool (Sterne et al., 2019). Each domain was rated as low risk, some concerns, or high risk. Disagreements were resolved by discussion or third-reviewer adjudication.

2.5. Statistical Analysis

Meta-analyses were performed using R software (version 4.5.3). Given the anticipated clinical and methodological heterogeneity, random-effects models with 95% confidence intervals estimated using the Hartung–Knapp–Sidik–Jonkman method were employed for all pooled estimates. Treatment effects on dichotomous outcomes were expressed as relative risk (RR). Mean difference (MD) and standardized mean difference (SMD) for continuous outcomes.Two-sided $P < 0.05$ was significant. Heterogeneity was quantified using Cochran's Q and I^2 (τ^2 for variance), with $I^2 > 50\%$ and Q $P < 0.10$ defining significance.Subgroup analyses found heterogeneity sources. Sensitivity used leave-one-out and fixed-effect replacement. Publication bias was evaluated via funnel plots and Egger's test. A two-sided $p<0.05$ on Egger's test, in conjunction with significant funnel plot asymmetry, was considered indicative of potential publication bias. Trim-and-fill was applied when bias was detected (Duval and Tweedie, 2000).

3. Results

3.1. Literature Search and Study Selection

The search output 615 records, 304 duplicates were removed. The remaining 311 were screened by title and abstract, with 205 excluded as irrelevant. Full-text review of 106 articles against eligibility criteria yielded 17 included studies. Figure 1 provides the PRISMA 2020 flow chart.

3.2. Characteristics of Included Studies

Seventeen RCTs with 2000 participants were included, equally divided between Qiliqiangxin Capsule (n = 1,000) and standard therapy (n = 1,000) (Boying et al., 2022; Changqing et al., 2021; Danmei and Zhengjian, 2017; Hua, 2017; Jiang, 2019; Jiaqi et al., 2025; Jinhua, 2019; Jinyu et al., 2020; Meijuan et al., 2024; Ronglai, 2020; Shige et al., 2024; Shisheng et al., 2020; Wang and Zhang, 2024; Xiling, 2020; Xinhua et al., 2014; Yaoqi et al., 2020; Yuxian et al., 2021) . The trials enrolled a minimum of 60 and a maximum of 236 participants, and treatment duration varied between 12 weeks and 6 months. Of the 17 studies, only one study employed placebo control (Changqing et al., 2021). All eligible studies reported comparable baseline characteristics between groups. Table 1 contains the baseline characteristics of the included studies.

Guo SS 2020	34/34	21/13	20/14	72.19 ± 4.53	71.84 ± 4.35	Random number table
Yang RL 2020	39/39	15/24	16/23	64.1 ± 12.2	63.6 ± 11.2	Random allocation
Zhao XL 2020	85/85	45/40	43/42	72.6 ± 2.3	73.5 ± 2.8	Random allocation
Chen YX 2021	116/116	63/53	61/55	58.35 ± 6.62	57.26 ± 7.05	Random number table
Xia CQ 2021	47/47	36/11	34/13	69.03 ± 6.84	68.12 ± 6.91	Random number table
Qin BY 2022	43/43	23/20	25/18	64.61 ± 4.68	64.58 ± 4.69	Randomized envelope
Li SG 2024	40/40	21/19	24/16	63.83 ± 6.14	62.97 ± 5.68	Random allocation
Qi MJ 2024	37/37	31/6	28/9	60.46 ± 8.45	61.65 ± 9.99	Random number table
Wang LJ 2024	79/79	38/41	39/40	59.48 ± 9.77	59.42 ± 9.72	Simple randomization
Huo JQ 2025	118/118	74/44	77/41	63.88 ± 7.69	63.57 ± 7.17	Simple randomization

Note: T, treatment group (Qiliqiangxin Capsule); C, control group; QLQX, Qiliqiangxin Capsule. ① Primary composite outcome (heart failure rehospitalization or all-cause mortality); ② LVEF; ③ LVEDD; ④ NT-proBNP; ⑤ 6MWD; ⑥ clinical response rate; ⑦ incidence of adverse events.

Table 1. Baseline characteristics of included studies (cont.)

Study	**Intervention**		**Treatment duration**	**Outcome**
	T	**C**		
Chen XH 2014	Standard therapy + QLQX	Standard therapy	6 months	①②③④
Yao DM 2017	Standard therapy + QLQX	Standard therapy	3 months	④
Wang H 2017	Standard therapy + QLQX	Standard therapy	6 months	②③④⑥
Yu J 2019	Standard therapy (bisoprolol fumarate) + QLQX	Standard therapy (bisoprolol fumarate)	3 months	②③⑦
Guo JH 2019	Standard therapy (trimetazidine) + QLQX	Standard therapy (trimetazidine)	3 months	②③⑤⑥
Chen YQ 2020	Standard therapy + QLQX	Standard therapy	6 months	②③④⑤⑥
Song JY 2020	Standard therapy (milrinone) + QLQX	Standard therapy (milrinone)	3 months	②③④⑤⑥
Guo SS 2020	Standard therapy (trimetazidine) + QLQX	Standard therapy (trimetazidine)	12 weeks	⑥
Yang RL 2020	Standard therapy + QLQX	Standard therapy	3 months	①②③⑥
Zhao XL 2020	Standard therapy (trimetazidine) + QLQX	Standard therapy (trimetazidine)	3 months	⑥

Chen YX 2021	Standard therapy + QLQX	Standard therapy	3 months	②③⑥
Xia CQ 2021	Standard therapy + QLQX	Standard therapy + placebo	12 weeks	②③④⑤⑥⑦
Qin BY 2022	Standard therapy (trimetazidine) + QLQX	Standard therapy (trimetazidine)	12 weeks	②③④⑤⑦
Li SG 2024	Standard therapy (sacubitril/valsartan) + QLQX	Standard therapy (sacubitril/valsartan)	3 months	②⑥⑦
Qi MJ 2024	Standard therapy (dapagliflozin) + QLQX	Standard therapy (dapagliflozin)	3 months	⑥
Wang LJ 2024	Standard therapy (trimetazidine) + QLQX	Standard therapy (trimetazidine)	6 months	②③④⑤⑥⑦
Huo JQ 2025	Standard therapy (sacubitril/valsartan) + QLQX	Standard therapy (sacubitril/valsartan)	12 weeks	②③④⑤⑥

Note: T, treatment group (Qiliqiangxin Capsule); C, control group; QLQX, Qiliqiangxin Capsule. ① Primary composite outcome (heart failure rehospitalization or all-cause mortality); ② LVEF; ③ LVEDD; ④ NT-proBNP; ⑤ 6MWD; ⑥ clinical response rate; ⑦ incidence of adverse events.

3.3. Methodological Quality Assessment

Each of the 17 studies were published as journal articles (Boying et al., 2022; Changqing et al., 2021; Danmei and Zhengjian, 2017; Hua, 2017; Jiang, 2019; Jiaqi et al., 2025; Jinhua, 2019; Jinyu et al., 2020; Meijuan et al., 2024; Ronglai, 2020; Shige et al., 2024; Shisheng et al., 2020; Wang and Zhang, 2024; Xiling, 2020; Xinhua et al., 2014; Yaoqi et al., 2020; Yuxian et al., 2021). For the randomization process, three studies (Jiaqi et al., 2025; Jinyu et al., 2020; Wang and Zhang, 2024) employed simple randomization, one (Boying et al., 2022) used a sealed envelope method, seven studies (Changqing et al., 2021; Jiang, 2019; Jinhua, 2019; Meijuan et al., 2024; Shisheng et al., 2020; Yaoqi et al., 2020; Yuxian et al., 2021) utilized a random number table to generate the allocation sequence, and all of these trials were rated at low risk; six studies merely stated that randomization was performed without specifying the method and were judged as some concerns (Danmei and Zhengjian, 2017; Hua, 2017; Ronglai, 2020; Shige et al., 2024; Xiling, 2020; Xinhua et al., 2014). Baseline characteristics were generally comparable across all included studies. Regarding deviations from intended interventions, one placebo-controlled trial was assessed as low risk (Changqing et al., 2021); the other 16 trials (non-placebo, unblinded) were high risk. For missing outcome data, no patient attrition or data loss occurred in any study, and they were classified as low risk. For measurement of the outcome, two studies (Ronglai, 2020; Xinhua et al., 2014) incorporated subjective endpoints without explicit assessor blinding and were classified as some concerns; the remaining studies employed objective outcome measurement criteria and were judged as low risk. For selection of the reported result, none of the reports referred to a prespecified protocol, and all were rated as some concerns. Figures S1 and S2 present the detailed outcomes of the bias assessment results.

3.4. Meta-Analysis Results

3.4.1. Primary Outcome

Two studies (Ronglai, 2020; Xinhua et al., 2014) reported the primary composite endpoint (HF rehospitalization or all-cause death), with 138 patients included (69 allocated to the Qiliqiangxin capsule arm and 69 to the control group). The pooled risk ratio was 0.38 (95% CI: 0.23–0.63), suggesting a significantly meaningful reduction in the Qiliqiangxin capsule arm (Figure 2). Heterogeneity was absent (I^2 = 0.0%, p = 0.4418). Sensitivity analysis using a fixed-effect model showed that the effect estimates remained consistent in direction.

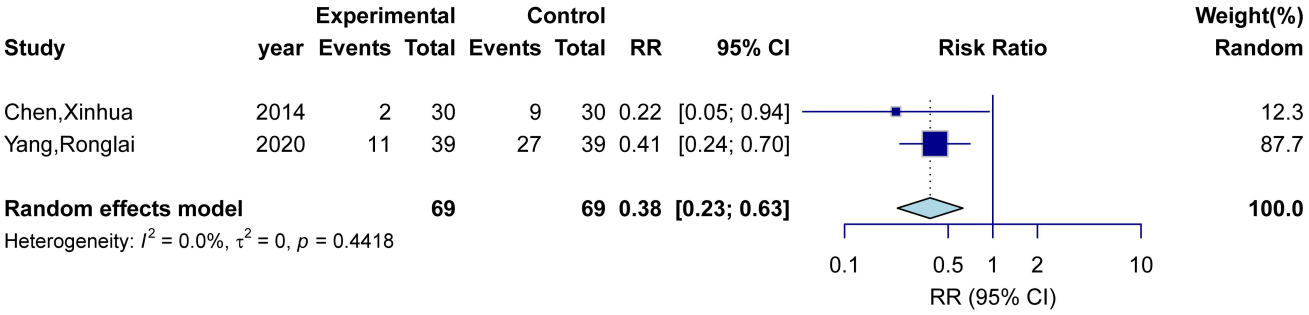


Figure 2. Forest Plot of the Primary outcome

3.4.2. LVEF

A total of 13 studies (Boying et al., 2022; Changqing et al., 2021; Hua, 2017; Jiang, 2019; Jiaqi et al., 2025; Jinhua, 2019; Jinyu et al., 2020; Ronglai, 2020; Shige et al., 2024; Wang and Zhang, 2024; Xinhua et al., 2014; Yaoqi et al., 2020; Yuxian et al., 2021) reported LVEF, comprising 1602 patients (801 allocated to the Qiliqiangxin capsule arm and 801 to the control arm). The pooled mean difference was 5.82 (95% CI: 4.68–6.96), indicating that Qiliqiangxin capsule significantly improved LVEF compared with control. Notable heterogeneity was observed across the studies, with an I^2 of 68.1% and p of 0.0002 (Figure 3A). A subgroup analysis was conducted by duration of treatment (≤3 months versus >3 months) to investigate the possible sources of heterogeneity (Figure S3). In the short-duration subgroup (≤3 months), heterogeneity remained substantial (I^2 = 77.4%, p <0.0001). In the long-duration subgroup (>3 months), heterogeneity was absent (I^2 = 0.0%, τ^2 = 0, p = 0.62). Treatment duration alone does not fully explain the observed between-study variability. Leave-one-out sensitivity analysis showed that effect estimates remained directionally consistent across all iterations; however, the removal of one study (Ronglai,2020) markedly reduced heterogeneity (I^2 = 36.2%, p =0.1008), yielding an adjusted pooled estimate of MD =5.39 (95% CI: 4.62, 6.16,) (Figure S4). Detailed inspection revealed that this study enrolled a population with a male-to-female ratio <1, whereas all other studies reported ratios ≥1, suggesting that differential sex distribution may have contributed to clinical heterogeneity. Attributable to the fact that women demonstrate higher stroke volume at identical end-diastolic volume (Arata et al.,2023), with consequent sex-based differences in ejection fraction. The funnel plot showed potentially asymmetric; however, Egger's test was not statistically significant (t = 0.97, P = 0.3538), suggesting absence of small-study effects (Figure S5).

3.4.3. NT-proBNP

A total of 9 studies (Boying et al., 2022; Changqing et al., 2021; Danmei and Zhengjian, 2017; Hua, 2017; Jiaqi et al., 2025; Jinyu et al., 2020; Wang and Zhang, 2024; Xinhua et al., 2014; Yaoqi et al., 2020) reported NT-proBNP, comprising 1114 patients (557 allocated to the Qiliqiangxin capsule group and 557 to the control group). Due to unit heterogeneity, SMD was used. A pooled analysis provided a SMD of -1.48 (95% CI: -2.40 to -0.55), indicating that Qiliqiangxin capsule significantly reduced NT-proBNP levels compared with control. Heterogeneity was considerable ($I^2 = 95.9\%$, $p < 0.0001$) (Figure 3B). Subgroup analyses were conducted by duration of treatment (≤3 months versus >3 months) to investigate possible sources of heterogeneity (Figure S6). In the short-duration subgroup (≤3 months), heterogeneity remained considerable ($I^2 = 91.6\%$, $p < 0.00001$), and in the long-duration subgroup (>3 months), heterogeneity remained considerable ($I^2 = 97.9\%$, $p = 0.37$), indicating that the duration of treatment does not represent a source of heterogeneity. Sensitivity analyses demonstrated directional consistency of effect estimates. Detailed inspection identified one study (Changqing et al., 2021) that substantially contributed to heterogeneity; this trial employed western conventional therapy plus placebo in the control group, whereas all other studies used blank control, representing a methodological design difference that may have introduced heterogeneity. Furthermore, one study (Wang and Zhang, 2024) used trimetazidine in both arms, potentially introducing clinical heterogeneity. Removal of these studies yielded a SMD of -0.82 (95% CI: -0.97 to -0.67) , and heterogeneity was reduced ($I^2 = 9.4\%$, $P = 0.3570$) (Figure S7).

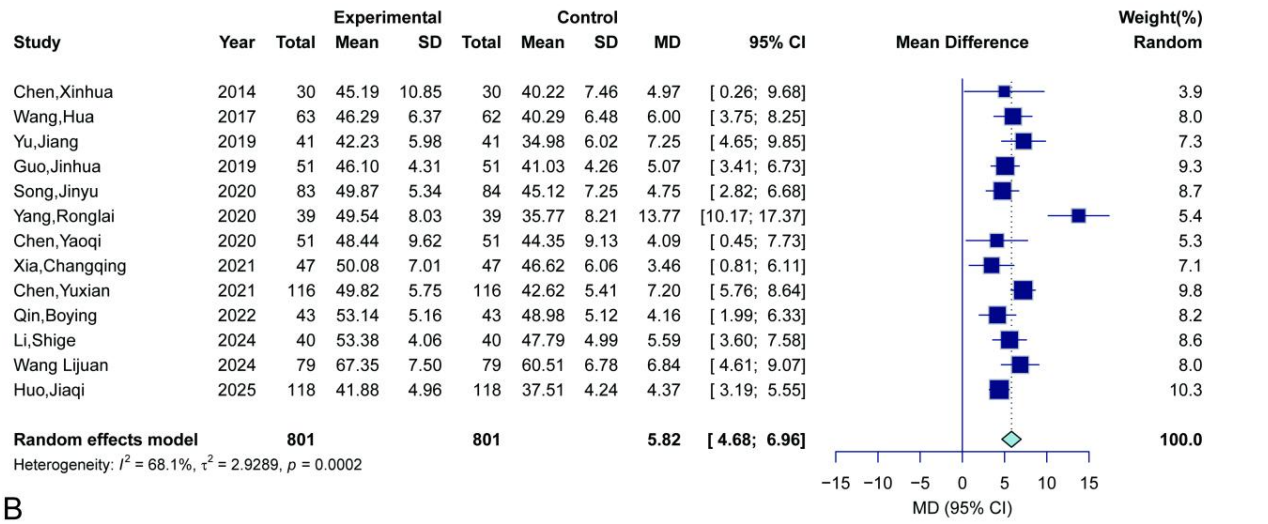
3.4.4. 6MWD

A total of 7 studies (Boying et al., 2022; Changqing et al., 2021; Jiaqi et al., 2025; Jinhua, 2019; Jinyu et al., 2020; Wang and Zhang, 2024; Yaoqi et al., 2020) reported 6MWD, comprising 945 patients (472 allocated to the Qiliqiangxin capsule arm and 473 to the control arm). The pooled MD was 39.05 meters (95% CI: 19.90 to 58.20), indicating that Qiliqiangxin capsule significantly improved 6MWD compared with control. Notable heterogeneity was observed across the studies, with an I^2 of 87.7% ($p < 0.0001$) (Figure 3C). In order to investigate the potential sources, we performed subgroup analyses that were stratified by NYHA class (II vs. III–IV) and duration of treatment. These findings (Figure S8,9) suggest that neither treatment duration nor baseline heart failure severity accounts for the observed clinical diversity. Variations in baseline patient age and disease duration across studies may represent potential sources of clinical heterogeneity. Leave-one-out approach and alternative statistical models demonstrated consistent directionality of effect estimates.

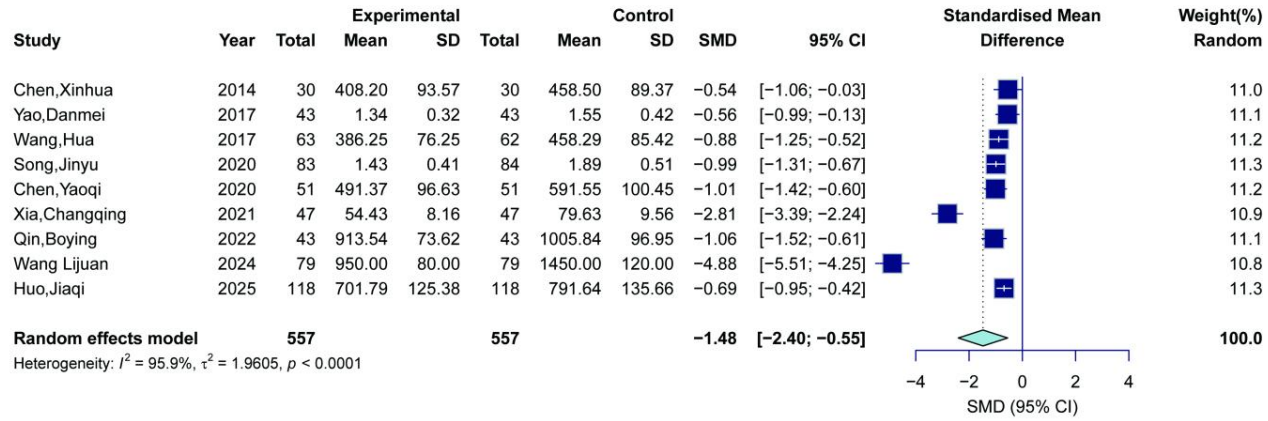
3.4.5. LVEDD

A total of 12 studies (Boying et al., 2022; Changqing et al., 2021; Hua, 2017; Jiang, 2019; Jiaqi et al., 2025; Jinhua, 2019; Jinyu et al., 2020; Ronglai, 2020; Wang and Zhang, 2024; Xinhua et al., 2014; Yaoqi et al., 2020; Yuxian et al., 2021) reported LVEDD, comprising 1522 patients (761 allocated to the Qiliqiangxin capsule arm and 761 to the control arm). The pooled MD was -4.93 (95% CI: -6.09 to -3.76) indicating that Qiliqiangxin capsule significantly reduced LVEDD compared with control. Heterogeneity was considerable ($I^2 = 80.5\%$, $p < 0.0001$) (Figure 4A). To investigate potential sources, we performed a subgroup analysis stratified by treatment duration (≤3 months versus >3 months) (Figure S10).

A



B



C

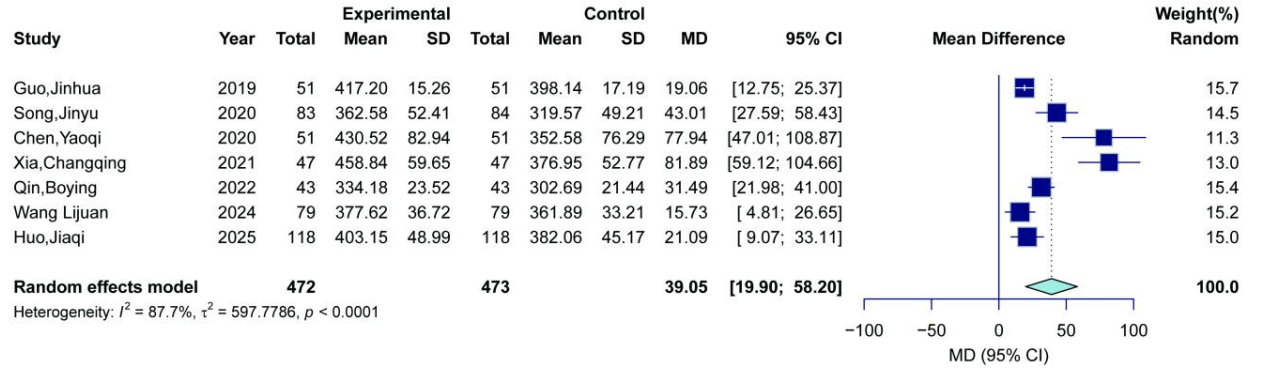


Figure 3. Forest Plot of LVEF , NT-pro BNP and 6MWD

In the short-duration subgroup (≤3 months), heterogeneity was negligible (I^2 = 0%, p = 0.438). In the long-duration subgroup (>3 months), heterogeneity remained substantial (I^2 = 70.4%, p = 0.018). Treatment duration alone does not fully explain the observed between-study variability. Sensitivity analyses demonstrated directional consistency of effect estimates. Detailed inspection of the long-duration subgroup identified one study (Yaoqi et al., 2020) enrolled a population in which 61 (59.8%) of 102 with CHF and CAD patients who had received percutaneous coronary intervention (PCI). This high prevalence of prior revascularization may have contributed to the observed clinical heterogeneity. Furthermore, the concomitant use of trimetazidine in both the experimental and control groups of one study (Wang and Zhang, 2024) may introduce clinical heterogeneity. Removal of these studies

yielded a MD of -4.86 (95% CI: -6.20 to -3.51), and heterogeneity was reduced (Figure S11). The funnel plot appeared potentially asymmetric; however, Egger's test was not statistically significant (t = -0.60, p = 0.5598), suggesting absence of small-study effects (Figure S12).

3.4.6. Clinical Response Rate

Thirteen studies (Changqing et al., 2021; Hua, 2017; Jiaqi et al., 2025; Jinhua, 2019; Jinyu et al., 2020; Meijuan et al., 2024; Ronglai, 2020; Shige et al., 2024; Shisheng et al., 2020; Wang and Zhang, 2024; Xiling, 2020; Yaoqi et al., 2020; Yuxian et al., 2021)reported clinical response rate, comprising a total of 1686 patients (843 allocated to the experimental arm and 843 to the control arm). The pooled risk ratio was 1.20 (95% CI:1.14,1.25) showed that the clinical response rate was significantly improved, with low between-study heterogeneity (I^2 = 0%, p =0.5022 for heterogeneity) (Figure 4B). Sensitivity analyses demonstrated directional consistency of effect estimates.

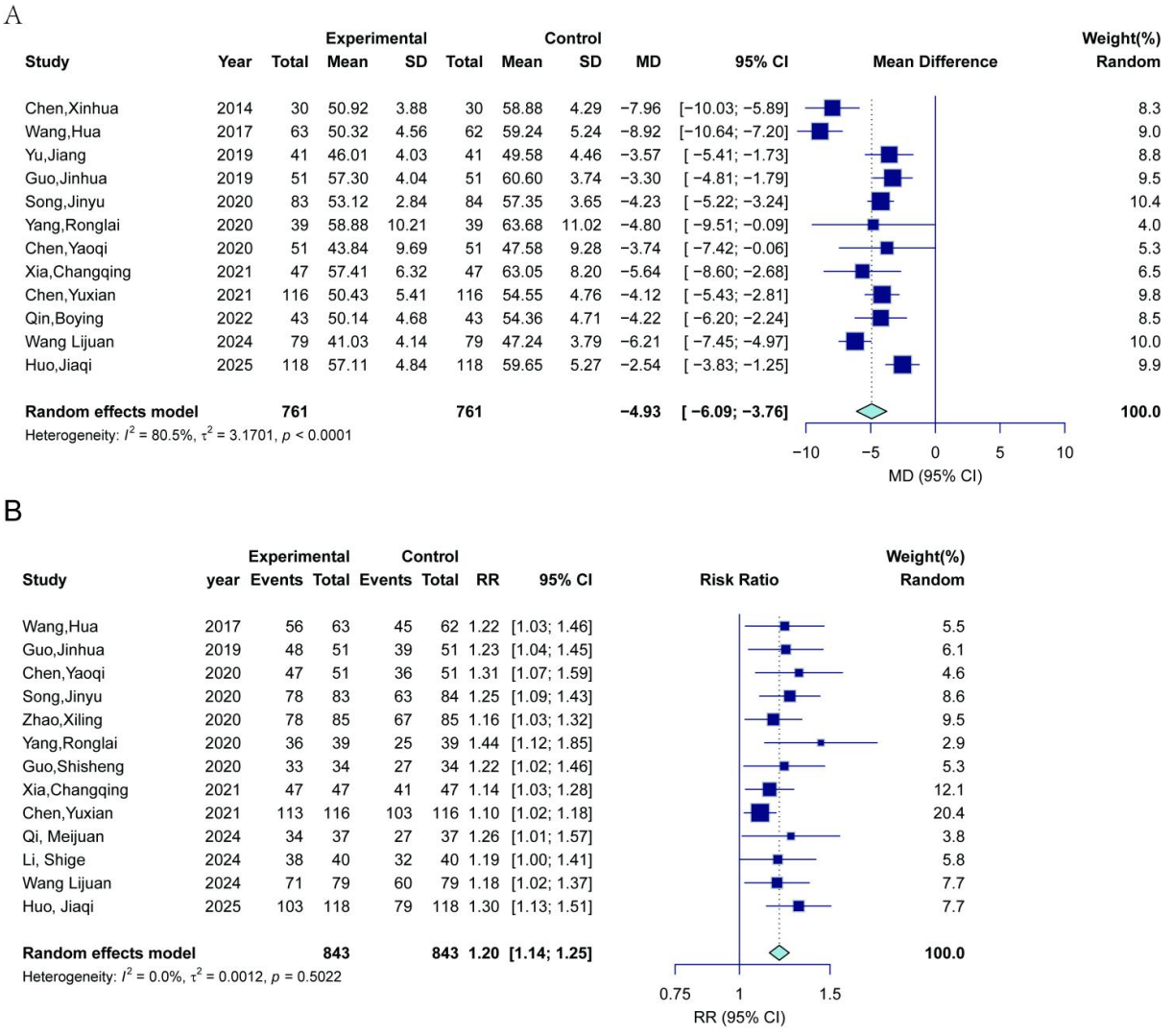


Figure 4. Forest Plot of LVEDD and Clinical Response Rate

3.5. Adverse Events

Eight studies (Boying et al., 2022; Changqing et al., 2021; Jiang, 2019; Jinhua, 2019; Jinyu et al., 2020; Shige et al., 2024; Wang and Zhang, 2024; Xiling, 2020) reported adverse events, of which three (Jinhua, 2019; Jinyu et al., 2020; Xiling, 2020) indicated no notable adverse events in either

group, and five (Boying et al., 2022; Changqing et al., 2021; Jiang, 2019; Shige et al., 2024; Wang and Zhang, 2024) provided detailed reports of specific adverse events. The control group reported 38 adverse events, the most common being headache and dizziness (n=10) and gastrointestinal dysfunction (n=9). In the experimental group, 34 adverse events were documented, among which dizziness and headache (n=9) and gastrointestinal discomfort (n=6) were the most common. Detailed information on adverse events is provided in Table S3. The pooled risk ratio was 0.95 (95% CI: 0.60 - 1.50), with between-study heterogeneity (I^2=13.6%, p=0.3275 for heterogeneity) (Figure 5), showing that adverse event rates did not differ significantly between groups. Sensitivity analyses employing a fixed-effect model and a leave-one-out approach demonstrated consistent directionality of effect estimates.

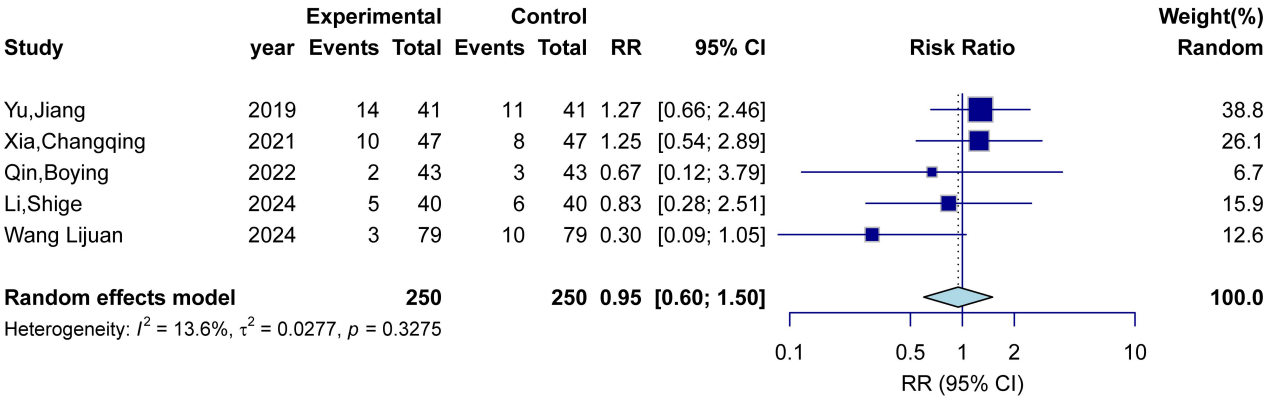


Figure 5. Forest Plot of Adverse Events

4. Discussion

The present meta-analysis for the first time found that Qiliqiangxin capsules combined with GDMT significantly reduced the composite outcome of HF rehospitalization or all-cause mortality in CHF patients complicated by CAD. In addition, Qiliqiangxin capsules also favorably modified markers of cardiac remodeling and ventricular function. These benefits were observed alongside a favorable safety profile, with no significant increase in adverse events. Collectively, these findings support the therapeutic relevance of Qiliqiangxin capsules in CHF with CAD, and highlight the need for further high-quality trials to refine patient selection and optimize integration with contemporary cardiovascular therapeutics.

CHF and CAD are characterized by a complex bidirectional interplay, wherein both conditions are tightly linked through shared pathophysiological mechanisms including myocardial ischemic injury, ventricular remodeling, neurohormonal activation, inflammatory response, oxidative stress, microcirculatory dysfunction, and metabolic remodeling.

CAD represents the most common etiology of heart failure. Atherosclerotic coronary stenosis or occlusion induces sustained myocardial hypoxia, precipitating myocardial infarction (MI). Necrotic myocardium is subsequently replaced by fibrotic scar tissue, causing pathological structure and function cardiac changes and ventricular remodeling (Jiang et al., 2023), thereby exacerbating heart failure. Heart failure induces hemodynamic derangement, reducing coronary perfusion pressure. Concurrently, sympathetic nervous system (SNS) activation increases oxygen demand, the supply–

demand mismatch exacerbates myocardial ischemia (Heusch, 2022). Simultaneously, myocardial injury triggers pathological overactivation of the renin-angiotensin-aldosterone system (RAAS) and the SNS (Jia et al., 2018), resulting in myocardial fibrosis, cytotoxic injury, and progressive ventricular remodeling that drives further deterioration of heart failure. This aberrant RAAS and SNS activation also increases myocardial oxygen consumption, promotes vasoconstriction, intensifies myocardial ischemia, and fosters a prothrombotic milieu. Furthermore, myocardial ischemia and hypoxia induce mitochondrial metabolic remodeling (Zhou and Tian, 2018), engendering oxidative stress, activating downstream signaling pathways, and triggering cytokine release, leading to cardiomyocyte apoptosis or necrosis and heart failure. Concurrently, oxidative activation and inflammatory response impair endothelial integrity, promoting plaque instability and aggravating vascular stenosis (Libby, 2002). Additionally, CAD induces coronary microcirculatory dysfunction (Vrints et al., 2024), precipitating sustained subclinical myocardial ischemia and culminating in heart failure with preserved or reduced ejection fraction (HFpEF/HFrEF). Insufficient myocardial perfusion exacerbates myocardial ischemia, stenosis, and plaque instability. Thus, CHF and CAD constitute a vicious cycle of mutually reinforcing pathologies, wherein each condition serves as both cause and consequence, significantly increasing the risks of recurrent hospitalization and all-cause mortality (Yan et al., 2020). Thus a novel strategy targeting this patient population is needed.

Qiliqiangxin capsules, a standardized commercial formulation comprising 11 herbal ingredients, has demonstrated multiple cardioprotective effects across diverse experimental and clinical settings. Mass spectrometry analysis has identified up to 173 potentially active compounds in Qiliqiangxin capsules, including astragaloside IV, tanshinone IIA, ginsenosides (Rb1, Rg1, and Re), periplocymarin, and alisol A (Packer, 2023). Astragaloside IV attenuates cardiomyocyte apoptosis (Jia et al., 2014) and enhances glucose uptake (Zhu et al., 2016); ginsenosides inhibit the pressure-overload heart failure (Yang et al., 2018), and reduce oxidative stress and proinflammatory signaling(Qin et al.,2019); tanshinone IIA ameliorates myocardial ischemia–reperfusion injury (Li et al., 2016). These experimental findings converge with the conceptual framework proposed by Packer, who posited that Qiliqiangxin capsules probably directly bind to RXRα, augmenting glucose and fatty acid oxidation, promoting mitochondrial health and mitophagy, and attenuating proinflammatory and profibrotic signaling. Collectively, these mechanisms may be the basis for the efficacy of Qiliqiangxin capsules in CHF complicated by CAD.

This study designated the composite hard outcome was identified as the primary outcome of HF rehospitalization or all-cause mortality, focusing on the interventional effect of Qiliqiangxin Capsule in CHF complicated by CAD. Compared with similar studies predominantly employing clinical response rate, heart failure biomarkers, and cardiac function-related indicators (Yahui et al., 2020; Yan et al., 2021), this approach more directly reflects patient survival status and confers stronger clinical guidance significance. Among them, LVEF, LVEDD, and NT-proBNP are indicative of cardiac function, whereas 6MWD and clinical response rate demonstrate patient exercise tolerance and quality of life. Furthermore, this study identified and elucidated sources of heterogeneity through subgroup analyses and leave-one-out sensitivity analyses. Additionally, publication bias for LVEF and LVEDD was evaluated by means of the funnel plot and Egger's linear regression test.

However, there are some limitations to this research. First, we found that the RCTs that we screened were all Chinese, which may compromise the generalizability of our results globally. Second, the primary outcome was reported in only two studies (Ronglai, 2020; Xinhua et al., 2014) compromising statistical credibility; furthermore, as the primary outcome encompassed merely two studies, Egger's linear regression test was underpowered and was therefore not performed for this outcome. Third, the methodological quality of the included RCTs was modest; several studies lacked explicit randomization protocols and blinding design, with only one RCT employing placebo control while the remainder utilized blank control. The risk of bias assessment yielded predominantly "high risk" judgments; this limitation may inflate the risk of bias. Fourth, for the 6MWD indicator, neither subgroup analyses stratified by treatment duration or heart failure severity classification nor leave-one-out approaches materially attenuated heterogeneity; this persistent heterogeneity may be attributable to multifactorial influences including patient age, sex, and disease duration. In response to these limitations, future large-scale, multicenter, high-quality RCTs conducted across multiple countries are warranted to confirm the superiority of these findings. Moreover, the therapeutic efficacy of Qiliqiingxin Capsule specifically regarding heart failure rehospitalization and all-cause mortality needs to be further validated by additional large-scale RCTs. With respect to study design, rigorous implementation of randomization protocols and blinding procedures should be emphasized to further corroborate these results.

5. Conclusion

Qiliqiangxin Capsule combined with guideline-directed medical therapy in patients with CHF complicated by CAD demonstrated superior efficacy compared with guideline-directed medical therapy alone in reducing the composite endpoint of HF rehospitalization or all-cause mortality, improving left ventricular ejection fraction, decreasing left ventricular end-diastolic dimension, reducing NT-proBNP levels, increasing 6-minute walk distance, and enhancing clinical response rate, without concomitant increase in adverse risk. Future large-scale, multicenter, randomized, double-blind, placebo-controlled clinical trials are needed to further confirm the reliability of these findings.

Author Contributions:

Conceptualization, Kaijuan Wang, Jingen Li, Jinhao Xu and Xiangying Zheng; methodology, Kaijuan Wang, Jingen Li, Jinhao Xu and Xiangying Zheng; software, Kaijuan Wang, Jingen Li, Jinhao Xu and Xiangying Zheng; validation, Kaijuan Wang, Jingen Li, Jinhao Xu and Xiangying Zheng; formal analysis,Kaijuan Wang, Jingen Li, Jinhao Xu and Xiangying Zheng; investigation, Kaijuan Wang, Jingen Li, Jinhao Xu and Xiangying Zheng; resources, Kaijuan Wang, Jingen Li, Jinhao Xu and Xiangying Zheng; data curation, Kaijuan Wang, Jingen Li, Jinhao Xu and Xiangying Zheng; writing—original draft preparation, Kaijuan Wang, Jingen Li, Jinhao Xu and Xiangying Zheng; writing—review and editing, Kaijuan Wang, Jingen Li, Jinhao Xu and Xiangying Zheng; visualization, Kaijuan Wang, Jingen Li, Jinhao Xu, Xiangying Zheng and Fengshuo Chang; supervision, Kaijuan Wang, Jingen Li, Jinhao Xu and Xiangying Zheng; project administration,

Kaijuan Wang, Jingen Li, Jinhao Xu and Xiangying Zheng; funding acquisition, Jingen Li. All authors have read and agreed to the published version of the manuscript.

Funding:

This research was funded by the Sponsored by Beijing Nova Program, grant number 20240484736; Beijing University of Chinese Medicine affiliated Dongzhimen Hospital's Youth Backbone Talent Program, grant number DZMG-QNGG007; Clinical Research and Achievement Commercialization Capacity Improvement Pilot Project of Beijing University of Chinese Medicine, Dongzhimen Hospital grant number DZMG-JBZX-25001; Capital's Funds for Health, grant number 2026-4-4196.

Institutional Review Board Statement:

Not applicable

Informed Consent Statement:

Not applicable

Data Availability Statement:

The original data presented in the study are openly available in CNKI, Wanfang, VIP, Sinomed, Pubmed, Web of Science and Embase.

Acknowledgments:

The authors thank the researchers of the included primary studies for their valuable contributions.

Conflict of Interest:

The authors declare no conflict of interest.

References

Arata, A., Ricci, F., Khanji, M. Y., et al. (2023). Sex Differences in Heart Failure: What Do We Know? J Cardiovasc Dev Dis, 10(7), 277.

Boying, Q., Yinglan, Y., and Ying, T. (2022). Effects of Qiliqiangxin Capsule and Trimetazidine on Serum NT pro BNP Level and Cardiac Function in Patients with Coronary Heart Disease and Heart Failure. Capit Food Med, 29(21).

Bozkurt, B., Ahmad, T., Alexander, K., et al. (2025). HF STATS 2024: Heart Failure Epidemiology and Outcomes Statistics An Updated 2024 Report from the Heart Failure Society of America. J Card Fail, 31(1), 66-116.

Changqing, X., Fang, W., Na, Z., et al. (2021). Curative Efficacy of Qili Qiangxin Capsules in Treatment of Heart Failure of Elderly Patients with Coronary Heart Disease. World Chin Med, 16(18), 2751-2756.

Cheang, I., Yao, W., Zhou, Y., et al. (2024). The traditional Chinese medicine Qiliqiangxin in heart failure with reduced ejection fraction: a randomized, double-blind, placebo-controlled trial. Nat Med, 30(8), 2295-2302.

Chinese Society of Cardiology, Chinese Medical Association, Chinese College of Cardiovascular Physician, C. H. F. a. O. C. M. D. A., and Cardiology, E. B. O. C. J. O. (2024). Chinese guidelines for the diagnosis and treatment of heart failure 2024. Chin J Cardiol 52(03), 235-275.

Danmei, Y., and Zhengjian, L. (2017). Application value of Qili Qiangxin capsule in the treatment of coronary heart disease combined with chronic heart failure. Clin Res Pract, 2(12), 33-34.

Duval, S., and Tweedie, R. (2000). Trim and fill: A simple funnel-plot-based method of testing and adjusting for publication bias in meta-analysis. Biometrics, 56(2), 455-463.

Fiuzat, M., Ezekowitz, J., Alemayehu, W., et al. (2020). Assessment of Limitations to Optimization of Guideline-Directed Medical Therapy in Heart Failure From the GUIDE-IT Trial: A Secondary Analysis of a Randomized Clinical Trial. JAMA Cardiol, 5(7), 757-764.

Haijing, G., and Zhigang, Z. (2022). Pharmacoeconomic evaluation of Qili qiangxin capsule in the treatment of chronic heart failure. China Pharm, 33(02), 209-216.

Heusch, G. (2022). Coronary blood flow in heart failure: cause, consequence and bystander. Basic Res Cardiol, 117(1), 1.

Hua, W. (2017). Effect of Qiliqiangxin capsule on Serum Adiponectin Levels and Heart Function in Patients with Coronary Heart Disease and Heart Failure. Mod J Integr Tradit Chin West Med, 26(22), 2450-2452.

Jia, G., Aroor, A. R., Hill, M. A., and Sowers, J. R. (2018). Role of Renin-Angiotensin-Aldosterone System Activation in Promoting Cardiovascular Fibrosis and Stiffness. Hypertension, 72(3), 537-548.

Jia, Y., Zuo, D., Li, Z., et al. (2014). Astragaloside IV inhibits doxorubicin-induced cardiomyocyte apoptosis mediated by mitochondrial apoptotic pathway via activating the PI3K/Akt pathway. Chem Pharm Bull (Tokyo), 62(1), 45-53.

Jiang, H., Fang, T., and Cheng, Z. (2023). Mechanism of heart failure after myocardial infarction. J Int Med Res, 51(10), 3000605231202573.

Jiang, Y. (2019). Investigation of the Effects of QiliQiangxin Capsule Combined with Bisoprolol on Vascular Endothelial Function and Cardiac Performance in Patients with Coronary Heart Disease and Heart Failure. Med J Chin People's Health, 31(14), 100-102.

Jiaqi, H., Houze, T., Yaling, Z., and Shifeng, X. (2025). Clinical observation of Qiliqiangxin capsule on patients with chronic heart failure complicated with coronary heart disease. Chin Arch Tradit Chin Med, 1-11.

Jinhua, G. (2019). Clinical observation of Qiliqiangxin capsule Combined with Trimetazidine on patients with Heart Failure of Coronary Heart Disease. Mod Diagn Treat, 30(01), 36-37.

Jinyu, S., Xin, D., Jihong, S., and Yongzhi, W. (2020). Effects of Qili Qiangxin Capsule Combined with Milrinone on Arterial Hemodynamics and Heart Function in Patients with Myocardial Infarction Complicated with Heart Failure. Shaanxi J Tradit Chin Med, 41(04), 493-495.

Li, Q., Shen, L., Wang, Z., et al. (2016). Tanshinone IIA protects against myocardial ischemia reperfusion injury by activating the PI3K/Akt/mTOR signaling pathway. Biomed Pharmacother, 84, 106-114.

Libby, P. (2002). Inflammation in atherosclerosis. Nature, 420(6917), 868-874.

Mcdonagh, T. A., Metra, M., Adamo, M., et al. (2021). 2021 ESC Guidelines for the diagnosis and treatment of acute and chronic heart failure. Eur Heart J, 42(36), 3599-3726.

Mcdonagh, T. A., Metra, M., Adamo, M., et al. (2023). 2023 Focused Update of the 2021 ESC Guidelines for the diagnosis and treatment of acute and chronic heart failure. Eur Heart J, 44(37), 3627-3639.

Meijuan, Qi., Han, Z., Fenfen, Z., et al. (2024). Efficacy of Qili Qiangxin capsule combined with dapagliflozin in treatment of newly developing heart failure after acute myocardial infarction. Chin J Drug Appl & Monit, 21(05), 661-664.

Packer, M. (2023). Qiliqiangxin: A multifaceted holistic treatment for heart failure or a pharmacological probe for the identification of cardioprotective mechanisms? Eur J Heart Fail, 25(12), 2130-2143.

Page, M. J., Mckenzie, J. E., Bossuyt, P. M., et al. (2021). The PRISMA 2020 statement: an updated guideline for reporting systematic reviews. Bmj, 372, n71.

Qin, Q., Lin, N., Huang, H., et al. (2019). Ginsenoside Rg1 ameliorates cardiac oxidative stress and inflammation in streptozotocin-induced diabetic rats. Diabetes Metab Syndr Obes, 12, 1091-1103.

Ronglai, Y. (2020). Effect of Qili Qiangxin Capsule on Serum APN， cTnI and Prognosis in Patients with Heart Failure of Coronary Heart Disease. Guangming J Chin Med, 35(17), 2711-2713.

Shige, L., Xiaodan, Z., and Zhangzheng, Y. (2024). Clinical Efficacy of Sacubitril Valsartan Combined with Qili Qiangxin Capsule in the Treatment of Coronary Heart Disease with Heart Failure. Shenzhen J Integr Tradit Chin West Med, 34(20), 33-36.

Shisheng, G., Donghua, L., and Jiwei, Z. (2020). Application of Trimetazidine Combined with Qili Qiangxin Capsule in Treatment of Heart Failure of Elderly Patients with Coronary Heart Disease. Cardiovasc Dis Electron J Integr Tradit Chin West Med, 8(17), 52-53.

Sterne, J. a. C., Savović, J., Page, M. J., et al. (2019). RoB 2: a revised tool for assessing risk of bias in randomised trials. Bmj, 366, l4898.

Vrints, C., Andreotti, F., Koskinas, K. C., et al. (2024). 2024 ESC Guidelines for the management of chronic coronary syndromes. Eur Heart J, 45(36), 3415-3537.

Wang, L., and Zhang, Q. (2024). Effectiveness of Qiliqiangxin Combined with Trimetazidine Hydrochloride Tablets in Treating Coronary Heart Disease with Concurrent Heart Failure: A Comparative Study. Curr Top Nutraceutical Res, 22(2), 446-451.

Xiling, Z. (2020). Effect of Qiliqiangxin capsule Combined with Trimetazidine on Plasma Brain Natriuretic Peptide and Vascular Endothelial Function in Elderly Patients with Coronary Heart Disease and Heart Failure. Mod J Integr Tradit Chin West Med, 29(01), 77-80.

Xinhua, C., Qi， Sun., Liang， Li., et al. (2014). Effect of Qiliqiangxin capsules on neurohumoral factors， left ventricular remodeling and heart function in the patients with ischemic heart disease with heart failure. Mod J Integr Tradit Chin West Med, 23(25), 2760-2763.

Yahui, C., Junpeng, X., Haiyue, Z., et al. (2020). Systematic Evaluation of Efficacy and Safety Qili Qiangxin Capsules in the Treatment of Acute Myocardial Infarction Complicated with Heart Failure. Eval Anal Drug-Use Hosp China, 20(06), 698-703.

Yan, Y., Xiaofang, H., Xiaoyun, L., et al. (2021). Systematic Review on Qili Qiangxin Capsules Combined with Conventional Western Therapy in Treatment of Coronary Heart Disease with Chronic Heart Failure. Chin J Inf TCM, 28(02), 39-45.

Yan, Z., Ting, M., Yaping, B., et al. (2020). Clinical features and prognosis of patients with different types of heart failure in relation to coronary artery disease. Natl Med J China, 100(15), 1142-1147.

Yang, T., Miao, Y., Zhang, T., et al. (2018). Ginsenoside Rb1 inhibits autophagy through regulation of Rho/ROCK and PI3K/mTOR pathways in a pressure-overload heart failure rat model. J Pharm Pharmacol, 70(6), 830-838.

Yaoqi, C., Jinxing, M., Yanxin, L., et al. (2020). Effect of Qiliqiangxin capsule on heart function，renal function and prognosis in patients with old myocardial infarction and heart failure Chin J Diffic and Compl Cas, 19(08), 785-790.

Yuxian, C., Shujun, Y., and Juping, D. (2021). Clinical Study on Qili Qiangxin Capsules Combined with Routine Western Medicine for Ischemic Cardiomyopathy Complicated with Heart Failure. J New Chin Med, 53(15), 40-43.

Zhou, B., and Tian, R. (2018). Mitochondrial dysfunction in pathophysiology of heart failure. J Clin Invest, 128(9), 3716-3726.

Zhu, R., Zheng, J., Chen, L., et al. (2016). Astragaloside IV facilitates glucose transport in C2C12 myotubes through the IRS1/AKT pathway and suppresses the palmitate-induced activation of the IKK/IκBα pathway. Int J Mol Med, 37(6), 1697-1705.

Supplementary Materials

Table S1. PRISMA_2020_checklist

Section and Topic	Item #	Checklist item	Location where item is reported
TITLE			
Title	1	Identify the report as a systematic review.	Title
ABSTRACT			
Abstract	2	See the PRISMA 2020 for Abstracts checklist.	Abstract
INTRODUCTION			
Rationale	3	Describe the rationale for the review in the context of existing knowledge.	Introduction
Objectives	4	Provide an explicit statement of the objective(s) or question(s) the review addresses.	Introduction
METHODS			
Eligibility criteria	5	Specify the inclusion and exclusion criteria for the review and how studies were grouped for the syntheses.	Section 2.1
Information sources	6	Specify all databases, registers, websites, organisations, reference lists and other sources searched or consulted to identify studies. Specify the date when each source was last searched or consulted.	Section 2.2 Search Strategy
Search strategy	7	Present the full search strategies for all databases, registers and websites, including any filters and limits used.	Table S2.
Selection process	8	Specify the methods used to decide whether a study met the inclusion criteria of the review, including how many reviewers screened each record and each report retrieved, whether they worked independently, and if applicable, details of automation tools used in the process.	Section 2.3
Data collection process	9	Specify the methods used to collect data from reports, including how many reviewers collected data from each report, whether they worked independently, any processes for obtaining or confirming data from study investigators, and if applicable, details of automation tools used in the process.	Section 2.3
Data items	10a	List and define all outcomes for which data were sought. Specify whether all results that were compatible with each outcome domain in each study were sought (e.g. for all measures, time points, analyses), and if not, the methods used to decide which results to collect.	Section 2.1.(iv) Outcome
	10b	List and define all other variables for which data were sought (e.g. participant and intervention characteristics, funding sources). Describe any assumptions made about any missing or unclear information.	Table 1.
Study risk of bias assessment	11	Specify the methods used to assess risk of bias in the included studies, including details of the tool(s) used,	Section 2.4

Section and Topic	Item #	Checklist item	Location where item is reported
		how many reviewers assessed each study and whether they worked independently, and if applicable, details of automation tools used in the process.	
Effect measures	12	Specify for each outcome the effect measure(s) (e.g. risk ratio, mean difference) used in the synthesis or presentation of results.	Section 2.5
Synthesis methods	13a	Describe the processes used to decide which studies were eligible for each synthesis (e.g. tabulating the study intervention characteristics and comparing against the planned groups for each synthesis (item #5)).	Section 2.5
	13b	Describe any methods required to prepare the data for presentation or synthesis, such as handling of missing summary statistics, or data conversions.	Section 2.5
	13c	Describe any methods used to tabulate or visually display results of individual studies and syntheses.	Section 3.4
	13d	Describe any methods used to synthesize results and provide a rationale for the choice(s). If meta-analysis was performed, describe the model(s), method(s) to identify the presence and extent of statistical heterogeneity, and software package(s) used.	Section 2.5
	13e	Describe any methods used to explore possible causes of heterogeneity among study results (e.g. subgroup analysis, meta-regression).	Section 2.5
	13f	Describe any sensitivity analyses conducted to assess robustness of the synthesized results.	Section 2.5
Reporting bias assessment	14	Describe any methods used to assess risk of bias due to missing results in a synthesis (arising from reporting biases).	Section 2.5
Certainty assessment	15	Describe any methods used to assess certainty (or confidence) in the body of evidence for an outcome.	Section 3.3
RESULTS			
Study selection	16a	Describe the results of the search and selection process, from the number of records identified in the search to the number of studies included in the review, ideally using a flow diagram.	Figure 1.
	16b	Cite studies that might appear to meet the inclusion criteria, but which were excluded, and explain why they were excluded.	Figure 1.
Study characteristics	17	Cite each included study and present its characteristics.	Table 1.
Risk of bias in studies	18	Present assessments of risk of bias for each included study.	Figures 2 and 3.
Results of individual studies	19	For all outcomes, present, for each study: (a) summary statistics for each group (where appropriate) and (b) an effect estimate and its precision (e.g. confidence/credible interval), ideally using structured tables or plots.	Section 3.4
Results of syntheses	20a	For each synthesis, briefly summarise the characteristics and risk of bias among contributing studies.	Section 3.4

Section and Topic	Item #	Checklist item	Location where item is reported
	20b	Present results of all statistical syntheses conducted. If meta-analysis was done, present for each the summary estimate and its precision (e.g. confidence/credible interval) and measures of statistical heterogeneity. If comparing groups, describe the direction of the effect.	Section 3.4
	20c	Present results of all investigations of possible causes of heterogeneity among study results.	Section 3.4
	20d	Present results of all sensitivity analyses conducted to assess the robustness of the synthesized results.	Section 3.4
Reporting biases	21	Present assessments of risk of bias due to missing results (arising from reporting biases) for each synthesis assessed.	Section 3.4
Certainty of evidence	22	Present assessments of certainty (or confidence) in the body of evidence for each outcome assessed.	
DISCUSSION			
Discussion	23a	Provide a general interpretation of the results in the context of other evidence.	Section 4
	23b	Discuss any limitations of the evidence included in the review.	Section 4
	23c	Discuss any limitations of the review processes used.	Section 4
	23d	Discuss implications of the results for practice, policy, and future research.	Section 4
OTHER INFORMATION			
Registration and protocol	24a	Provide registration information for the review, including register name and registration number, or state that the review was not registered.	Section 2
	24b	Indicate where the review protocol can be accessed, or state that a protocol was not prepared.	Section 2
	24c	Describe and explain any amendments to information provided at registration or in the protocol.	Section 2
Support	25	Describe sources of financial or non-financial support for the review, and the role of the funders or sponsors in the review.	Funding
Competing interests	26	Declare any competing interests of review authors.	Conflict of Interest
Availability of data, code and other materials	27	Report which of the following are publicly available and where they can be found: template data collection forms; data extracted from included studies; data used for all analyses; analytic code; any other materials used in the review.	

Table S2. Search Strategy

Database	Search terms
CNKI	（篇关摘：心衰 + 心力衰竭 + 心功能不全) AND （冠心病 + 冠状动脉粥样硬化性心脏 + 缺血性心肌病 + 心肌梗死） AND (篇关摘：芪苈强心 + 芪苈强心胶囊) AND (篇关摘：随机 + 对照 + 临床 + RCT) (Title/Keywords/Abstract: "heart failure" + "cardiac failure" + "cardiac insufficiency") AND ("coronary heart disease" + "coronary atherosclerotic heart disease" + "ischemic cardiomyopathy" + "myocardial infarction") AND (Title/Keywords/Abstract: "Qiliqiangxin" + "Qiliqiangxin Capsule") AND (Title/Keywords/Abstract: "randomized" + "controlled" + "clinical" + "RCT")
WanFang	题名或关键词:(心衰 OR 心力衰竭 OR 心功能不全) and 题名或关键词:(冠心病 OR 冠状动脉粥样硬化性心脏病 OR 缺血性心肌病 OR 心肌梗死) and 题名或关键词:(芪苈强心) and 题名或关键词:(随机 OR 对照 OR 临床 OR RCT) Title or Keywords: ("heart failure" OR "cardiac failure" OR "cardiac insufficiency") AND Title or Keywords: ("coronary heart disease" OR "coronary atherosclerotic heart disease" OR "ischemic cardiomyopathy" OR "myocardial infarction") AND Title or Keywords: ("Qiliqiangxin") AND Title or Keywords: ("randomized" OR "controlled" OR "clinical" OR "RCT")
VIP	(((((题名或关键词=心衰 OR 题名或关键词=心力衰竭) OR 题名或关键词=心功能不全) AND (((题名或关键词=冠心病 OR 题名或关键词=冠状动脉粥样硬化性心脏) OR 题名或关键词=缺血性心肌病) OR 题名或关键词=心肌梗死)) AND 题名或关键词=芪苈强心) AND (((题名或关键词=随机 OR 题名或关键词=对照) OR 题名或关键词=临床) OR 题名或关键词=RCT)) (((((Title or Keywords = "heart failure" OR Title or Keywords = "cardiac failure") OR Title or Keywords = "cardiac insufficiency") AND (((Title or Keywords = "coronary heart disease" OR Title or Keywords = "coronary atherosclerotic heart disease") OR Title or Keywords = "ischemic cardiomyopathy") OR Title or Keywords = "myocardial infarction")) AND Title or Keywords = "Qiliqiangxin") AND (((Title or Keywords = "randomized" OR Title or Keywords = "controlled") OR Title or Keywords = "clinical") OR Title or Keywords = "RCT"))
Sinomed	("心衰"[摘要] OR "心力衰竭"[摘要] OR "心功能不全"[摘要]) AND("冠心病"[摘要] OR "冠状动脉粥样硬化性心脏病"[摘要] OR "缺血性心肌病"[摘要] OR "心肌梗死"[摘要]) AND "芪苈强心"[摘要] AND("随机"[摘要] OR "对照"[摘要] OR "临床"[摘要] OR "RCT"[摘要]) ("heart failure"[Abstract] OR "cardiac failure"[Abstract] OR "cardiac insufficiency"[Abstract]) AND ("coronary heart disease"[Abstract] OR "coronary atherosclerotic heart disease"[Abstract] OR "ischemic cardiomyopathy"[Abstract] OR "myocardial infarction"[Abstract]) AND "Qiliqiangxin"[Abstract] AND ("randomized"[Abstract] OR "controlled"[Abstract] OR "clinical"[Abstract] OR "RCT"[Abstract])
Pubmed	((((((((((((("Heart Failure"[Mesh]) OR (Cardiac Failure[Title/Abstract])) OR (Heart Decompensation[Title/Abstract])) OR (Decompensation, Heart[Title/Abstract])) OR (Congestive Heart Failure[Title/Abstract])) OR (Heart Failure, Congestive[Title/Abstract])) OR (Heart Failure, Right-Sided[Title/Abstract])) OR (Right-Sided Heart Failure[Title/Abstract])) OR (Heart Failure, Left-Sided[Title/Abstract])) OR (Left-Sided Heart Failure[Title/Abstract])) OR (Myocardial Failure[Title/Abstract])) OR (HF[Title/Abstract])) AND ((("Coronary Disease"[Mesh]) OR (((((((((Coronary Diseases[Title/Abstract]) OR (Disease, Coronary[Title/Abstract])) OR (Diseases, Coronary[Title/Abstract])) OR (Coronary Heart Disease[Title/Abstract])) OR (Coronary Heart Diseases[Title/Abstract])) OR (Disease, Coronary Heart[Title/Abstract])) OR

	(Diseases, Coronary Heart[Title/Abstract])) OR (Heart Disease, Coronary[Title/Abstract])) OR (Heart Diseases, Coronary[Title/Abstract]))) OR (("Myocardial Infarction"[Mesh]) OR ((((((((((((Infarction, Myocardial[Title/Abstract]) OR (Infarctions, Myocardial[Title/Abstract])) OR (Myocardial Infarctions[Title/Abstract])) OR (Heart Attack[Title/Abstract])) OR (Heart Attacks[Title/Abstract])) OR (Myocardial Infarct[Title/Abstract])) OR (Infarct, Myocardial[Title/Abstract])) OR (Infarcts, Myocardial[Title/Abstract])) OR (Myocardial Infarcts[Title/Abstract])) OR (Cardiovascular Stroke[Title/Abstract])) OR (Cardiovascular Strokes[Title/Abstract])) OR (Stroke, Cardiovascular[Title/Abstract])) OR (Strokes, Cardiovascular[Title/Abstract])))))) AND ((((("qiliqiangxin" [Supplementary Concept]) OR (QLQX[Title/Abstract])) OR (qiliqiangxin[Title/Abstract])) OR (qili qiangxin[Title/Abstract]))) AND (((((("Randomized Controlled Trial" [Publication Type]) OR (randomized clinical trial[Title/Abstract])) OR (random[Title/Abstract])) OR (RCT[Title/Abstract]))))
WOS	#1.TS=(Heart Failure OR Cardiac Failure OR Heart Decompensation OR Decompensation, Heart OR Congestive Heart Failure OR Heart Failure, Congestive OR Heart Failure, Right-Sided OR Right-Sided Heart Failure OR Heart Failure, Left-Sided OR Left-Sided Heart Failure OR Myocardial Failure OR HF) #2.TS=(Coronary Disease OR Disease, Coronary OR Diseases, Coronary OR Coronary Heart Disease OR Coronary Heart Diseases OR Disease, Coronary Heart OR Diseases, Coronary Heart OR Heart Disease, Coronary OR Heart Diseases, Coronary OR Myocardial Infarction OR Infarction, Myocardial OR Infarctions, Myocardial OR Myocardial Infarctions OR Heart Attack OR Heart Attacks OR Myocardial Infarct OR Infarct, Myocardial OR Infarcts, Myocardial OR Myocardial Infarcts OR Cardiovascular Stroke OR Cardiovascular Strokes OR Stroke, Cardiovascular OR Strokes, Cardiovascular) #3.((TS=(qiliqiangxin)) OR TS=(QLQX)) OR TS=(qili qiangxin) #4.(((TS=(randomized controlled trial)) OR TS=(randomized clinical trial)) OR TS=(random)) OR TS=(RCT) #1 AND #2 AND #3 AND #4
Embase	#1 'heart failure'/exp OR 'heart failure':ti,ab,kw OR 'backward failure, heart':ti,ab,kw OR 'cardiac backward failure':ti,ab,kw OR 'cardiac decompensation':ti,ab,kw OR 'cardiac failure':ti,ab,kw OR 'cardiac incompetence':ti,ab,kw OR 'cardiac insufficiency':ti,ab,kw OR 'cardiac stand still':ti,ab,kw OR 'cardial decompensation':ti,ab,kw OR 'cardial insufficiency':ti,ab,kw OR 'chronic heart failure':ti,ab,kw OR 'chronic heart insufficiency':ti,ab,kw OR 'decompensatio cordis':ti,ab,kw OR 'decompensation, heart':ti,ab,kw OR 'heart backward failure':ti,ab,kw OR 'heart decompensation':ti,ab,kw OR 'heart incompetence':ti,ab,kw OR 'heart insufficiency':ti,ab,kw OR 'insufficientia cardis':ti,ab,kw OR 'myocardial failure':ti,ab,kw OR 'myocardial insufficiency':ti,ab,kw #2 'ischemic heart disease'/exp OR 'coronary artery insufficiency':ti,ab,kw OR 'coronary insufficiency':ti,ab,kw OR 'heart disease, ischaemic':ti,ab,kw OR 'heart disease, ischemic':ti,ab,kw OR 'ischaemia heart disease':ti,ab,kw OR 'ischaemic cardiac disease':ti,ab,kw OR 'ischaemic cardial disease':ti,ab,kw OR 'ischaemic cardiopathy':ti,ab,kw OR 'ischaemic heart disease':ti,ab,kw OR 'schaemic heart disease':ti,ab,kw OR 'ischemic cardiac disease':ti,ab,kw OR 'ischemic cardiopathy':ti,ab,kw #3 'qiliqiangxin'/exp OR 'qiliqiangxin capsule'/exp #4 'randomized controlled trial'/exp OR 'randomized controlled trial':ti,ab,kw OR 'controlled trial, randomized':ti,ab,kw OR 'randomised controlled study':ti,ab,kw OR 'randomised controlled trial':ti,ab,kw OR 'randomized controlled study':ti,ab,kw OR 'trial, randomized controlled':ti,ab,kw #5 #1 AND #2 AND #3 AND #4

Table S3. Detailed adverse events reported in five studies

Adverse Event	Control Group (n)	Experimental Group (n)
Sleep disorders / Somnolence	3	3
Headache and dizziness / Dizziness and headache	10	9
Chest distress with abnormal heartbeat / palpitations	4	5
Lower extremity edema	1	2
Gastrointestinal dysfunction / discomfort	9	6
Constipation	3	1
Rash	2	0
Hypotension	2	4
Mild anemia	1	2
Elevated serum creatinine	2	1
Elevated serum potassium	1	1
Total	38	34

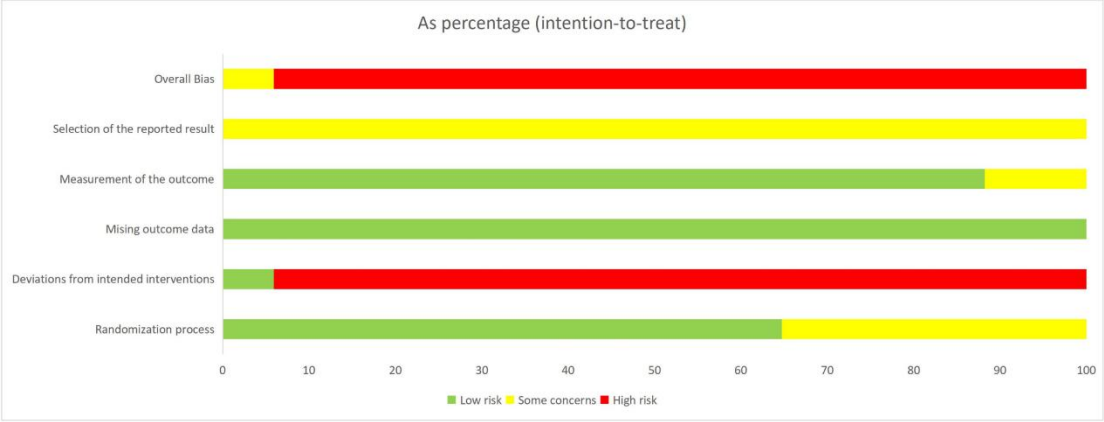


Figure S1. Risk of Bias Assessment

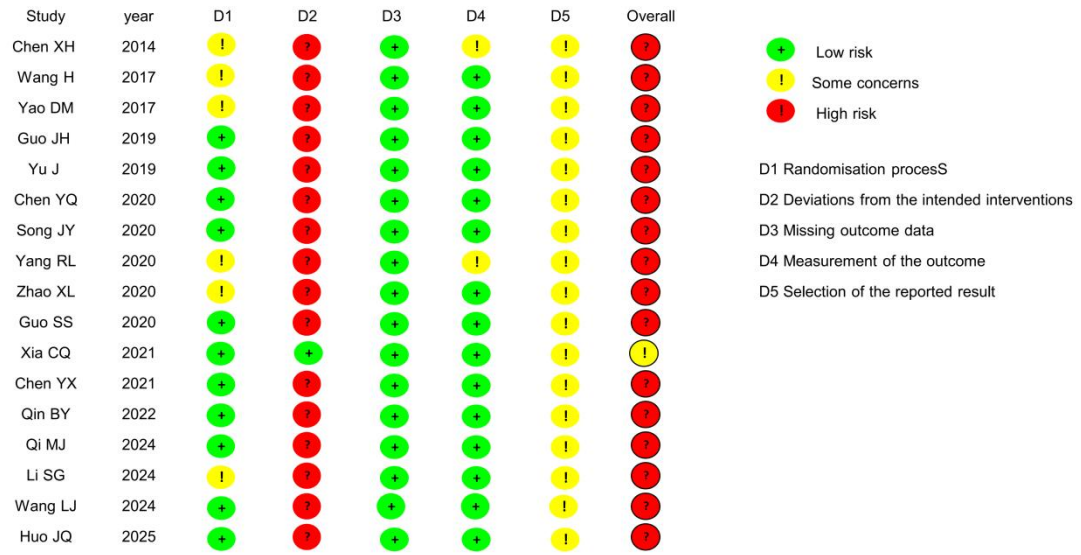


Figure S2. Quality assessment of the included trials

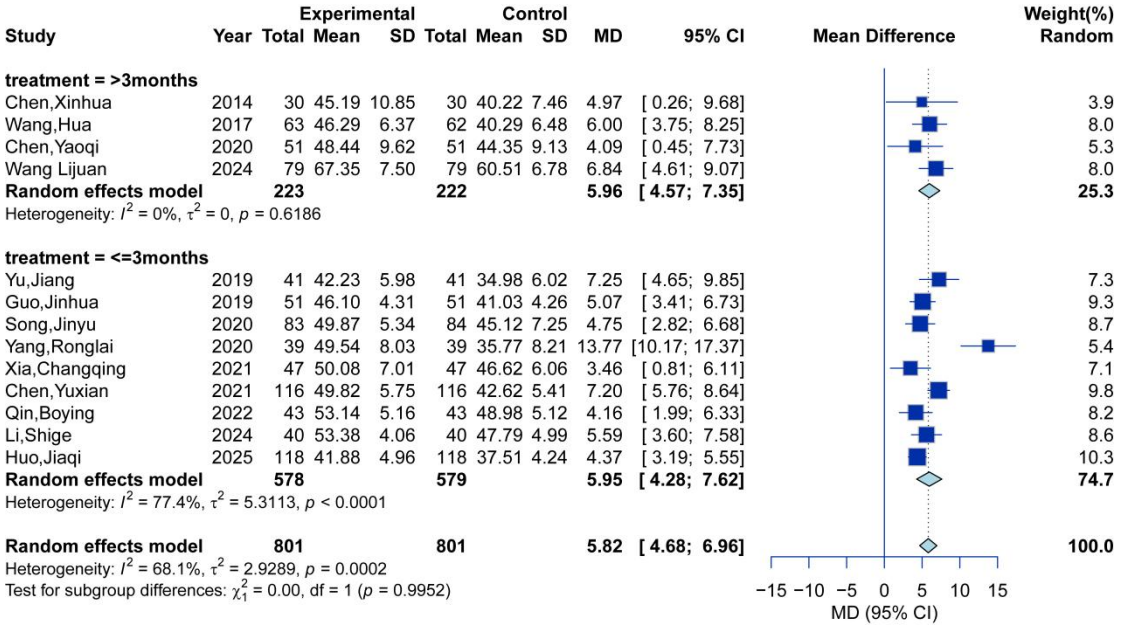


Figure S3. Forest Plot of LVEF Subgroup Analysis

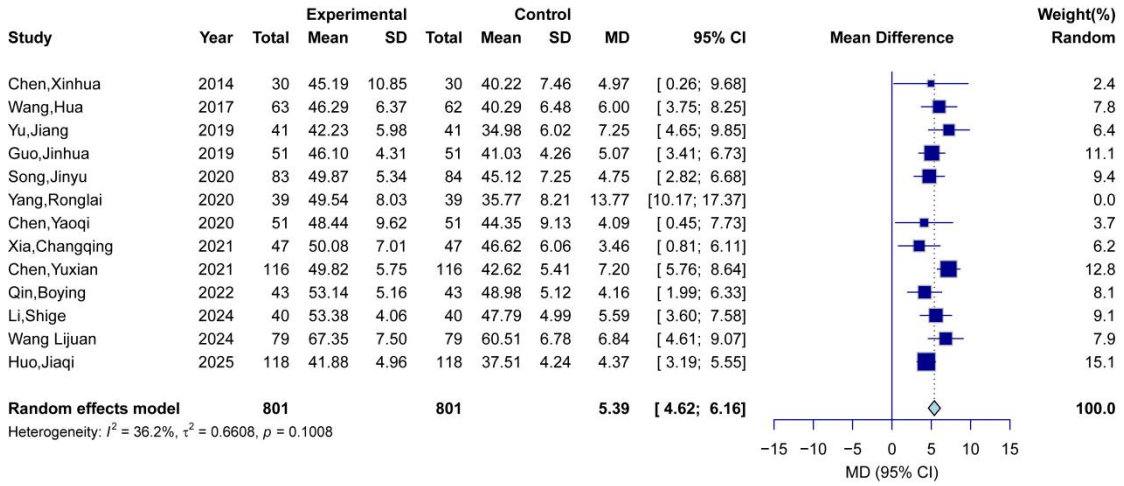


Figure S4. Forest Plot of LVEF Sensitivity Analysis

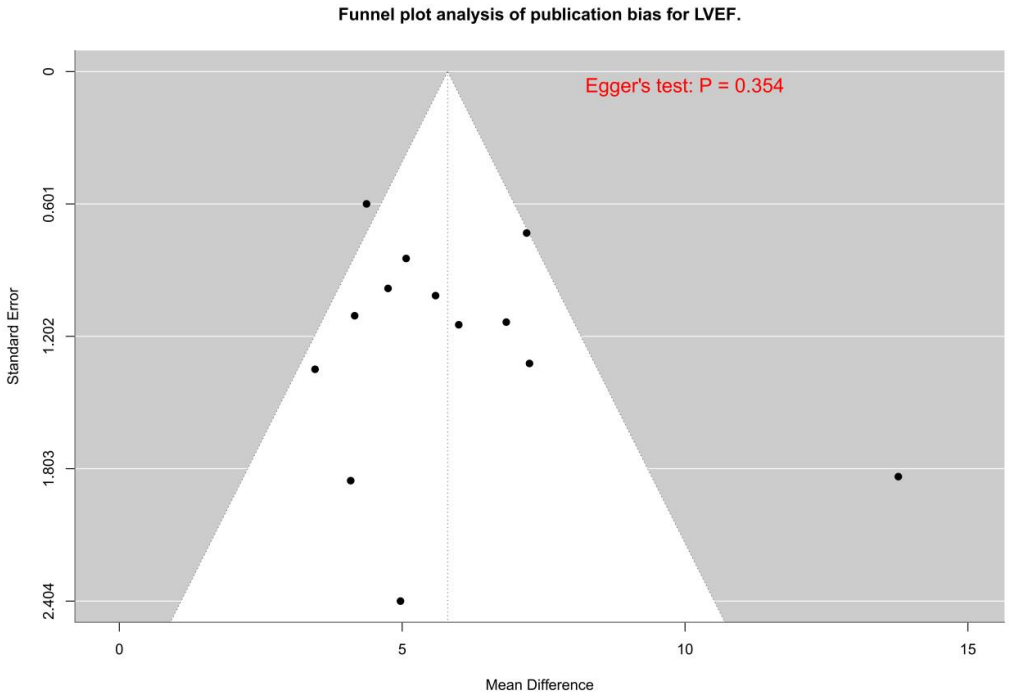


Figure S5. Funnel plot analysis of publication bias for LVEF

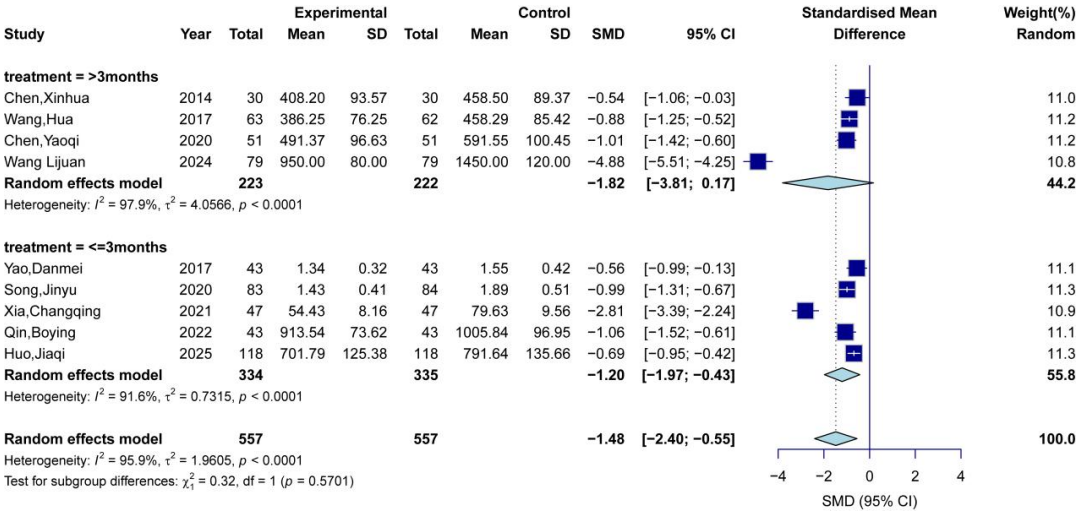


Figure S6. Forest Plot of NT-proBNP Subgroup Analysis

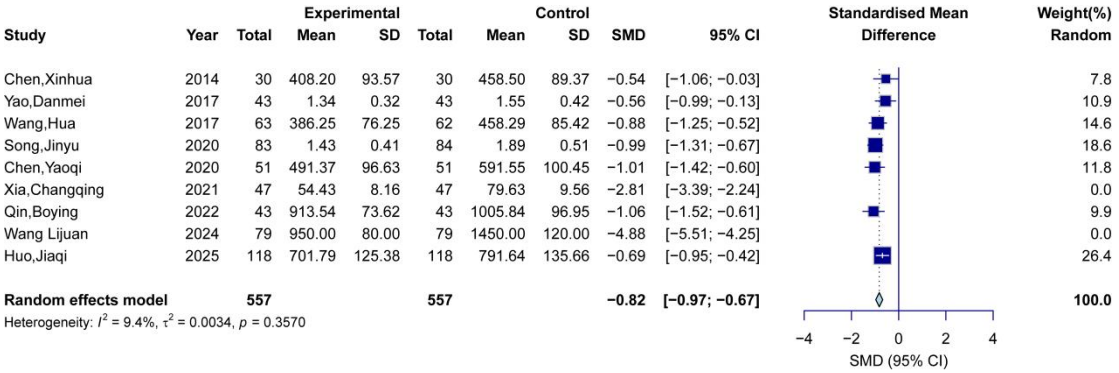


Figure S7. Forest Plot of NT-proBNP Sensitivity Analysis

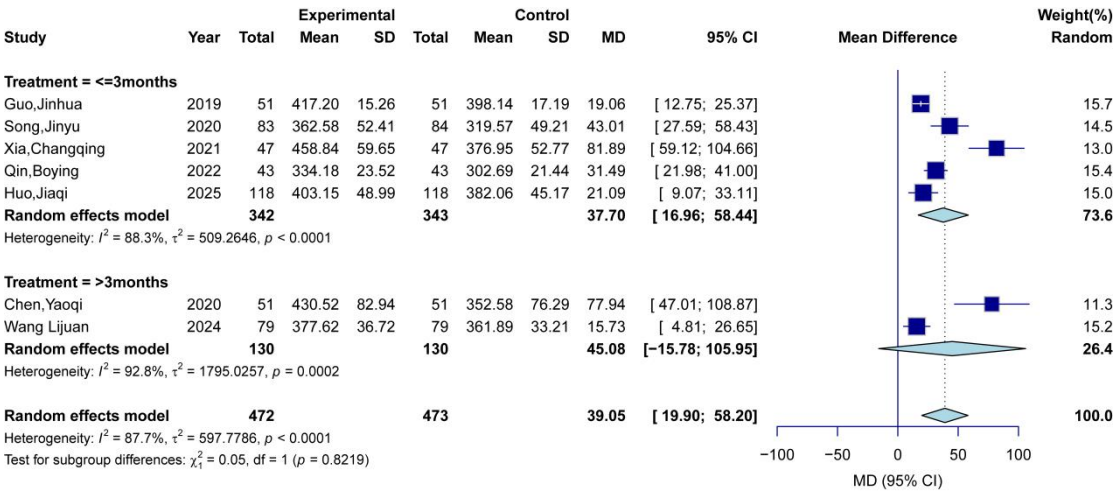


Figure S8. Forest Plot of 6MWD Subgroup Analysis of Treatment

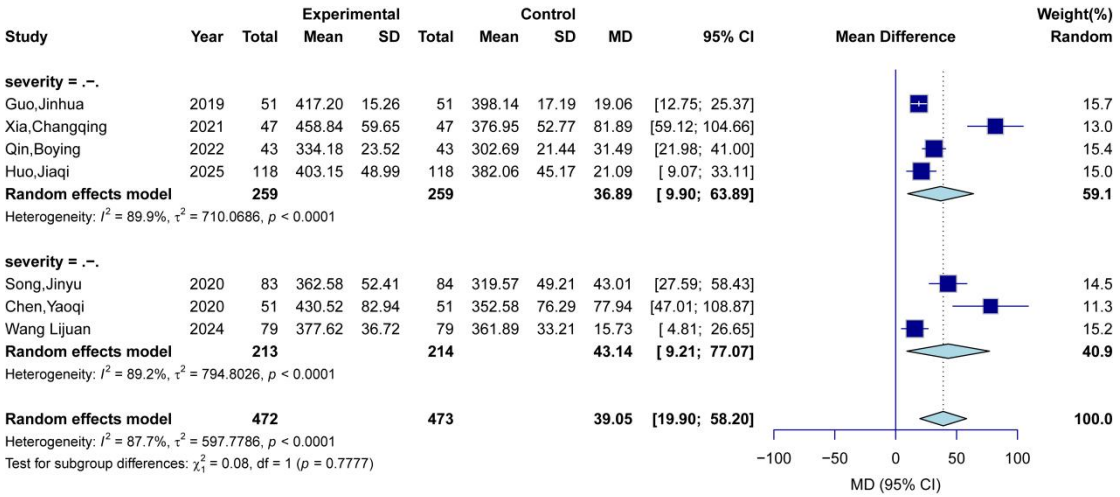


Figure S9. Forest Plot of 6MWD Subgroup Analysis of Class

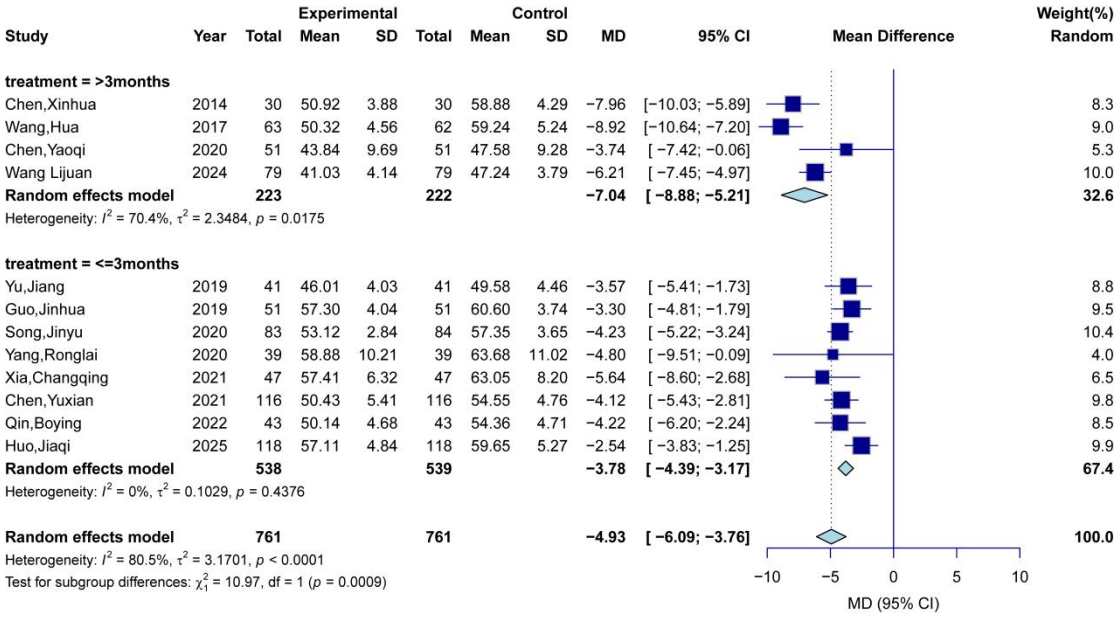


Figure S10. Forest Plot of LVEDD Subgroup Analysis

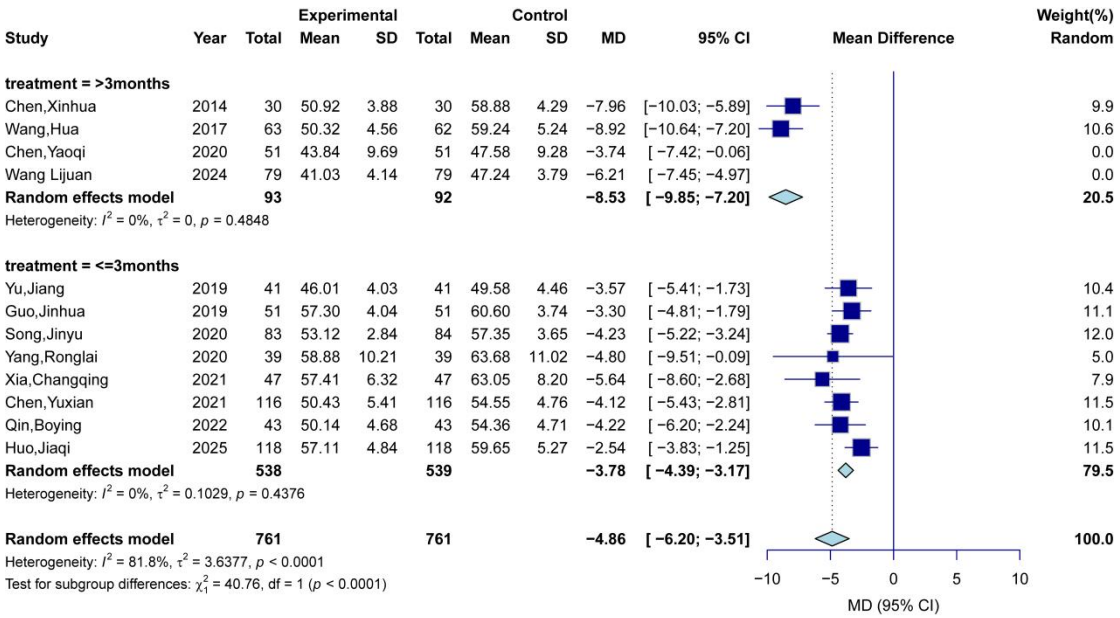


Figure S11. Forest Plot of LVEDD Sensitivity Analysis

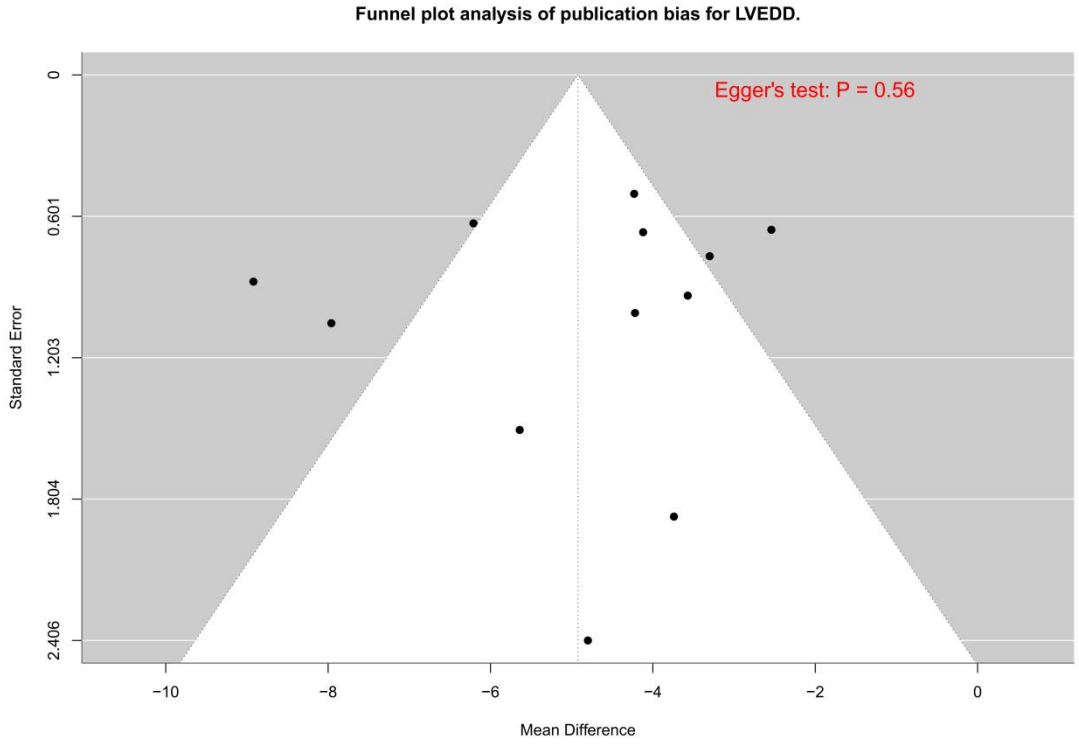


Figure S12. Funnel plot analysis of publication bias for LVEDD

License: Copyright (c) 2026 Author.
All articles published in this journal are licensed under the Creative Commons Attribution 4.0 International License (CC BY 4.0). This license permits unrestricted use, distribution, and reproduction in any medium, provided the original author(s) and source are properly credited. Authors retain copyright of their work, and readers are free to copy, share, adapt, and build upon the material for any purpose, including commercial use, as long as appropriate attribution is given.

Advances in World Medical Research, 2026, 2(3), 78-86
https://doi.org/10.71204/dkzdp879

CD8+ T Cell Exhaustion and Tumor Immune Checkpoint Blockade: Mechanisms, Heterogeneity, and Combination Intervention Strategies

Gang Liu [1, *]

[1] International Sakharov Environmental Institute, Belarusian State University, Minsk 220114, Belarus

*** Correspondence**:

Gang Liu

lg6666699@163.com

Received: 1 September 2026/ Accepted: 27 September 2026/ Published online: 30 September 2026

Abstract

CD8+ T cells are the core effector cells in anti-tumor immunity, but under continuous tumor antigen stimulation and inhibitory microenvironment, they gradually enter a state of dysfunction, showing reduced effector secretion, decreased proliferation, persistent expression of inhibitory receptors, and abnormal metabolic adaptation, which are driven by a unified transcriptional, epigenetic, metabolic, and microenvironmental exhaustion program. T cell exhaustion is a major reason why immune checkpoint blockade (ICB) therapy has limited effectiveness and also a key target for combination treatment strategies. In recent years, single-cell sequencing, spatial transcriptomics, and functional immunology studies have shown that exhausted T cells are not a single state-they include heterogeneous subgroups such as progenitor exhausted T cells (Tpex), intermediate exhausted T cells, and terminal exhausted T cells. Blocking PD-1/PD-L1 and CTLA-4 can partly restore T cell function, but primary and secondary resistance are still common. This article reviews the unified mechanisms of CD8+ T cell exhaustion and, organized around the axis of 'mechanism–heterogeneity–ICB response–combination strategies', explores potential strategies for immune checkpoint blockade related to CD8+ T cell exhaustion, and also discusses biomarkers and future research directions.

Keywords: CD8+ T Cells; T Cell Exhaustion; Immune Checkpoint Blockade; Tumor Microenvironment; Immunotherapy

1. Introduction

Tumor immunotherapy, especially with immune checkpoint inhibitors, has changed the treatment landscape for many types of cancers (Pardoll, 2012; Topalian et al., 2015).PD-1/PD-L1 blockade, CTLA-4 blockade, and CAR-T cell therapy have shown significant clinical benefits in melanoma, non-small cell lung cancer, Hodgkin lymphoma, and blood cancers (June et al., 2018;

Sharma & Allison, 2015).However, only some patients are able to achieve a lasting response, and most solid tumors still have primary or secondary resistance. Increasing evidence suggests that $CD8^+$ T cell exhaustion is one of the key factors limiting anti-tumor immune responses and the effectiveness of ICB.Increasing evidence suggests that $CD8^+$ T cell exhaustion is one of the key factors limiting anti-tumor immune responses and the effectiveness of ICB (Chow et al., 2022; Dolina et al., 2021; Raskov et al., 2021).

T cell exhaustion was first systematically described in chronic viral infections, and was later found to also exist in tumors, autoimmune conditions, and chronic inflammatory environments (Ahmed & Gray, 1996; Wherry & Kurachi, 2015).Unlike memory T cells formed after acute infections, exhausted T cells can still recognize antigens, but their proliferation, cytokine secretion, and cytotoxic functions are significantly impaired, and they express high levels of multiple inhibitory receptors. This article aims to review the key mechanisms of $CD8^+$ T cell exhaustion and, in light of the latest advances in tumor immunotherapy, explore potential strategies to overcome exhaustion.

2. Literature Search Strategy and Scope

A comprehensive literature search was conducted in PubMed, Web of Science, and Scopus databases up to October 2026. The search terms included combinations of "$CD8^+$ T cell exhaustion," "immune checkpoint blockade," "tumor microenvironment," "Tpex," "epigenetic regulation," and "combination therapy." Articles published in English were prioritized.

Regarding the IL-17 pathway, although it plays a complex and context-dependent role in tumor immunity, it is not a canonical driver of the CD8+ T cell exhaustion program and its role in immune checkpoint blockade resistance remains controversial. Therefore, the IL-17 pathway is not included within the core scope of this review, so as to maintain focus on the established transcriptional, epigenetic, metabolic, and microenvironmental exhaustion axes. Its potential involvement in tumor microenvironment remodeling may be explored in future studies.

3. The Unified Exhaustion Program of $CD8^+$ T Cells

T cell exhaustion refers to a state where T cells progressively lose their function due to continuous antigen stimulation and inflammatory signals. Its typical features include reduced production of IFN-γ, TNF-α, and IL-2, decreased expression of granzyme B and perforin, weaker proliferation ability, and co-expression of inhibitory receptors like PD-1, TIM-3, LAG-3, and TIGIT(Wherry & Kurachi, 2015; Wherry et al., 2007).Exhaustion isn't just simple 'functional silence'; it's a stable state maintained by a combination of transcription, epigenetics, and metabolism.

In tumors and chronic infections, CD8 T cells can differentiate into precursor exhausted T cells (Tpex), intermediate exhausted T cells (Giles et al., 2022; Zheng et al., 2021), and terminal exhausted T cells. Tpex usually express TCF1, SLAMF6, and PD-1, retaining the ability to self-renew and differentiate into effector cells, making them an important source of cells that respond to ICB; whereas terminally exhausted T cells highly express TOX, CD39, TIM-3, and LAG-3, have

low effector function, and are hard to reverse with just PD-1 blockade(Hashimoto et al., 2018; McLane et al., 2019).This differentiation trajectory provides a framework for understanding ICB responses and resistance (Figure 1).

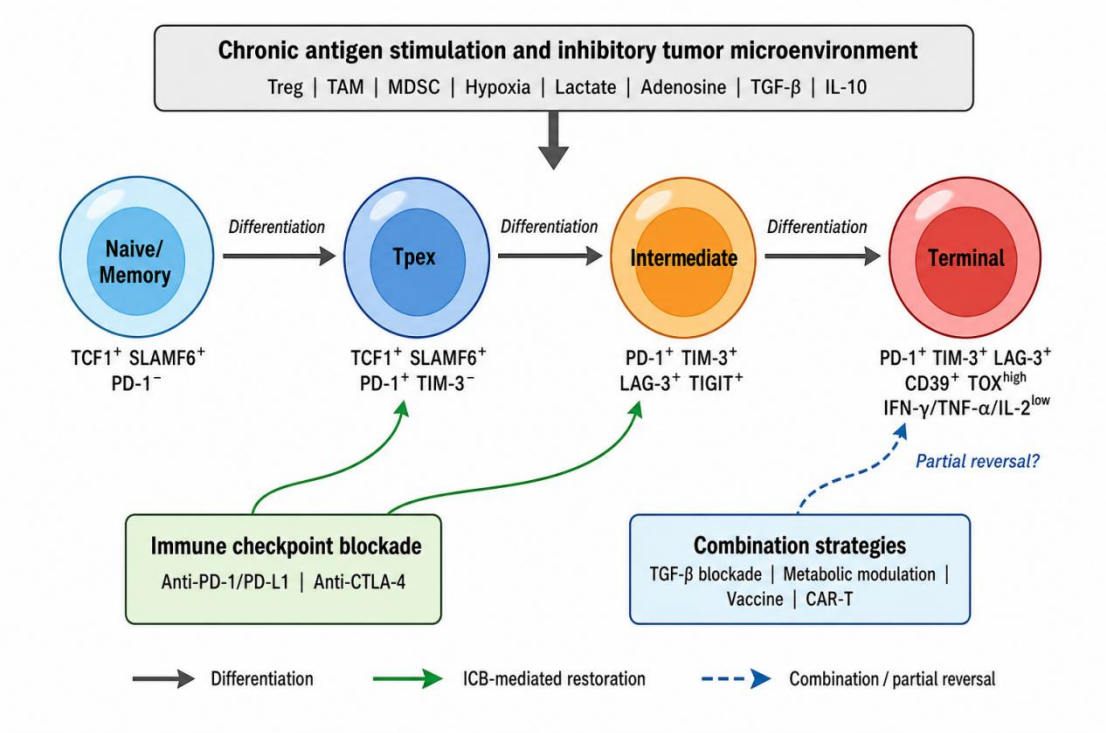


Figure 1. Schematic of the unified CD8+ T cell exhaustion program and differentiation trajectory, highlighting mechanisms, heterogeneity, and therapeutic interventions.

Chronic antigen stimulation and the inhibitory tumor microenvironment (driven by Tregs, TAMs, MDSCs, hypoxia, lactate, and adenosine) induce a unified exhaustion program via transcriptional (TOX, TCF1, NR4A, BATF), epigenetic (PDCD1, HAVCR2, LAG3 loci opening), and metabolic (mitochondrial dysfunction, ROS accumulation) rewiring. This drives the differentiation from memory-like cells to Tpex (TCF1$^+$, SLAMF6$^+$, PD-1$^+$, TIM-3$^+$), intermediate exhausted (PD-1$^+$, TIM-3$^+$, LAG-3$^+$, TIGIT$^+$), and terminal exhausted cells (PD-1high, TIM-3$^+$, LAG-3$^+$, CD39$^+$, TOX$^+$, low IFN-γ/TNF-α/IL-2). ICB (anti-PD-1/PD-L1, anti-CTLA-4) can restore Tpex proliferation and differentiation. Combination strategies (TGF-β blockade, metabolic modulators, vaccines, CAR-T) may partially reverse terminal exhaustion and CAR-T might enhance the reversal effect.Exhaustion is not merely functional silencing, but a stable state maintained by an integrated network of transcription, epigenetics, and metabolism, driven by the tumor microenvironment.These epigenetic and transcriptional changes lock the exhaustion program, which is further reinforced by metabolic and microenvironmental constraints (Abdel-Hakeem et al., 2021; Belk et al., 2022; Yates et al., 2021).TOX is considered a key regulator of the exhaustion program, helping to boost inhibitory receptor expression and keep the cells exhausted, while TCF1 is linked to maintaining Tpex cells and their memory potential (Khan et al., 2019).

The steady state of exhausted T cells depends on a series of transcription factors and epigenetic remodeling. TOX is considered a key regulator of the exhaustion program, helping to boost inhibitory receptor expression and keep the cells exhausted, while TCF1 is linked to maintaining Tpex cells and their memory potential. In addition, transcription factors like NR4A, BATF, IRF4,

and NFAT are involved in regulating the expression of genes related to exhaustion. On the epigenetic side, in exhausted T cells, gene sites like PDCD1, HAVCR2, and LAG3 show an open chromatin state, while effector gene sites like IL2 and IFNG gradually close, making it hard to completely reverse the exhausted state through short-term stimulation.These epigenetic and transcriptional changes lock the exhaustion program, which is further reinforced by metabolic and microenvironmental constraints.Tregs, tumor-associated macrophages (TAMs), and myeloid-derived suppressor cells (MDSCs) can boost suppression through IL-10, TGF-β, VEGF, arginase, and tryptophan-metabolizing enzymes (Tauriello et al., 2022).

The tumor microenvironment suppresses T cell function through nutrient competition, hypoxia, lactate buildup, adenosine signaling, and abnormal lipid metabolism. Exhausted T cells have impaired mitochondrial function, an imbalance between glycolysis and oxidative phosphorylation, and accumulation of reactive oxygen species, which further weakens their ability to proliferate and kill. Tregs, tumor-associated macrophages (TAMs), and myeloid-derived suppressor cells (MDSCs) can boost suppression through IL-10, TGF-β, VEGF, arginase, and tryptophan-metabolizing enzymes. So, exhaustion isn't just an internal program of T cells; it's also the result of the combined effects of the microenvironment.Therefore, exhaustion is a unified program integrating intrinsic T cell rewiring and extrinsic microenvironmental suppression.

4. Molecules Related to Exhaustion and Immune Checkpoints

4.1. Inhibitory Receptors

PD-1 is one of the most classic markers of exhausted T cells. After binding with PD-L1/PD-L2, it recruits SHP-2 and suppresses TCR signaling and co-stimulatory pathways (Pardoll, 2012; Topalian et al., 2015).CTLA-4 mainly controls early T cell activation and Treg function by competitively binding to CD80/CD86 and sending inhibitory signals.TIM-3, LAG-3, TIGIT, BTLA, and VISTA are often co-expressed with PD-1 in exhausted T cells, working together to suppress activity. The combination of different inhibitory receptors is closely linked to how exhausted the cells are, treatment responses, and resistance mechanisms(Table 1) (Korman et al., 2022; Kraehenbuehl et al., 2022).

Table 1. Main Markers and Functions of $CD8^+$ T Cell Exhaustion

Category	Marker	Main Expression/Function	Clinical & Biological Significance	Clinical Stage
Inhibitory Receptor	PD-1	Continuous expression; suppresses TCR signaling via SHP-2	Main ICB target; expression alone does not define terminal exhaustion	Approved (Multiple cancers)
Inhibitory Receptor	CTLA-4	Competes with CD80/CD86; inhibits co-stimulation	CTLA-4 blockade boosts T cell activation and depletes Tregs	Approved (Melanoma)
Inhibitory	TIM-3	Co-expressed with PD-	Correlates with severe	Phase III (Various)

Receptor		1; regulates T cell exhaustion	exhaustion; target for combination therapy	
Inhibitory Receptor	LAG-3	Binds MHC-II; suppresses T cell proliferation	Relatlimab (anti-LAG-3) combined with PD-1 blockade shows benefit	Approved (Melanoma)
Inhibitory Receptor	TIGIT	Binds CD155/CD112; suppresses NK and T cell activity	Tiragolumab combined with PD-L1 blockade under investigation	Phase III (NSCLC)

4.2. Soluble Factors and Cell Interactions

TGF-β is an important factor that promotes exhaustion and fibrosis, and it can suppress the effector function of $CD8^+$ T cells while promoting Treg differentiation. IL-10, VEGF, adenosine, and prostaglandin E2 also play a role in immune suppression (Thommen & Schumacher, 2018; Topalian et al., 2015).Tumor cells can escape immune attacks by upregulating PD-L1, downregulating MHC-I, losing antigens, and activating the Wnt/β-catenin pathway. Also, TAMs and MDSCs can suppress T cells through metabolic competition and cell contact. So, just blocking a single checkpoint usually isn’t enough to fully restore anti-tumor immunity.The molecular mechanisms of exhaustion directly shape the heterogeneous states of T cells in the TME, which in turn dictate ICB responses and inform combination strategies.

5. Heterogeneity of exhausted T cells in the tumor microenvironment

Single-cell RNA sequencing studies have shown that tumor-infiltrating $CD8^+$ T cells are highly heterogeneous Sade-Feldman and colleagues identified T cell states linked to ICB response in melanoma, finding that Tpex-like and effector-like cells are associated with good responses, while terminally exhausted cells are linked to resistance (Sade-Feldman et al., 2018).Spatial transcriptomics further shows that exhausted T cells are often found at the tumor edges or in areas rich in suppressive cells, and their spatial distance from tumor cells, TAMs, and Tregs affects their functional recovery.

Tpex cells are the key 'seed' population for ICB response. After PD-1 blockade, Tpex can proliferate and differentiate into effector-like cells, but if the Tpex pool is insufficient or the epigenetic exhaustion program is already fixed, it's hard to get a lasting response. So, treatment strategies shouldn't just focus on 'lifting inhibition,' but also on protecting or expanding Tpex and improving their differentiation environment.Sade-Feldman and colleagues identified T cell states linked to ICB response in melanoma, finding that Tpex-like and effector-like cells are associated with good responses, while terminally exhausted cells are linked to resistance (Oliveira & Wu, 2023).

6. Immune Checkpoint Blockade and Combined Interventions

Based on the mechanisms and heterogeneity described above, current ICB and combination strategies aim to target the exhaustion program at different levels.

6.1. PD-1/PD-L1 and CTLA-4

PD-1/PD-L1 blockade produces long-lasting responses in various tumors by restoring TCR signaling and effector functions. CTLA-4 blockade mainly works on the activation stage of T cells in lymph nodes and the tumor microenvironment, and it can also deplete Tregs. Combining PD-1 and CTLA-4 blockade shows a synergistic effect in melanoma, but it comes with increased toxicity. Clinical responses are linked to tumor mutation burden, PD-L1 expression, TIL infiltration, MSI-H status, and Tpex abundance (Litchfield et al., 2021).

6.2. Combination Strategy

To overcome exhaustion and drug resistance, combination therapy has become the main approach. Chemotherapy and radiotherapy can trigger immunogenic cell death and increase antigen release; anti-angiogenic treatments can improve T cell infiltration and reduce MDSCs; blocking TGF-β, inhibiting the adenosine pathway, and metabolic regulation can improve the microenvironment. LAG-3 blockade combined with PD-1 blockade has shown benefits in melanoma, and targets like TIGIT and TIM-3 are under clinical investigation (Tawbi et al., 2022). In addition, tumor vaccines, adoptive T cell therapy, and CAR-T cell therapy can supplement or reshape the T cell pool (Gumber & Wang, 2022; Lin et al., 2022; Weber et al., 2021). In addition, neoadjuvant or radical PD-1 blockade has further shown clinical benefits in long-term follow-ups for resectable NSCLC, locally advanced MMR-deficient rectal cancer, and PD-L1 high-expressing NSCLC (Cercek et al., 2022; Forde et al., 2022; Reck et al., 2021).

Table 2. Representative Immune Checkpoint Targets and Combination Strategies

Target	Representative Drugs/Strategies	Main Mechanism	Combined Direction	Clinical Stage
PD-1	Pembrolizumab, Nivolumab	Blocking PD-1/PD-L1 to restore T cell function	Chemotherapy, radiotherapy, CTLA-4, LAG-3	Approved
PD-L1	Atezolizumab, Durvalumab	Blocking PD-L1 binding to PD-1/CD80	Anti-angiogenesis, chemotherapy	Approved
CTLA-4	Ipilimumab	Boost T cell activation, deplete Tregs	PD-1 blockade	Approved
LAG-3	Relatlimab	Relieve LAG-3 mediated inhibition	PD-1 blockade	Approved (Melanoma)
TIGIT	Tiragolumab	Blocking TIGIT/CD155	PD-L1 blockade	Phase III

7. Biomarkers and Predicting Treatment Response

Currently, the commonly used clinical predictors include PD-L1 expression, tumor mutation burden, MSI-H/dMMR, TIL density, and dynamic changes in ctDNA. However, all of these markers have their limitations. Single-cell and spatial omics suggest that things like Tpex abundance, T cell states, co-expression patterns of inhibitory receptors, and the spatial structure of the microenvironment might be better at predicting ICB responses.Gut microbiota, host genetic background, and immune-related side effects might also affect treatment efficacy. For patient selection, integrating Tpex abundance, spatial immune profiles, and circulating tumor DNA (ctDNA) dynamics is crucial to identify those most likely to benefit from ICB. Biomarker-guided combination therapy, such as using LAG-3 or TIGIT expression to guide dual blockade, represents a promising avenue for personalized immunotherapy. In the future, we'll need multidimensional integrated models to achieve personalized immunotherapy.

8. Challenges and Outlook

Even though ICB has had major success, T cell exhaustion, antigen loss, MHC downregulation, immunosuppressive microenvironments, and irAEs are still the main challenges. The toxicity of combination therapies, particularly the increased risk of severe irAEs with dual checkpoint blockade (e.g: PD-1 plus CTLA-4 or LAG-3), necessitates careful patient stratification and toxicity management. Future research should focus on: understanding the plasticity and epigenetic reversibility of exhausted T cells; developing combination strategies targeting the expansion and differentiation of Tpex; using spatial multi-omics and AI to predict responses and identify new targets; optimizing the therapeutic window to balance efficacy and toxicity in biomarker-guided combination regimens; and optimizing the persistence and safety of CAR-T in solid tumors. By deeply integrating basic immunology with clinical translational research, it's possible to turn 'exhaustion' from a treatment hurdle into a target that can be intervened.

Author Contributions:

All author shave read and agreed to the published version of the manuscript.

Funding:

Not applicable.

Institutional Review Board Statement:

Not applicable.

Informed Consent Statement:

Not applicable.

Data Availability Statement:

Not applicable.

Conflict of Interest:

The authors declare no conflict of interest.

References

Abdel-Hakeem, M. S., Manne, S., Beltra, J. C., et al. (2021). Epigenetic scarring of exhausted T cells hinders memory differentiation upon eliminating chronic antigenic stimulation. Nature Immunology, 22(8), 1008–1019. https://doi.org/10.1038/s41590-021-00975-5

Ahmed, R., & Gray, D. (1996). Immunological memory and protective immunity: Understanding their relation. Science, 272(5258), 54–60. https://doi.org/10.1126/science.272.5258.54

Belk, J. A., Yao, W., Ly, N., et al. (2022). Genome-wide CRISPR screens of T cell exhaustion identify chromatin remodeling factors that limit T cell persistence. Cancer Cell, 40(7), 768–786.e7. https://doi.org/10.1016/j.ccell.2022.06.001

Cercek, A., Lumish, M., Sinopoli, J., et al. (2022). PD-1 blockade in mismatch repair-deficient, locally advanced rectal cancer. New England Journal of Medicine, 386(25), 2363–2376. https://doi.org/10.1056/NEJMoa2201445

Chow, A., Perica, K., Klebanoff, C. A., & Wolchok, J. D. (2022). Clinical implications of T cell exhaustion for cancer immunotherapy. Nature Reviews Clinical Oncology, 19(12), 775–790. https://doi.org/10.1038/s41571-022-00689-z

Dolina, J. S., Van Braeckel-Budimir, N., Thomas, G. D., & Salek-Ardakani, S. (2021). CD8+ T cell exhaustion in cancer. Frontiers in Immunology, 12, Article 715234. https://doi.org/10.3389/fimmu.2021.715234

Forde, P. M., Spicer, J., Lu, S., et al. (2022). Neoadjuvant nivolumab plus chemotherapy in resectable lung cancer. New England Journal of Medicine, 386(21), 1973–1985. https://doi.org/10.1056/NEJMoa2202170

Giles, J. R., Ngiow, S. F., Manne, S., et al. (2022). Shared and distinct biological circuits in effector, memory and exhausted CD8+ T cells revealed by temporal single-cell transcriptomics and epigenetics. Nature Immunology, 23(11), 1600–1613. https://doi.org/10.1038/s41590-022-01338-4

Gumber, D., & Wang, L. D. (2022). Improving CAR-T immunotherapy: Overcoming the challenges of T cell exhaustion. eBioMedicine, 77, Article 103941. https://doi.org/10.1016/j.ebiom.2022.103941

Hashimoto, M., Kamphorst, A. O., Im, S. J., et al. (2018). CD8 T cell exhaustion in chronic infection and cancer: Opportunities for interventions. Annual Review of Medicine, 69, 301–318. https://doi.org/10.1146/annurev-med-012017-043208

June, C. H., O'Connor, R. S., Kawalekar, O. U., et al. (2018). CAR T cell immunotherapy for human cancer. Science, 359(6382), 1361–1365. https://doi.org/10.1126/science.aar6711

Khan, O., Giles, J. R., McDonald, S., et al. (2019). TOX transcriptionally and epigenetically programs CD8+ T cell exhaustion. Nature, 571(7764), 211–218. https://doi.org/10.1038/s41586-019-1325-x

Korman, A. J., Garrett-Thomson, S. C., & Lonberg, N. (2022). The foundations of immune checkpoint blockade and the ipilimumab approval decennial. Nature Reviews Drug Discovery, 21(7), 509–528. https://doi.org/10.1038/s41573-021-00345-8

Kraehenbuehl, L., Weng, C. H., Eghbali, S., et al. (2022). Enhancing immunotherapy in cancer by targeting emerging immunomodulatory pathways. Nature Reviews Clinical Oncology, 19(1), 37–50. https://doi.org/10.1038/s41571-021-00552-7

Lin, M. J., Svensson-Arvelund, J., Lubitz, G. S., et al. (2022). Cancer vaccines: The next immunotherapy frontier. Nature Cancer, 3(8), 911–926. https://doi.org/10.1038/s43018-022-00418-6

Litchfield, K., Reading, J. L., Puttick, C., et al. (2021). Meta-analysis of tumor- and T cell-intrinsic mechanisms of sensitization to checkpoint inhibition. Cell, 184(3), 596–614.e14. https://doi.org/10.1016/j.cell.2021.01.002

McLane, L. M., Abdel-Hakeem, M. S., & Wherry, E. J. (2019). CD8 T cell exhaustion during chronic viral infection and cancer. Annual Review of Immunology, 37, 457–495. https://doi.org/10.1146/annurev-immunol-041015-055318

Oliveira, G., & Wu, C. J. (2023). Dynamics and specificities of T cells in cancer immunotherapy. Nature Reviews Cancer, 23(5), 295–316. https://doi.org/10.1038/s41568-023-00560-y

Pardoll, D. M. (2012). The blockade of immune checkpoints in cancer immunotherapy. Nature Reviews Cancer, 12(4), 252–264. https://doi.org/10.1038/nrc3239

Raskov, H., Orhan, A., Christensen, J. P., & Gögenur, I. (2021). Cytotoxic CD8+ T cells in cancer and cancer immunotherapy. British Journal of Cancer, 124(2), 359–367. https://doi.org/10.1038/s41416-020-01048-4

Reck, M., Rodríguez-Abreu, D., Robinson, A. G., et al. (2021). Five-year outcomes with pembrolizumab versus chemotherapy for metastatic non-small-cell lung cancer with PD-L1 tumor proportion score ≥ 50%. Journal of Clinical Oncology, 39(21), 2339–2349. https://doi.org/10.1200/JCO.21.00174

Sade-Feldman, M., Yizhak, K., Bjorgaard, S. L., et al. (2018). Defining T cell states associated with response to checkpoint immunotherapy in melanoma. Cell, 175(4), 998–1013. https://doi.org/10.1016/j.cell.2018.10.038

Sharma, P., & Allison, J. P. (2015). The future of immune checkpoint therapy. Science, 348(6230), 56–61. https://doi.org/10.1126/science.aaa8172

Tauriello, D. V. F., Sancho, E., & Batlle, E. (2022). Overcoming TGFβ-mediated immune evasion in cancer. Nature Reviews Cancer, 22(1), 25–44. https://doi.org/10.1038/s41568-021-00413-6

License: Copyright (c) 2026 Author.
All articles published in this journal are licensed under the Creative Commons Attribution 4.0 International License (CC BY 4.0). This license permits unrestricted use, distribution, and reproduction in any medium, provided the original author(s) and source are properly credited. Authors retain copyright of their work, and readers are free to copy, share, adapt, and build upon the material for any purpose, including commercial use, as long as appropriate attribution is given.

Call for Papers: Advances in World Medical Research

An International Double-Blind Peer-Reviewed Journal Dedicated to Cutting-Edge Medical Innovations and Translational Research.

Journal Overview

Advances in World Medical Research (AWMR) Journal is an open-access, peer-reviewed academic journal committed to disseminating high-quality research findings, clinical experiences, and technological advancements across the entire spectrum of medical and health sciences. We aim to build a global platform for researchers, clinicians, engineers, medical students and policymakers to exchange innovative ideas, promote interdisciplinary collaboration, and accelerate the translation of basic research into clinical practice and public health solutions.

Scope of Interest

We welcome original contributions that address critical issues and novel developments in the following areas (but not limited to):

Clinical Medicine & Healthcare: Diagnosis, treatment, prognosis, and management of various diseases (e.g., cardiovascular, neurological, infectious diseases, oncology, ophthalmology, otorhinolaryngology); clinical trials, evidence-based medicine, and clinical decision-making.

Basic Biomedical Research: Molecular biology, cell biology, genetics, immunology, physiology, pathology, pharmacology, and mechanisms of human diseases.

Biomedical Engineering & Technology: Medical imaging, biomaterials, tissue engineering, medical devices, rehabilitation engineering, and point-of-care testing (POCT) technologies.

Biomedical Technology Translation: Conversion of laboratory discoveries into clinical applications, technology transfer, and commercialization of medical innovations.

Health Management: Preventive medicine, public health, health education, elderly care, chronic disease management, digital health, and health informatics.

AI & Medicine: Machine learning/deep learning in medical diagnosis, prognostic modeling, drug discovery, medical data analysis, telemedicine, and AI-assisted clinical workflows (manuscripts should emphasize clinical relevance and methodological rigor).

Ethnomedicine: Traditional medicine practices, herbal medicine, ethnic healthcare systems, and their integration with modern medicine.

Accepted Manuscript Types

Original Research Articles: Novel, completed research with comprehensive data, detailed

methods, and significant scientific contributions.

Case Reports: Rare clinical cases, unusual disease presentations, or innovative treatment outcomes with clinical insights.

Clinical Research Protocols: Detailed descriptions of planned clinical trials (including study design, objectives, methods, and ethical considerations).

Review Articles: Systematic reviews, narrative reviews, or scoping reviews that summarize the latest research progress, identify knowledge gaps, and propose future research directions (preferably with meta-analysis for systematic reviews).

Short Communications: Concise reports of preliminary but impactful research findings or technical innovations.

Contact Information

For inquiries regarding submission guidelines, peer review, or publication fees, contact:

Editorial Office of Advance of World Medical Research

Email: chi_editor@cscholar.com

Website: https://awmr.cscholar.com/index

We look forward to receiving your outstanding contributions and advancing global medical research together!

PUBLISHER INFORMATION
Publisher: ConnectSix Scholar Publishing Inc.
Address: 6547 N Academy Blvd, #2265,
Colorado Springs, CO 80918, USA
Email: authorsupport@cscholar.com
Official Website: https://www.cscholar.com/
Journal Portfolio: https://journal.cscholar.com/

